JPC 438

Report Number
TM-67-6

An Experimental Investigation of the Gaseous Phase Reaction Zone in a Composite Solid Propellant

by

R. L. Derr
J. R. Osborn

Grant NsG 592

September 1967

JET PROPULSION CENTER
PURDUE UNIVERSITY

SCHOOL OF MECHANICAL ENGINEERING
LAFAYETTE, INDIANA

ERRATA SHEET

Page	Line	Correction
vii	24	Change "chlorine" to "chloride"
3	13	Change in (1) and (2) to in (5)
14	17	Change cal/cm-sec/c to cal/cm-sec-c
17	22	Change end of line to read "from Planck's"
28	17	Change beginning of line to read "was to"
50		Equation should be

$$T_F = \frac{\lambda}{C_2}\left[\ell n\left\{\frac{I_L - I_{L-F}}{I_F}\left[\exp(C_2/\lambda T_L)-1\right]+1\right\}\right]^{-1}$$

113	14	Equation should be

$$T_F = \frac{\lambda}{C_2}\left[\ell n\left\{\left[\frac{\omega_1 A_1}{\omega_2 A_2}\right]\left[\frac{I_L - I_{L-F}}{I_F}\right]\left[\exp\,(C_2/\lambda T_L{}')-1\right]+1\right\}\right]^{-1}$$

113		Equation (14) should be

$$T_F = \frac{\lambda}{C_2}\left[\ell n\left\{\frac{I_L - I_{L-F}}{I_F}\left[\exp\,(C_2/\lambda T_L)-1\right]+1\right\}\right]^{-1}$$

JPC 438

Report Number

TM-67-6

PURDUE UNIVERSITY

AND

PURDUE RESEARCH FOUNDATION

Lafayette, Indiana

AN EXPERIMENTAL INVESTIGATION OF THE GASEOUS PHASE REACTION ZONE IN A COMPOSITE SOLID PROPELLANT

by

R. L. Derr

J. R. Osborn

Technical Memorandum

Grant NsG 592

Jet Propulsion Center
Purdue University

September 1967

ACKNOWLEDGMENTS

The authors wish to express their gratitude to Dr. J. D. Hoffman for his helpful assistance and suggestions during the investigation.

The authors also appreciate the efforts of the following people: Mesdames F. Haniford and S. Waszilycsak for their typing skills; Messrs. F. Berg, D. Brown, R. Malinowski, and L. Wheeler for their assistance in conducting the experiments and preparing drawings; and Messrs. C. Merkel, W. Timmons, T. Miller, G. Hurst, and T. Virgin for fabricating the experimental equipment and maintaining the apparatus.

The research program reported herein was sponsored by the National Aeronautics and Space Administration, Contract Nos. NsG 383 and NsG 592. Reproduction of this document in full or in part is permitted for any use of the United State Government.

The author also wishes to thank Mr. R. Wall and Dr. D. Flanigan of Thiokol Chemical Corporation, Huntsville, Alabama, and Mr. W. Gin of Jet Propulsion Laboratory, Pasadena, California for supplying the propellants used in this research program.

TABLE OF CONTENTS

LIST OF TABLES

LIST OF FIGURES

Figure | Page

ABSTRACT

This report discusses an experimental investigation of the gaseous reaction zone located above the burning surface of a composite solid propellant. In the investigation, the temperature profile within the gaseous reaction zone was measured with a modified line reversal pyrometer. In conjunction with this, a servo-controlled feedshaft was employed to drive the strand of propellant toward the temperature measurement region at the same rate at which the strand burned. This technique enabled a zone in the flame to be examined over a controlled length of time.

A polysulfide-ammonium perchlorate solid propellant was used in the study. The effect of oxidizer size on the temperature profile was investigated by using a propellant containing a fine oxidizer grind ($\overline{d}$=6μ) and a propellant containing a coarse oxidizer grind ($\overline{d}$=50μ). The propellants were burned at pressures ranging from atmospheric to 215 psia.

A motion picture study was conducted in which the gaseous reaction zone and burning surface of a propellant sample were photographed as the servomechanism operated. The results of this study demonstrated that the servomechanism was capable of positioning the burning surface satisfactorily.

The results of the temperature measurements showed that the gaseous reaction zone cannot be represented by a one-dimensional temperature profile. It was also found that the gaseous reaction zone is not confined to a thin region adjacent to the surface; rather, at the pressures examined, the reaction zone extends up to a distance of approximately 1 mm from the surface, a measurement which is greater than that found by some researchers.

INTRODUCTION

In the past fifteen years a considerable amount of experimental and theoretical research has been directed towards understanding the steady state combustion of composite solid propellants. Upon noting the extensive amount of work in this area, one might erroneously conclude that the sole motivation for this research is based upon the need for a steady state burning rate theory which will allow a priori burning rate prediction for those propellants. Certainly, the development of such a steady state model would be helpful; but, unfortunately, other phenomena associated with the combustion process introduce effects which must also be dealt with when designing a solid propellant rocket motor. Several of the more important effects are as follows:

1. the effect of erosive burning which is introduced when combustion products sweep over the burning surface,

2. the effect of unstable burning which results from both acoustic and nonacoustic interactions between the hot combustion products and the burning solid propellant, and

3. the effect of acceleration forces which are present when the rocket is spinning or experiencing a high rate of acceleration.

Recognizing the existence of these and other effects, it can be seen, then, that the objective of steady state propellant research is much more far reaching than just a steady state solution to solid propellant combustion which allows a priori burning rate predictions. Rather, the importance lies in the basic understanding of the combustion process which will give a foundation for understanding the complex problems mentioned previously.

Experimental research to date has been occupied with many aspects of the steady state combustion process which includes studies of solid phase reactions, gas phase reactions, and combinations of these reactions. Theoretical work has been directed towards analyzing the above reactions; however, no theoretical model for steady state combustion has been developed to date which reliably predicts the burning characteristics of a composite propellant.

One of the most widely debated issues of the steady state combustion of composite solid propellants is the contribution of the heat generated in the gaseous reaction zone to the total heat necessary to sustain the controlling surface reactions. Indeed, the flame structure above the burning surface is not well understood and has been approximated as:

1. occurring adjacent to the burning surface such that all energy required by the surface reactions originates from the gas phase reactions (1)*;

---

*Numbers in parentheses indicate publications listed in the List of References.

2. occurring at an intermediate distance from the burning surface whereby only a fraction of the heat necessary to sustain the surface reaction comes from the gas phase reactions (2,3); and

3. occurring at a distance from the burning surface great enough that the surface reactions must depend on subsurface reactions for their sustaining energy (4).

The prime reason for the confusion is the lack of agreement in the results of experiments which are designed to determine the structure of the flame zone. Results have been obtained which show that the adiabatic flame temperature of the gas phase reaction occurs very close to the burning surface (5). However, other results (6,7) have shown that the reaction zone is very extensive (by two orders of magnitude) over that of the results presented in (1) and (2).

The objective of this research program was to develop a technique for measuring the temperature profile above the burning surface of a composite propellant and to relate the results of the measurement to previous experimental investigations of the gaseous combustion zone.

REVIEW OF THE LITERATURE

General Discussion

Over the past two decades, solid propellant rocket propulsion has been accepted as the propulsion source in various military and space applications. The acceptance of the solid propellant rocket has led to extensive investigations into the nature of steady state combustion for many different types of rocket propellants. The most thoroughly investigated class of propellants is that of the double-base propellant which is simply a colloidal mixture of nitrocellulose and an explosive plasticizer, usually nitroglycerin, to which additives and ballistic modifiers are added to obtain desired propellant characteristics. Several excellent reviews of the combustion of double-base propellants can be found in References (8, 9, and 10).

In recent years, the composite type of propellant has received a great deal of attention in the literature (11,12). The composite type of propellant consists of a finely divided grind (from about 5μ to 200μ) of oxidizer crystal dispersed throughout a matrix of plastic or elastomeric compound which also serves as the fuel for the combustion reaction. In many instances additives are added to the matrix compound in order to increase the energy release of the combustion process.

Description of the Combustion of Composite Solid Propellants

The overall combustion process of a composite solid propellant appears to be a complex interplay of reactions in both the solid and the gaseous phase of the burning propellant. In order to examine the process, it is expedient to isolate each of the important reactions and examine them separately. The sketch in Fig. 1 illustrates a simple composite propellant consisting of a typical polymetric binder (such as polysulfide, polyurethane, or polybutadiene-acrylic acid) and a bimodal (two sizes: fine and coarse) distribution of ground ammonium perchlorate crystals as oxidizer. In the combustion of such a propellant, the following reactions can be isolated for discussion purposes:

1. The exothermic heterogeneous reaction between the binder and the oxidizer interface,

2. The endothermic pyrolysis of the binder or fuel,

3. The exothermic decomposition of the oxidizer crystal, and

4. The exothermic gaseous reaction between the oxidizer decomposition products and the fuel pyrolysis products.

The existence of a subsurface reaction is based on the premise that heat transferred from the hot surface of the propellant to submerged oxidizer crystal surfaces just below the propellant surface is sufficient to decompose intermosaic blocks of the perchlorate oxidizer particles such that gaseous products diffuse to the oxidizer particle-fuel interface. When such conditions arise, a heterogeneous reaction between the resulting gaseous oxidizer and fuel yields a source

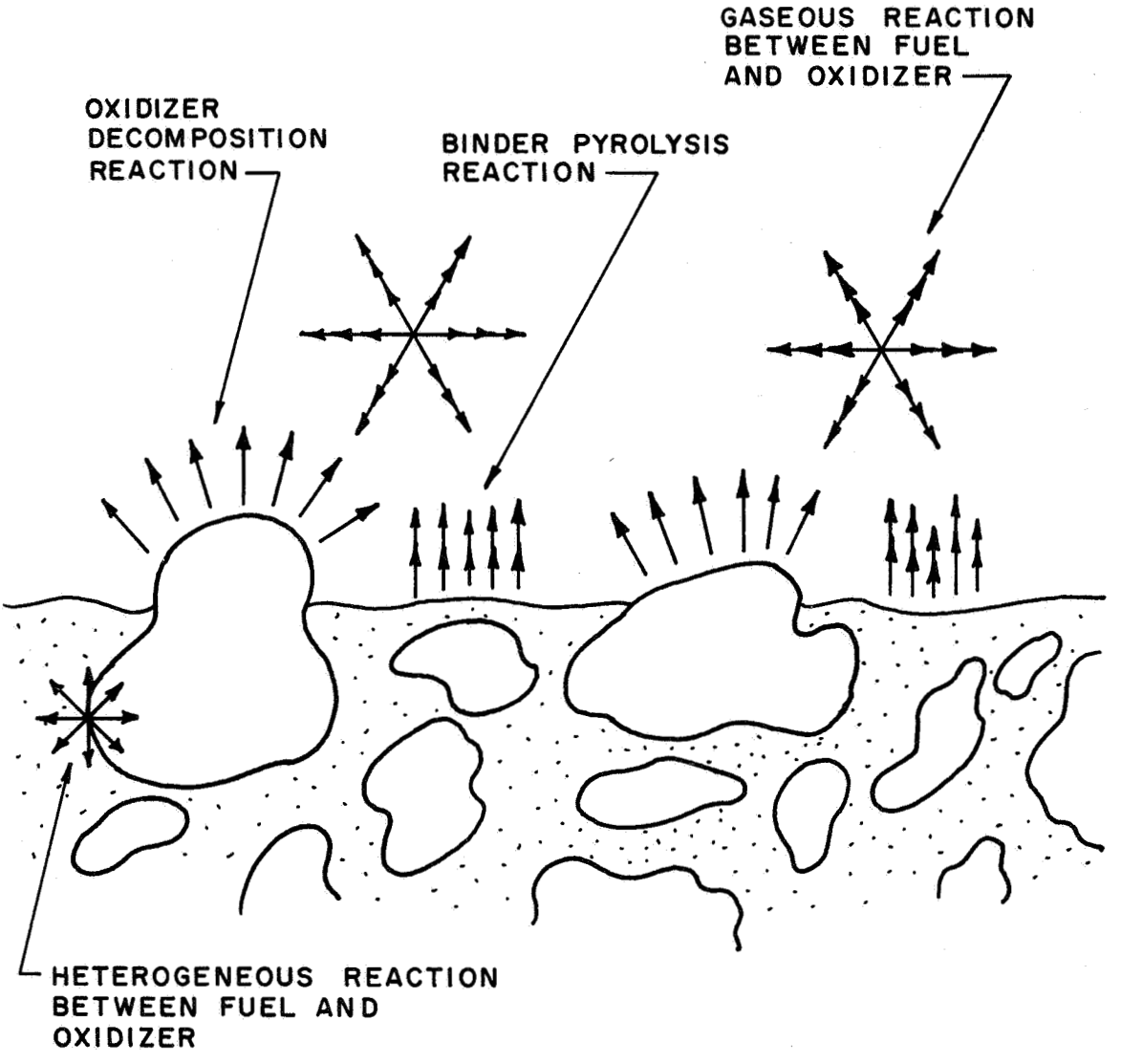

FIG. 1 ILLUSTRATIVE SCHEMATIC OF COMBUSTION PROCESSES IN A COMPOSITE SOLID PROPELLANT

of heat which must be recognized in the overall combustion process because of its close proximity to those reactions which require heat to sustain them.

There is a great deal of controversy in the literature pertaining not only to the importance of a subsurface reaction but also to the actual existence of such a reaction. The case for heterogeneous subsurface reactions was first presented by Anderson and co-workers (13) in a study of the ignition of solid propellants. In that study, oxidizers such as flourine and chlorine triflouride were used to ignite composite solid propellant hypergolically. The experiments demonstrated that the ignition process proceeds as a result of spontaneous heterogeneous reactions occurring at the oxidizer interface. Encouraged by this, Anderson (14) proposed that heat released from heterogeneous reactions must play an important role in steady state combustion of solid propellants.

The pyrolysis of the fuel or binder results when heat is transferred to the binder from some heat source. Whether the binder is located on the surface or below the surface, the result is the thermal degradation and vaporization of small fragments of the polymer which serves as one of the reactants in the gaseous fuel-oxidizer reaction. In a realistic sense, the pyrolysis of binder is not restricted to the surface of the propellant; rather, the possibility of small pieces of binder protruding and breaking from the surface allow pyrolysis to occur even in the gaseous zone.

The decomposition of the oxidizer crystal involves the transformation of the crystal into the oxidizing gas which then reacts with the binder pyrolysis products. The chemical process by which this transformation occurs varies according to the type of oxidizer crystal considered. The most widely used oxidizers in composite solid propellants are potassium perchlorate, ammonium perchlorate, and ammonium nitrate. Of those, ammonium perchlorate is used more extensively because it yields little residue or smoke and the oxidizer makes a substantial contribution to the gas phase when burned in a given propellant formulation. As a result, attention is directed toward that oxidizer crystal throughout the following discussion.

The final reaction which was isolated in the generalized discussion of the solid propellant combustion was that of the gaseous reaction zone. This reaction takes place above the burning surface where pyrolyzed binder or fuel and the oxidizer decomposition products are reactants. It is this reaction which yields the high temperature attributed to the combustion of a given solid propellant. The heat generated from this reaction occurs at varying distances above the burning surface due to the irregular nature of the propellant surface and inhomogeneities of the reaction zone. The energy released in the reaction could yield sufficient energy to sustain the combustion reaction; however, the reaction does not necessarily occur close enough to the surface to supply the energy required for steady state combustion.

Quite clearly, a complete understanding of each of these isolated reactions would not yield a complete understanding of the overall combustion process. Rather, the interaction phenomena associated with these reactions must be known before any realistic conclusion can be made about the combustion of a solid propellant. Interactions can occur between the isolated reactions by means of reaction heterogeneity and energy transfer between the exothermic and endothermic reactions.

Reaction heterogeneity occurs as a result of any two of the reactions combining. For instance, the previously mentioned breakage of unpyrolyzed binder or fuel particles from the surface and the subsequent ejection of these particles into the gaseous fuel-oxidizer reaction environment produces a heterogeneous interaction. Another example of this type of interaction is the introduction of pyrolyzed binder as a reactant in the oxidizer decomposition flame. If this should occur, the altered oxidizer decomposition reaction must show a marked change from that of the isolated oxidizer decomposition reaction.

The energy transfer form of interaction is probably the most important interplay between the reaction. It is that transfer which supplies the necessary energy to the endothermic reaction and sustains the overall combustion process. For example, the energy required to pyrolyze the binder must originate from some other reaction or reactions. Also, in some pressure regimes, the oxidizer decomposition flame is not self sustaining and a source of energy must be available for this reaction to be completed. Thus, it can

be seen that the combustion of a composite solid propellant is quite complex.

Upon examining this complex problem with the intention of representing the overall combustion process by an analytical model which can yield insight into the combustion of solid propellant, the question arises as to what approach should be followed in formulating a model. The answer to this can be readily seen when one observes that for a given set of conditions, the combustion of a solid propellant proceeds at a given rate and that this rate must be dependent upon some controlling reaction which is sustained by a source of energy generated directly from the reaction itself or from some other reaction. Thus, the logical approach is to determine the controlling reaction and then examine all of the limiting influences which can affect the reaction.

In an attempt to determine the location of the controlling reactions, Gutman (15) examined the interaction of important rate processes occurring in composite solid propellant combustion and established the following five logical rules:

1. It is important to consider whether the processes in question are in series or in parallelwith respect to the mass flow.

2. If in parallel, their influences are added as conductances; if in series, they are added as resistances.

3. If one of two parallel influences is much larger, it will be controlling.

4. If the upstream of two series influences is limiting, it will be controlling.

5. If a downstream of two series influences is limiting, the system will not work.

For an example of rule five, Gutman cites the situation of a propellant burning where an upstream flow has been established and the pressure falls so low that the reaction rate in the flame cannot accommodate the flow without thickening excessively, causing the flame to quench or to oscillate. Thus, one might be led to believe that the downstream reactions of two series influences cannot be limiting and that only the upstream reaction need be considered. Upon closer observation, however, it becomes obvious that this line of reasoning is not true in the general case when combustion interactions are present. In particular, the presence of energy feedback from a downstream reaction necessary to sustain an upstream reaction presents a situation where the rate of the downstream reaction determines the position of the energy source and thereby the amount of energy feedback to the upstream reaction. Thus, the downstream reaction rate becomes as important as the upstream reaction rate. It would appear that the insertion of the word "independent" before the words "series influence" and the note that dependent series influences must be considered jointly would correct these rules and make Gutman's approach for determining controlling reactions more realistic.

Several immediate conclusions can be made at this point with the modified rules stated by Gutman. First, models of solid propellant

combustion which include only the gaseous reaction zone such as postulated in the work of Boys and Corner (16) for double-base propellants are not realistic because they consider only the downstream reaction of a series of dependent reactions (solid zone -- foam zone -- fizz zone -- flame zone). Thus, this reaction cannot be the controlling reaction and cannot establish the burning characteristics of the propellant. Second, if the downstream gaseous reaction between the oxidizer and fuel pyrolysis products in a composite propellant can be shown to occur at a sufficient distance from the burning surface such that heat transfer to the surface is not a factor in sustaining the pyrolysis reactions, then the parallel pyrolysis reactions of binder and oxidizer can be considered to be the controlling reaction combination of the solid propellant and the downstream reactions can be ignored. Third, the same parallel pyrolysis reactions can be considered to be controlling and the gaseous reaction ignored if the existence of a heat source due to heterogeneous reactions at oxidizer and fuel interfaces is established with sufficient energy to sustain the pyrolysis reactions. Lastly, if the gaseous reaction is coupled with the parallel pyrolysis by heat feedback, all of these reactions become important.

Thus, two basic questions arise which if answered would yield valuable insight into the combustion characteristics of a composite solid propellant:

1. What fraction of the heat generated in the gaseous reaction zone is transferred back to the burning surface of the propellant?

2. What fraction of heat is generated at and below the burning surface of the propellant due to heterogeneous reactions?

In the following discussion a review from the literature is presented of experimental work that has been directed towards answering the question pertaining to energy source location.

2.3 Experimental Investigations

The importance of establishing the location of energy sources in the combustion of composite solid propellants has been established. In the past, experimental investigations concerned with the location of the reaction zones above and below the burning surface, have been conducted. Unfortunately, no one experimental approach yields results definitely establishing the sites of energy release which influence the controlling reaction of the combustion process of even the most simple composite solid propellants. In the following, some of the more important experimental findings are discussed in terms of results which indicate the energy source location of the combustion process.

2.3.1 Experiments Supporting Significant Energy Transfer From the Gas Phase to the Burning Surface

There are two categories of experiments which support the premise that the gaseous phase reaction between the oxidizer and fuel supplies a large fraction of the energy necessary to sustain the surface reactions. The first is a direct experimental approach in which the gaseous reaction zone is examined and the gaseous reaction

between the oxidizer and fuel is found to occur very close to the burning surface of the propellant such that steep temperature gradients exist at the surface. The second is an indirect experimental approach, in which the subsurface reaction zone is examined and a conclusion is made pertaining to the gaseous reaction zone. In this type of experiment, results indicate that no subsurface reaction exists such that subsurface heating is nonexistent. As a result, it can be inferred that the surface reactions must rely upon heat transfer from the gas phase reactions in order to be sustained.

Considering the investigations of the gaseous reaction zone, it is helpful to make a rough estimate of the thickness of the reaction zone required in order that a significant energy transfer from that zone to the surface can exist. Friedman (17) assumed that a heat flux of approximately 400 cal/cm^2 - sec was necessary to vaporize the surface of a typical composite solid propellant burning at a rate of one cm/sec. By equating the heat flux to $\lambda \frac{\Delta T}{\Delta X}$, where λ is the gas conductivity, and assuming λ = 0.0002 cal/cm-sec/C and ΔT = 2000 C, Friedman found that the height of the flame above the surface must be about 10 microns. It can be seen, then, that the gaseous reaction zone is quite small for the case of complete energy transfer from the gas phase to the surface.

Sutherland (5) has investigated the reaction zone of a styrene-base polyester resin-ammonium perchlorate propellant with an optical pyrometer which yielded temperature measurements in the gaseous reaction as a function of distance from the surface. The technique employed was

a modified sodium line reversal method which measured temperatures over a range of 1400 K to 2500 K with a spatial resolution of 50 microns by 300 microns and a time resolution of approximately 3 msec.

The procedure followed in measuring the profile consisted of allowing the propellant strand to burn by the temperature measurement region and measuring the temperature as a function of time. The burning rate of the strand was measured concurrently by means of a beam splitter arrangement and a 35 mm frame camera. Thus with the burning rate and temperature-time data, the temperature profile was easily calculated.

The results of Sutherland's experiments showed that the active reaction zone occupies only 100 microns or less adjacent to the propellant surface. Thus, the results found by Sutherland are consistent with the rough calculations of the flame height as noted by Friedman; and, it would appear from these results that the gaseous reaction between the fuel and the oxidizer is linked with the surface reactions whereby the two cannot be considered independently when examining the overall combustion process. Further comments on this work are deferred to a later section.

Turning attention to solid phase combustion studies, Hightower (18) has attempted to observe the heterogeneous reaction at the interface of the solid binder and oxidizer crystal. In these experiments two-dimensional propellant sandwiches consisting of a thin binder layer between two single crystals have been burned and extinguished.

The binder was polybutadine - acrylic acid (PBAA) and the oxidizer was a thin sheet of ammonium perchlorate cleaved from a single crystal. The sandwiches were burned at pressures between 100 and 1200 psig. After extinguishment, it was noted that in no case was the surface regression led by the oxidizer-binder interface as would be expected if a heterogeneous reaction occurred along these surfaces. A second study of subsurface reactions by McGurk (19) seems to substantiate Hightower's results. In McGurk's work extinguished composite propellant samples were cut to thin wafers with a microtome allowing microscopic investigation of the subsurface reaction zones. The crystallographic changes of the oxidizer were analyzed by means of a polarized light technique. In the examination of an ammonium perchlorate propellant, McGurk noted that oxidizer crystals within a few microns from the surface do not show visible effects while protected by a very thin coat of binder.

Thus, the direct observations of Hightower and McGurk do not show the existence of the heterogeneous subsurface reactions that have been postulated by Anderson and co-workers. If this result is accepted, it would appear that all heat necessary to pyrolyze the solids must originate from the gas phase.

Experiments Not Supporting Significant Energy Transfer From the Gas Phase to the Surface

Experiments which support the premise that the gaseous phase reaction between the oxidizer and fuel supplies only a small fraction of the energy necessary to sustain the surface reactions fall into two categories. The first is a direct experimental approach where the gaseous reaction zone is examined and the oxidizer-fuel reaction is found to occur over an extensive region such that steep temperature gradients do not exist at the propellant surface. The second is an indirect experimental approach where the subsurface reaction zone is examined and a conclusion is made pertaining to the gaseous zone. In this case, the existence of subsurface reactions is established and from this it is inferred that the energy transfer from the gaseous reaction zone is not dominant in sustaining the surface reactions.

Penzias (6) has measured the temperature profiles above the surface of a polyvinyl-chloride-ammonium perchlorate propellant, with a rapid scanning infrared pyrometer. In this study, strands of propellant were burned past the location of the zone of a fixed temperature measurement and the infrared spectral radiance and absorptance of the gases above the burning surface were measured in the 1-5 micron region. From these data, the temperature was calculated from Planck's Law as a function of time; and, in a manner similar to that of Sutherland, these data were converted to temperature as a function of distance from

the burning surface. The height of the temperature measurement region was 80 microns and the time resolution of the measurement was 50 milliseconds.

The results of this experiment are shown in Fig. 2 for a pressure of 600 psig. The results show that the maximum temperature is attained at a distance of approximately 1000 microns. Thus, following the rough calculation scheme of Friedman, the heat transferred back to the surface must be reduced by two orders of magnitude. Such a reduction would essentially eliminate the influence of the gaseous reaction between the oxidizer and fuel on the overall combustion of the propellant.

Temperature profiles have also been measured in composite solid propellant flames employing fine bead thermocouples. Sabadell (7) fabricated thermocouples from Wollanstan platinum and platinum-10% rhodium wire of 7.5 micron diameter. The thermocouples were embedded in samples of a PBAA-ammonium perchlorate propellant and temperature-time profiles were obtained by recording the thermocouple output as the burning surface passed over the thermocouple junction. Temperature-distance profiles were then calculated from burning rate data as described previously. The results of this investigation yielded temperature profiles through the solid reaction zone as well as the gaseous reaction zone. Temperature profiles for pressures of 30 psig, 100 psig, and 150 psig are presented in Fig. 3. As a result of the low melting point of the thermocouple material, the profile does not extend to the high temperatures resulting from the gaseous fuel-oxidizer reaction. However, the temperatures recorded prior to thermocouple

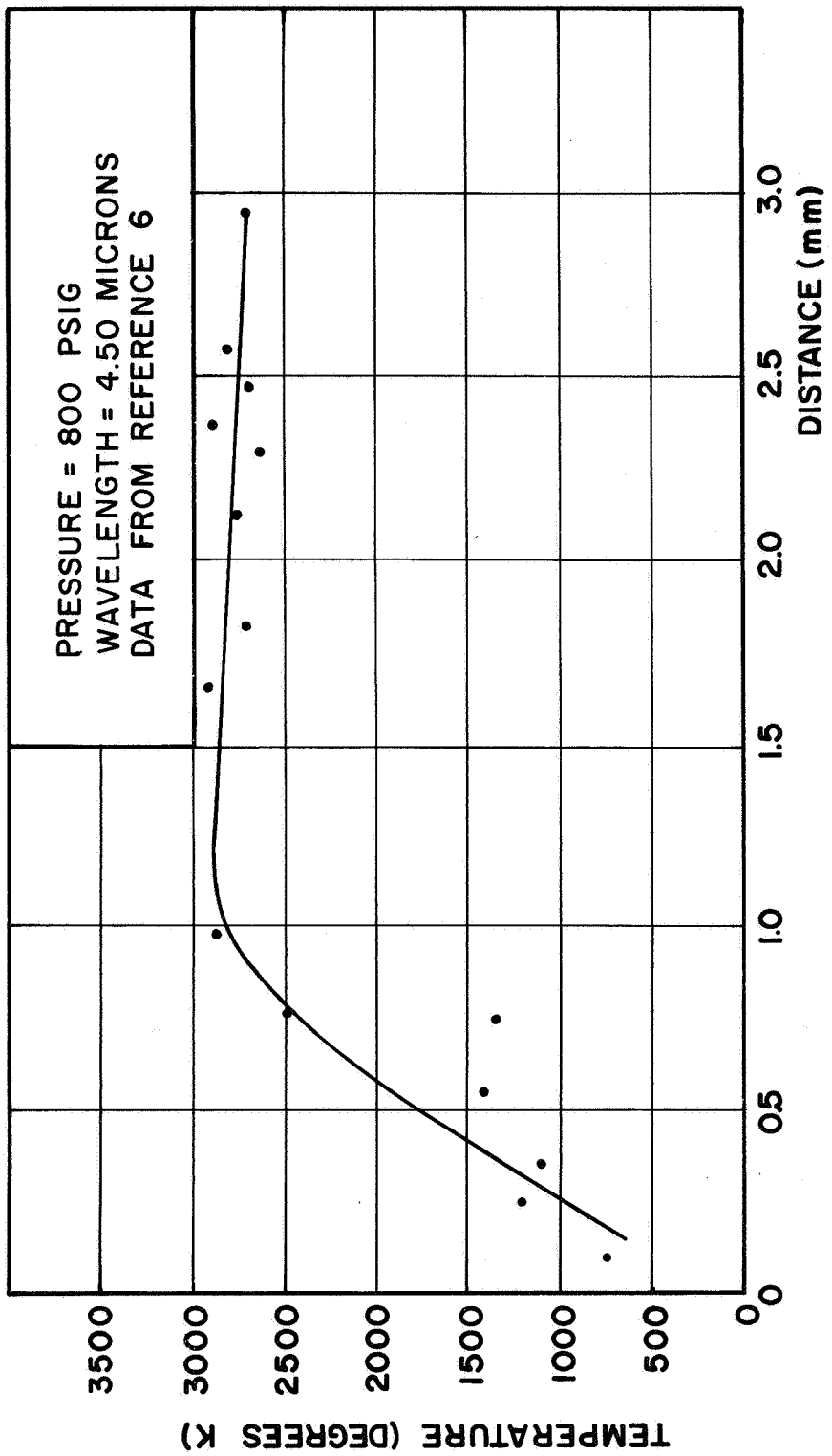

FIG. 2 TEMPERATURE PROFILE OF POLYVINYL-AP FLAME

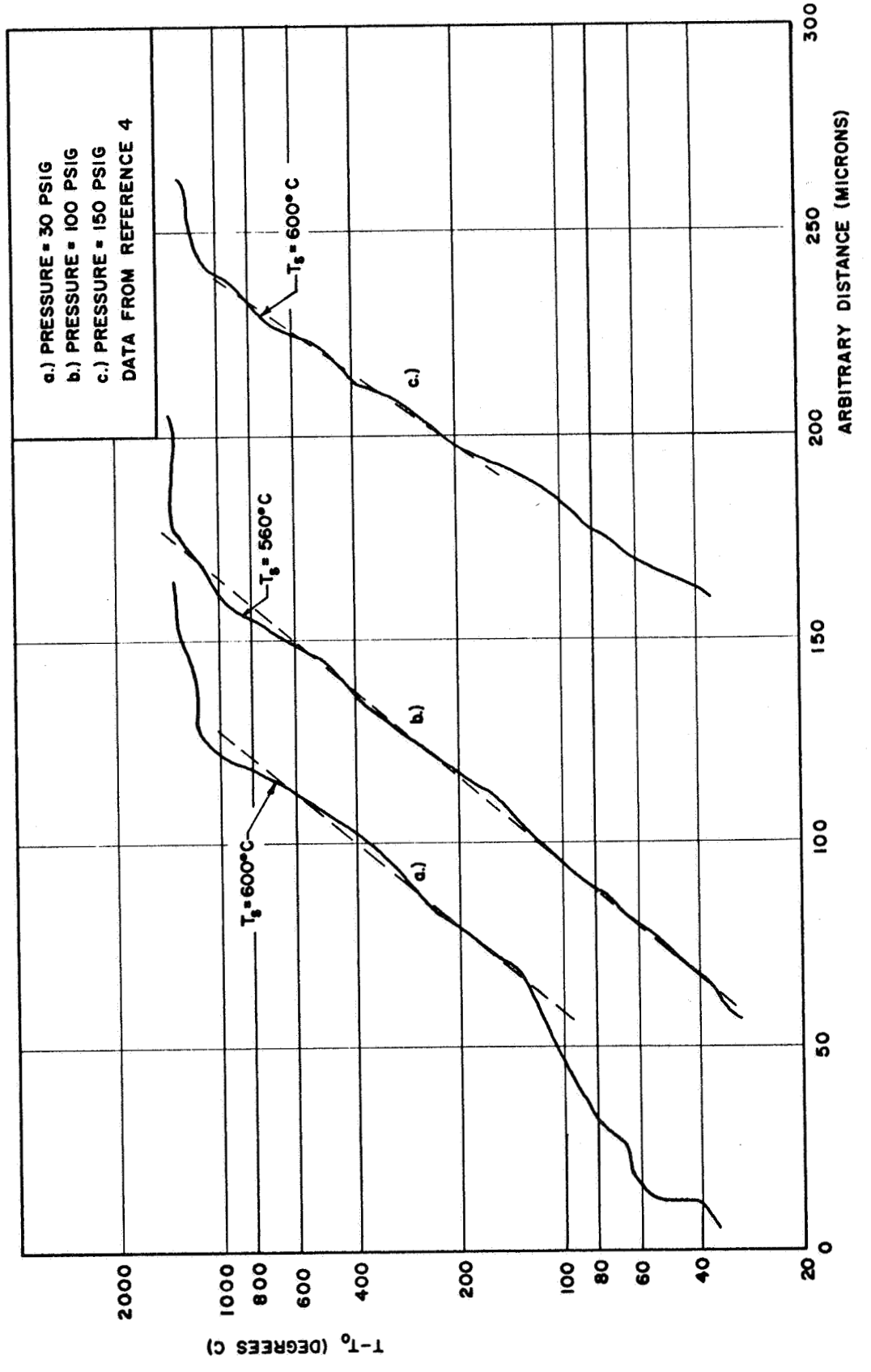

FIG. 3 TEMPERATURE PROFILE OF PBAA-AP FLAME

"burnup", show that the gradient at the surface is of the order 30 C/micron which is much smaller than that found from Friedman's rough calculation. Thus the results of this investigation again show that the temperature gradient in the gas is insufficient to supply all of the energy necessary to vaporize the solid.

Several spectroscopic studies of the gaseous reaction zone have been conducted in the past (20,21). In these studies the spatial distribution of transient emitters in the ultraviolet and visible regions of the spectrum was measured. These emitters give an indication both of the reactions which are occurring and the locations of the reactions. In the work of Povinelli (20), the intensity of CN emission at 3883 $\mathring{A}$ was measured as a function of distance above the burning surface of a polybutadiene-acrylic acid, ammonium perchlorate ($\bar{d}\simeq 11\mu$) propellant. The CN emission was chosen because it is believed that this specie is formed only from a reaction between the binder and oxidizer for the propellant chosen in the experiment. The results of this experiment showed that at atmospheric pressure, the CN emission was maximum at a distance of 275 microns from the surface and extended to a distance of approximately 2 mm. By assuming that the level of CN emission is negligible past the reaction zone, Povinelli ascribes the reaction zone thickness to be 2 mm. Unfortunately, no results were obtained at pressures above atmospheric due to the high intensity of carbon continuum which obscured the CN lines at these higher pressures; however, the results indicate that at atmospheric pressure, the gas

phase reaction between the gaseous fuel and binder is not occurring adjacent to the surface such that a steep temperature profile exists at that point.

A more recent spectrographic study of the propellant flame zone by Waesche (21) has extended this approach to pressures above atmospheric. Waesche has examined the spectrum of NF - ammonium perchlorate propellants over a pressure range of atmospheric to 20 atmospheres and noted the spatial distribution of the CN band. The results of this investigation were in agreement with those of Povinelli. At atmospheric pressure the CN emission was again found to extend above the burning surface a distance of 2 mm. At a pressure of 20 atmospheres, the region diminished to 1 mm. Thus, the results again indicate that the reaction zone is too extensive for the reaction between the gaseous fuel and oxidizer to be the sole source of energy for the surface reactions.

Experiments of the indirect type, which support the premise that the gaseous reaction between the fuel and oxidizer is not the sole provider of energy to the surface reactions, have dealt with the differential thermal analysis of solid propellant samples. Waesche and Wenograd (4) have examined the condensed phase thermal decomposition reactions of ammonium perchlorate composite propellants using the technique of differential scanning calorimetry. In these experiments, a small test sample and a reference inert material were

heated at a programmed rate of temperature rise. Energetic reactions from the test sample were indicated by a differential readout of the heat rates necessary to maintain equal temperature rises in the reference material and sample holders. The most significant result of this experiment was obtained when the heat release rate for samples of ammonium perchlorate were compared to the heat release rate for samples of PBAA ammonium perchlorate. The results were expressed in the form of a thermogram in which the rate of heat evolution was plotted against the temperature of the reference and test sample holders. The resulting thermogram for the previously mentioned comparison of AP and PBAA-AP samples at atmospheric pressure is given in Fig. 4. Integration of the two thermograms shows that the heat release for the propellant is about four times greater than that for the oxidizer alone. The results were found to differ only slightly at a pressure of 250 psig. As a result of their determination of the heat release rate, Waesche and Wenograd concluded that condensed-phase reactions are rapid and intense enough to supply a significant portion of the energy required to maintain the combustion of a solid propellant.

Similar experiments with the differential thermal analysis technique have been reported by Stammler (22). In these tests, the conclusion is also made that the combustion of propellant is governed by some solid phase reactions.

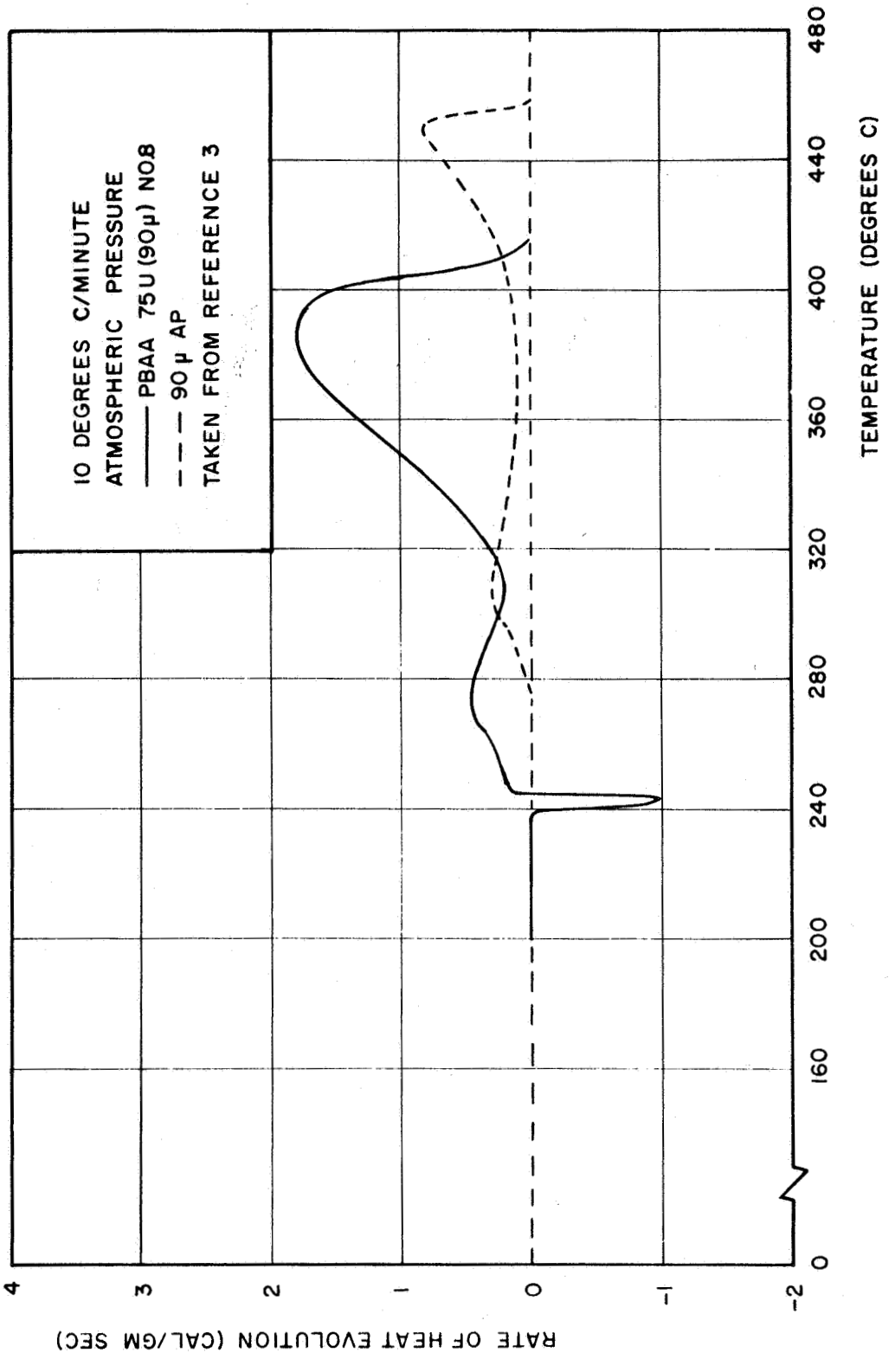

FIG. 4 THERMAL DECOMPOSITION OF AP AND PBAA-AP PROPELLANT

Summary and Comments

The foregoing discussion has dealt with an intuitive look at the important reactions which occur in the overall combustion process of a composite solid propellant. Also, the importance of interaction between the basic reactions was emphasized. From this discussion, it was concluded that the controlling reactions of the combustion process are the surface reactions which receive their sustaining energy from either subsurface or gaseous phase reactions or from both of these sources. Experimental work in the past has attempted to determine the origin of the sustaining energy; however, to date little or no agreement in that respect can be found between the various experimental approaches.

In the case of the indirect measurements (examination of the subsurface reactions in order to infer a result of the gaseous phase heat release contributions) several remarks can be made which should reduce the confusion in the comparison of the results presented. In the case of the sandwich propellant strand investigations the criticism can be made that the experiment does not represent the true combustion process which occurs between small crystals of oxidizer dispersed in a binder matrix. Also, the comment has been made that the crystal structure of the AP slab does not agree with that found in a true propellant. Conversely, the experiments of the subsurface reactions which confirm exothermic reactions below the surface have certain limitation problems.

For the results of differential thermal analysis, there is a possibility of gaseous phase reactions entering into

the results. Since the technique monitors the temperature of a sample holder rather than the sample itself, there is always the possibility that gases pyrolyzing from the surface between the sample and the holder are reacting and yielding the exotherms noted in these experiments. Thus, the results of the indirect type of experiment performed to date have not yielded information from which a definite conclusion of energy source location can be made.

Probably the most perplexing results of the experiments reviewed are those of the direct type in which the temperature profile in the gaseous phase is measured. In the measurements of Sutherland (5), Penzias (6), and Sabadell (7), one finds that the results are so varied that no conclusion can be made about the contribution of the gas phase reaction between the oxidizer and fuel to the surface reactions. This is surprising; because, although the experimental techniques are not the same, certain qualitative similarities should exist between these results. Certainly the difference in techniques should allow some variation in the temperature values measured; however, the large variation in the temperature change and the location of the region of maximum temperature cannot be explained simply on the basis of different temperature technique. As a result of this discrepancy and the importance of determining the contribution of the energy feedback from the gas phase to the propellant surface, it was deemed important to reconcile these differences in this research program.

METHOD OF INVESTIGATION

General Discussion

The importance of determining the structure of the gaseous reaction zone above the burning surface of a composite propellant has been established. In this research program, an experimental approach has been employed to determine the structure of that zone. Two types of experiments have been conducted. First, the temperature profile of the burning surface of a polysulfide-ammonium perchlorate propellant has been measured by a modified line reversal technique similar to that employed by Sutherland (5). Second, color motion pictures have been taken of the burning surface and gaseous reaction zone of the propellant.

The following is a general description of the temperature measurement system designed to measure the temperature profile. In addition, the specific experiments conducted in this research program are described. A detailed discussion of the design criteria for the temperature measurement system can be found in Appendix B.

The Temperature Measurement System

A considerable amount of effort was given to determining what experimental technique should be employed for the temperature profile measurement. It was recognized that two measurements were necessary in order to measure the temperature profile in the gases above a burning solid propellant; viz., the temperature of the gas over a small region

above the burning surface and the distance from the region of temperature measurement to the burning surface. The system which was developed for the measurement consisted of a modified line reversal pyrometer and a servo-controlled propellant feedshaft that drives a burning propellant strand towards the temperature measurement region at the same rate at which the propellant strand burns. To facilitate the discussion of the temperature measurement system, the system is divided into three parts:

1. the servomechanism system,
2. the modified line reversal pyrometer, and
3. the combined system.

The Servomechanism System

The servomechanism system served two purposes in the temperature measurement system. The first was to drive the propellant strand upward at the same rate at which it is burning, enabling the examination of a flame zone for a controlled length of time, and the second was to locate the burning surface with respect to the temperature measurement zone at any given time.

The feasibility of employing a closed loop servomechanism system to drive a sample of burning solid propellant at the same rate at which it burns was first introduced by Osborn, Burick, and Panella (23). That system was originally designed incorporating a gamma ray-scintillation probe technique to detect the burning surface. In this research program, that servomechanism system was modified so that the surface detection technique could be adapted to the temperature

measurement system. In the following discussion, the basic principles of operation for the servomechanism are presented.

The servomechanism system as employed in the temperature measurement system consisted of three basic components:

1. the surface detection components,
2. the electrical components, and
3. the mechanical components.

A block diagram showing these components is presented in Fig. 5.

The successful operation of the servomechanism system consisted in the DC servomotor imparting a linear velocity to the propellant feed shaft equal and opposite to that of the burning surface of the propellant strand. When this condition prevailed, the burning surface remained in a fixed position as the strand burned.

It was the purpose of the detection and electrical components to supply a feedback to the servomotor in order for the correct motor speed to be attained. In particular, the detection components located the position of the burning surface within the confines of a visible light beam. The detection of the surface was accomplished by a photomultiplier tube circuit which had an output proportional to the position of the surface within the light beam.

The purpose of the electrical components was to amplify this detection signal and provide power to the DC servomotor. Since the detection signal increased as the surface receded in the direction of burning and decreased as the surface was driven in the opposite

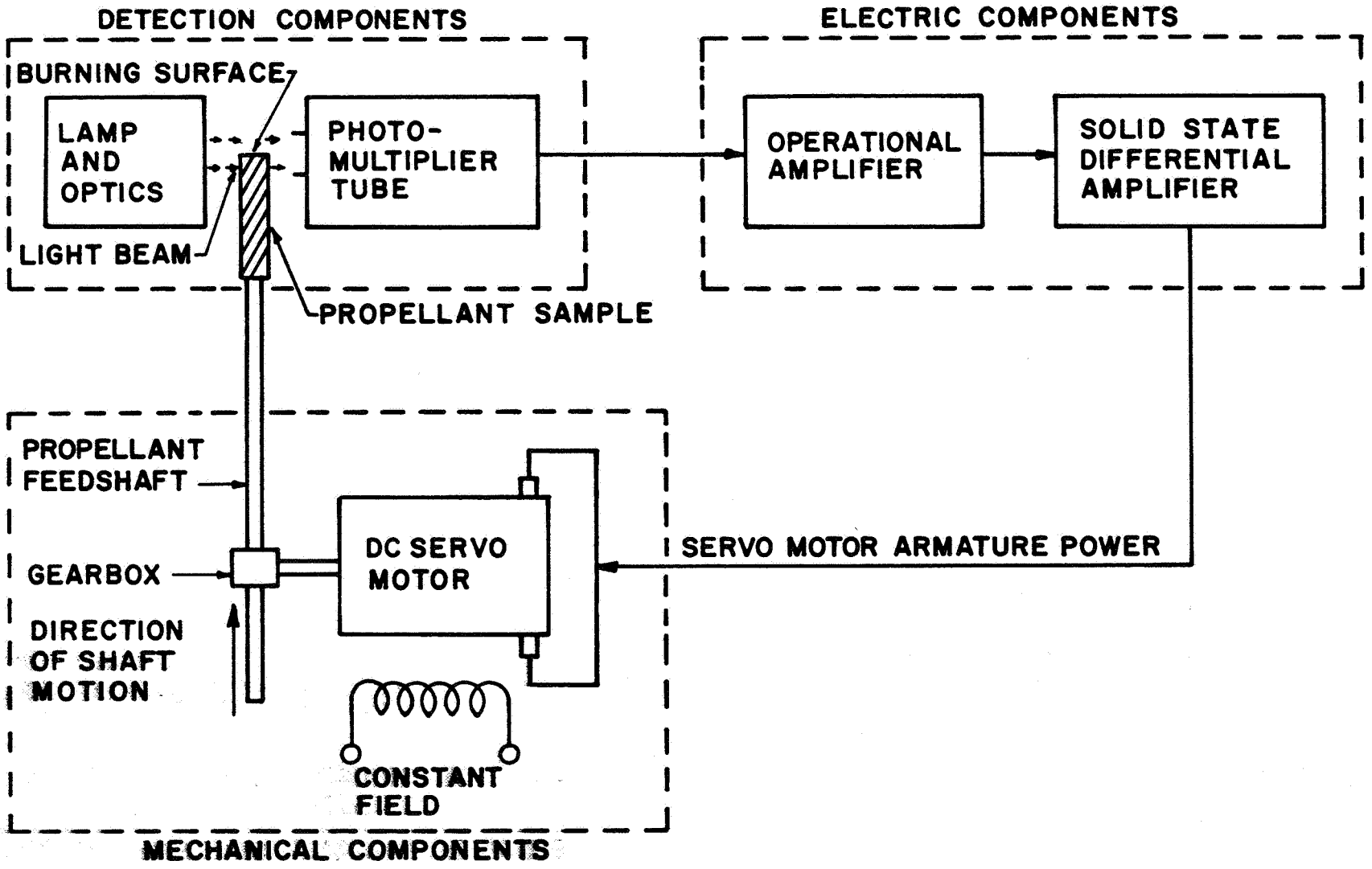

FIG. 5 SERVOMECHANISM COMPONENT DIAGRAM

direction (at a speed greater than the burning rate), the burning propellant surface sought a position of equilibrium dependent upon the gain of the operational amplifier. It should be noted, however, that if the operational amplifier gain was below a critical limit, established by the propellant burning rate, the system was inoperative; i.e., the maximum feedshaft velocity was less than the propellant burning rate.

The Surface Detection Components. As mentioned previously, the surface detection technique employed in the original servomechanism system of Osborn, Burick, and Panella (23) consisted of a collimated beam of gamma rays passing over the burning surface of the propellant which was detected by a scintillation probe. In this research program it was necessary to employ a visible light beam position detection system (hereafter referred to as VLBPDS) rather than a radioactive source. The VLBPDS had the advantage of lower cost and eliminated the hazards of the gamma ray system.

Figure 6 illustrates schematically the VLBPDS. In that system lenses L_1 and L_2 form an image of a glowing tungsten ribbon within the combustion bomb at the plane of the propellant strand. Lenses L_3 and L_4 serve to magnify this image on a razor blade slit, S_1, such that only a narrow portion of the lamp image is detected by the position photomultiplier tube (hereafter referred to as the PPM tube). The width of the slit, S_1, then dictated the width

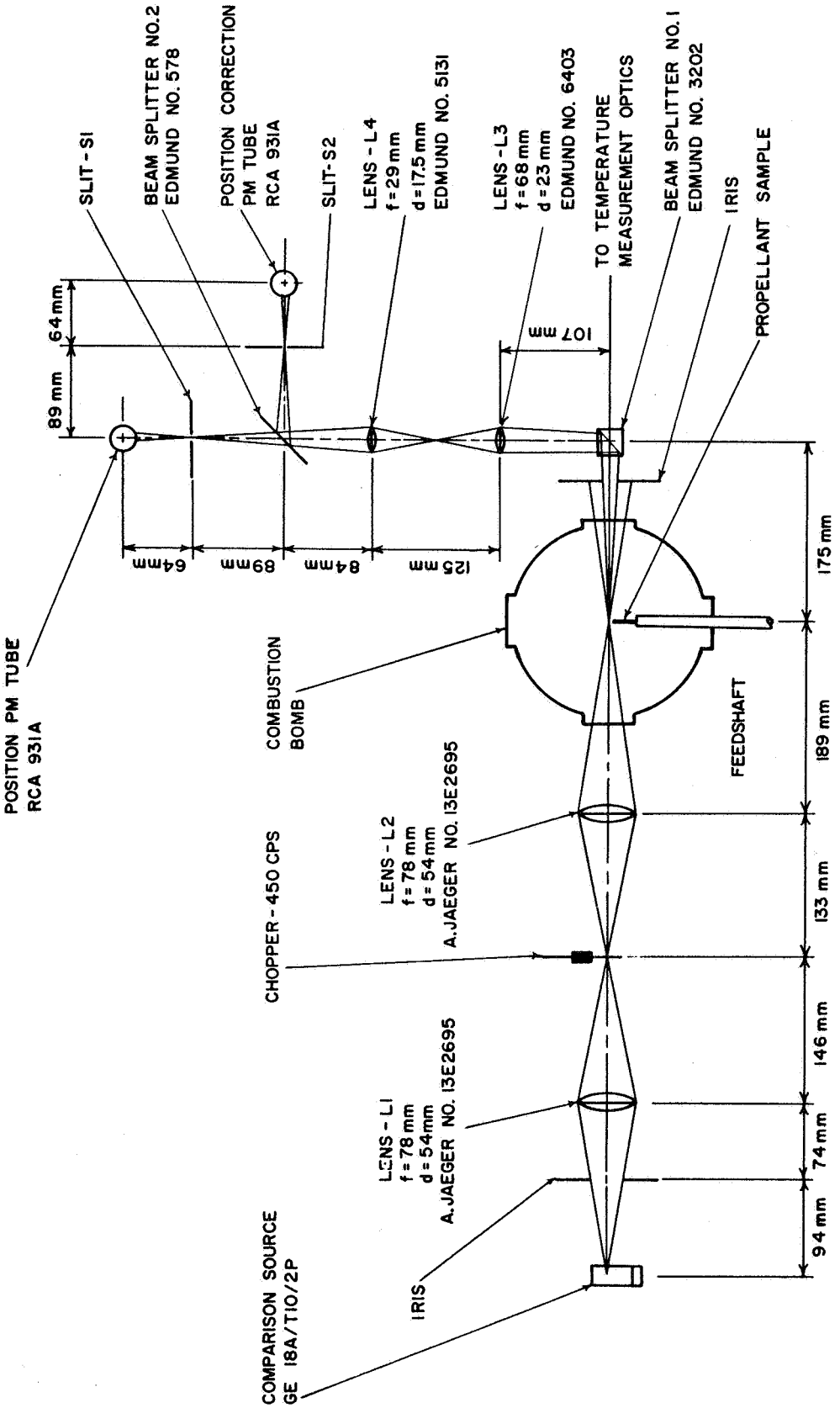

FIG. 6 OPTICAL SCHEMATIC OF VISIBLE LIGHT BEAM POSITION DETECTION SYSTEM (VLBPDS)

of propellant surface seen by the PPM tube; thus, the effect of burning surface tilt could be minimized by reducing the slit width. The width of slit S_1 and the combination of the previously mentioned lenses were such that the PPM tube viewed a rectangular region 50 microns in width and 1800 microns in height centered within the 2 mm by 8 mm lamp image.

Thus, the feedback characteristics of the VLBPDS can be seen readily. If the burning surface of the propellant strand is below the tungsten strip image, the PPM tube output is a maximum. If the burning surface is above the tungsten strip image such that the beam is blocked, the PPM tube output is zero. By proper design of the photomultiplier tube circuit (discussed below) and the slit size, the output of the PPM tube will be linear with position for intermediate positions of the burning surface.

To permit discrimination between the radiation from the tungsten strip lamp and the luminosity of the combustion zone, the light beam emanating from the lamp was chopped at a low audio frequency (450 cps) before passing over the burning surface. By passing the PPM tube output through a blocking capacitor and a full wave rectifier, the DC component due to the flame luminosity was eliminated and the AC output originating from the chopped lamp luminosity was converted to a DC signal.

A typical calibration curve for the VLBPDS is presented in Fig. 7. The plot depicts the rectified output of the PPM tube versus

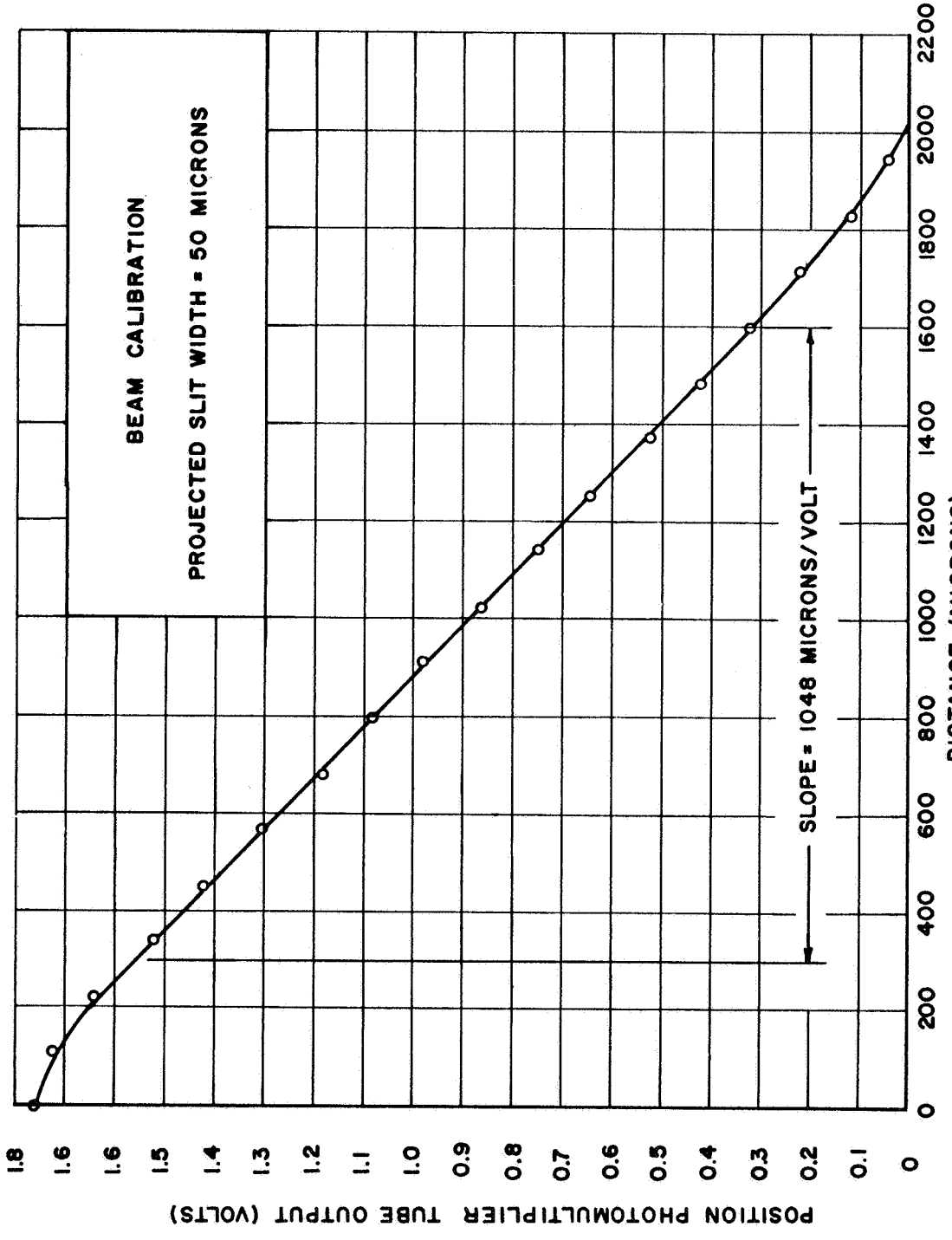

FIG.7 VLBPDS CALIBRATION CURVE

the distance traversed by a propellant sample at the lamp image formed within the combustion bomb. It can be seen that the curve is linear over the central portion of the curve; however, near the edges of the lamp, nonlinearities are observed. The cause of the nonlinearity is primarily a result of temperature gradients existing near the edge of the tungsten strip. However, since the operation of the system was confined to the central portions of the tungsten strip image, no adverse effects were derived from the nonlinearities. A detailed discussion of the calibration technique for the VLBPDS can be found in Appendix C.

The fact that the VLBPDS is dependent upon the fraction of visible light passing over the propellant surface introduces the possibility of an error in the PPM tube output due to smoke or haze attenuating the light beam. For this reason, a second photomultiplier tube, termed the position correction photomultiplier tube (hereafter referred to as the PCPM tube), was incorporated in the VLBPDS. The PCPM tube was located adjacent to the PPM tube shown in Fig. 6, and the output from the PCPM tube was passed through a separate photomultiplier tube circuit, blocking capacitor, fullwave rectifier, and smoothing capacitor. The PCPM tube viewed, by means of a beam splitter and slit, S_2, the same narrow portion of the lamp image viewed by the PPM tube. However, the slit, S_2, was further restricted, over the slit S_1, to allow only the upper portion of the narrow image to enter the PCPM tube. That is, the PCPM tube viewed a region of the lamp image which was not interrupted by the surface when the

system was operating satisfactorily. Therefore, the only source of light attenuation observed by the PCPM tube was that due to window clouding and excessive reflection and scattering in the flame zone.

By recording the PCPM tube output before igniting the propellant strand and monitoring its output during the burning of the strand, it was possible to determine at what time attenuation occurred due to the previously mentioned effects. Thus, a means of knowing when the VLBPDS was unreliable was available during a given propellant sample burning.

The Electrical Components. The electronics for the servomechanism system is presented in a block diagram in Fig. 8 and consisted of the following components:

1. the photomultiplier tube circuit,
2. the operational amplifier, and
3. the differential amplifier.

The photomultiplier tube circuits and operation amplifiers for the PPM and PCPM tubes are illustrated schematically in Fig. 9. The photomultiplier tubes employed were both RCA Model 931A tubes and the voltage divider circuits were designed to allow voltage divider currents of 3 ma. The load resistance seen by each of the photomultiplier tubes was adjusted for maximum linearity by means of separate 1 meg ohm potentiometers linked by blocking capacitors to the primary windings of an interstage transformer. The function of the transformer in both cases was to isolate the photomultiplier tube

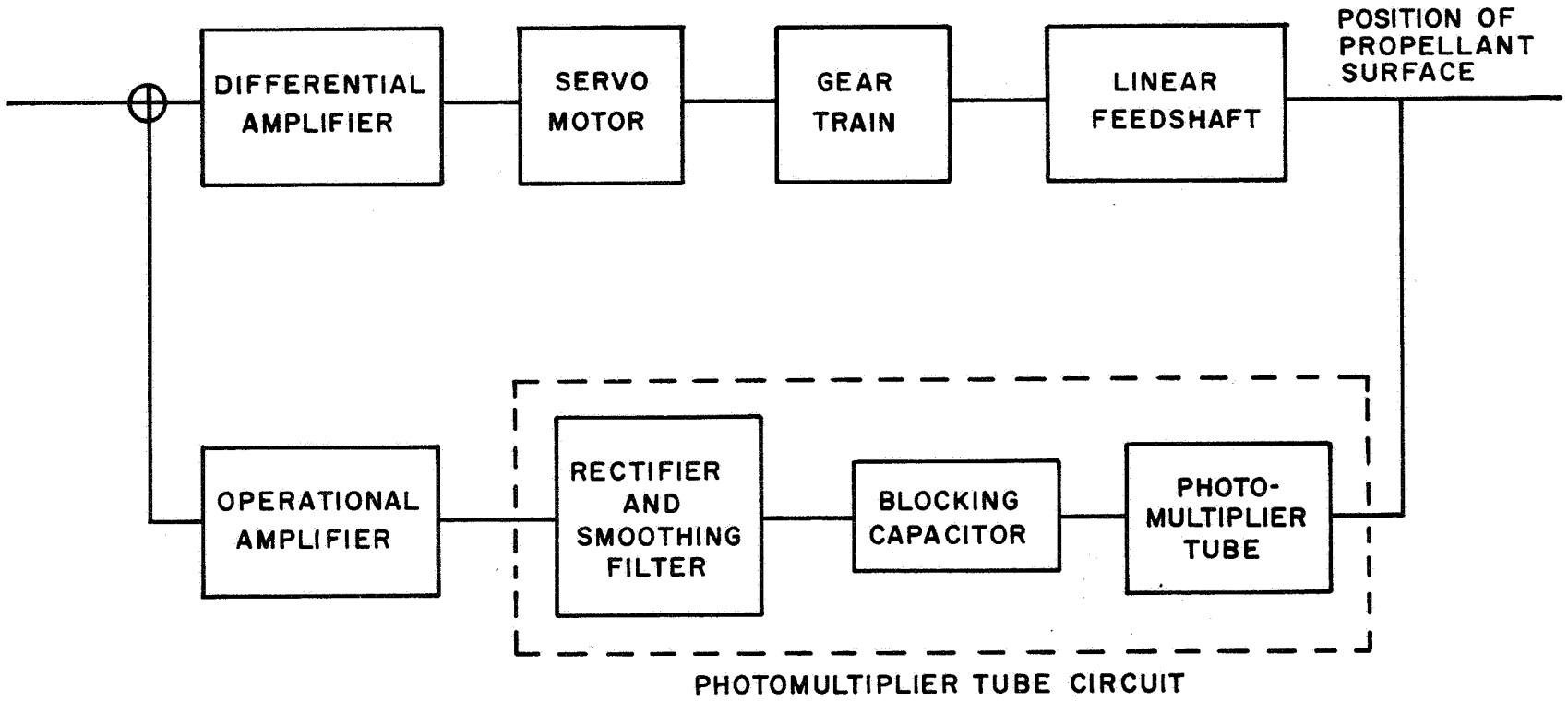

FIG. 8 BLOCK DIAGRAM OF ELECTRICAL COMPONENTS

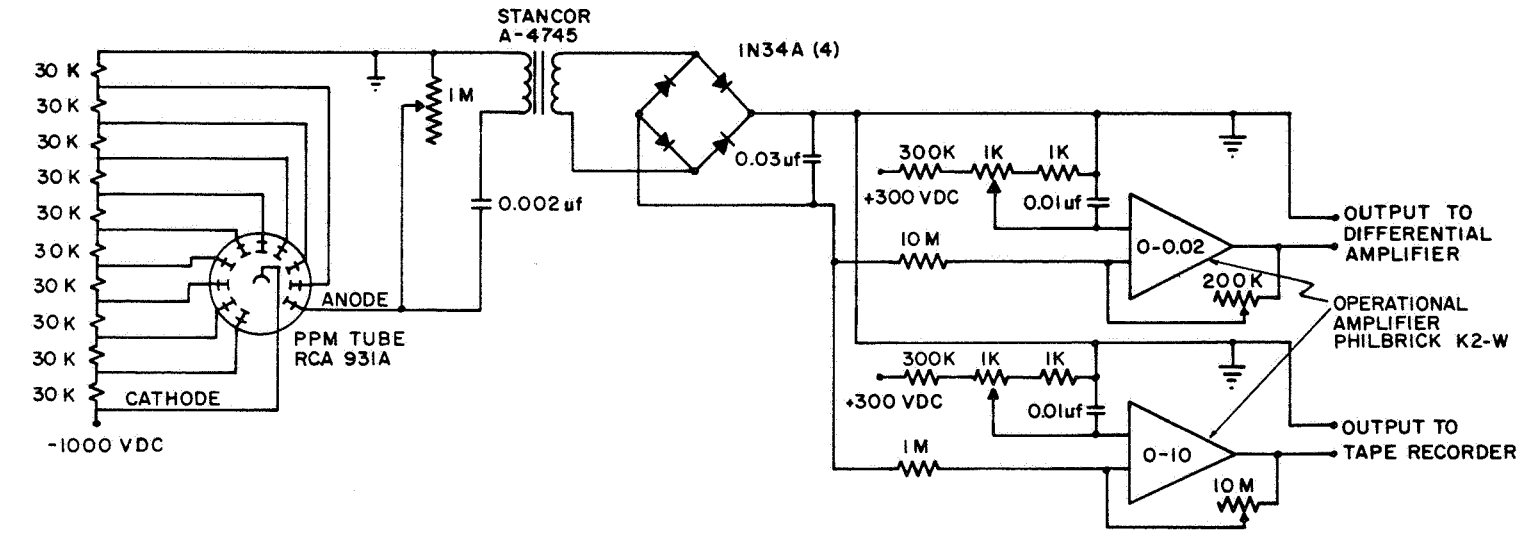

A. POSITION PHOTOMULTIPLIER TUBE ELECTRICAL SCHEMATIC

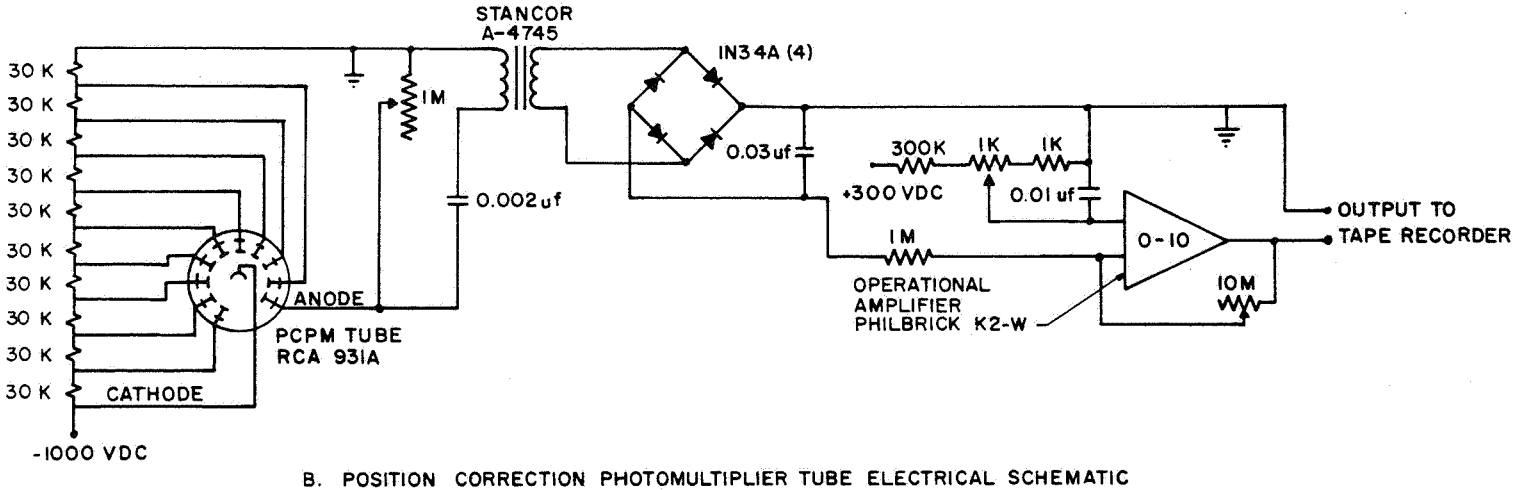

B. POSITION CORRECTION PHOTOMULTIPLIER TUBE ELECTRICAL SCHEMATIC

FIG. 9 DETECTION PHOTOMULTIPLIER TUBES - ELECTRICAL SCHEMATIC

from the respective rectifier bridges allowing full wave rectification of the AC voltage developed across the load resistors.

The operational amplifiers served two purposes. First, the gain of the photomultiplier tube circuit outputs could be varied by the operational amplifiers over a wide range. Second, the operational amplifiers served as a high impedance coupling between the photomultiplier tube circuits and other associated electronics. In the case of the PPM tube circuit, two operational amplifiers were employed such that the rectified output of the PPM tube could be inputed to the differential amplifier and one channel of an Ampex Tape Recorder. The PCPM tube circuit output was linked to a single operational amplifier and the output of this amplifier was inputed to a second channel of the tape recorder.

The differential amplifier (designed and built by the Department of Electrical Engineering, Purdue University) is illustrated schematically in Figs. 10 and 11. The differential amplifier derived power for the DC servomotor armature by combining two full wave rectifier bridges in parallel as shown in Fig. 10. Control of the power was accomplished by employing silicon control rectifiers (hereafter referred to as SCR) in the bridges. The SCR's were triggered in such a manner that the integrated voltage output to the motor armature was linear with respect to the signal received from the PPM tube operational amplifier.

The trigger circuit for the SCR's is presented in Fig. 11 and consists of a differential amplifier (dual-transistor 2N264) which

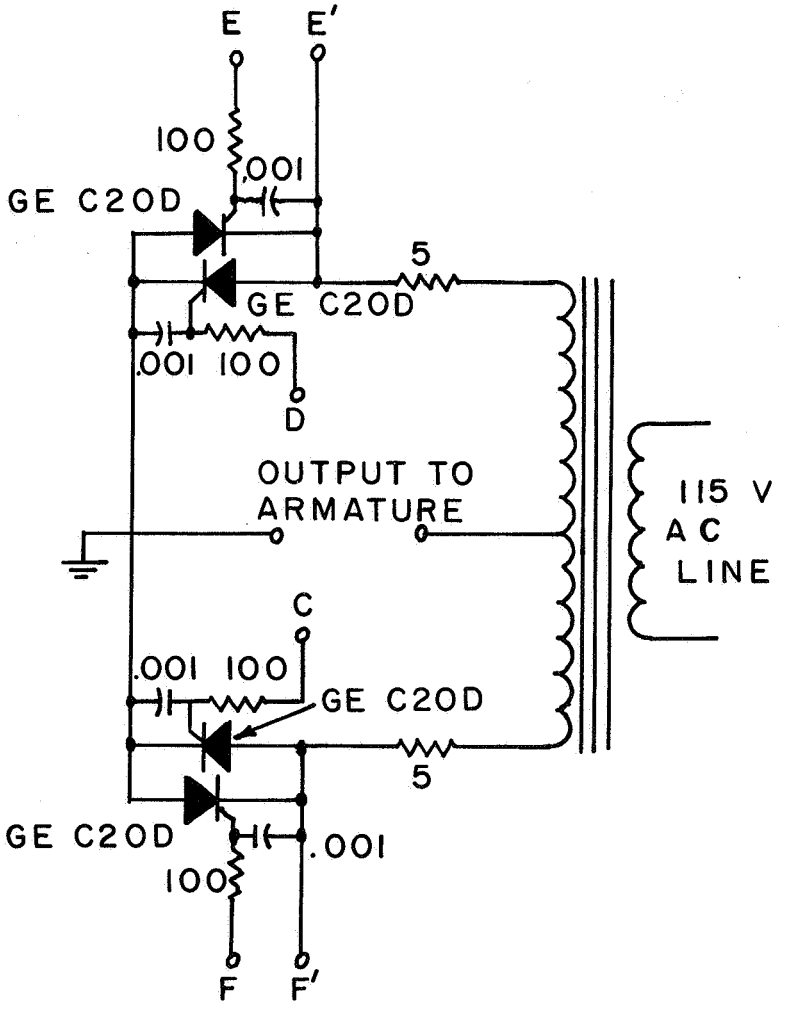

FIG. 10 BASIC SCR BRIDGE CIRCUIT

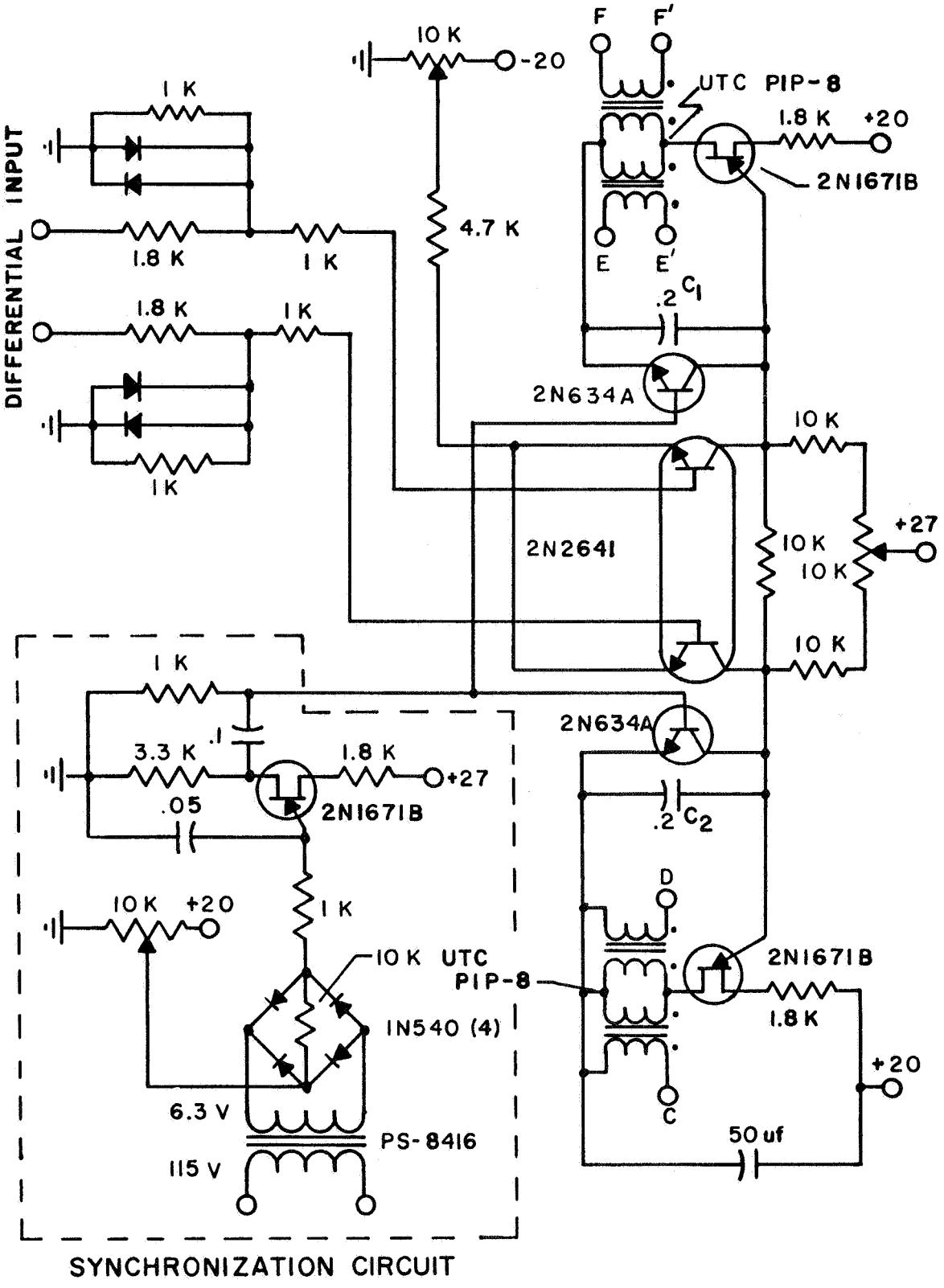

FIG. 11 SCR AMPLIFIER TRIGGER CIRCUIT

controls the charging rate of the two capacitors C_1 and C_2. When a signal is received from the PPM tube operational amplifier, at the differential input, the trigger circuit fires the SCR's in the SCR circuit and power is delivered to the armature.

The Mechanical Components. The mechanical components of the servomechanism system consisted basically of the DC servomotor, a gear reduction box, and the propellant feedshaft. The purpose of the mechanical components was to convert the angular rotation of the servomotor into translational motion of the propellant feedshaft such that the DC servomotor developed sufficient torque to drive the propellant feedshaft into the pressurized combustion bomb.

A photograph of the mechanical components is presented in Fig. 12. The angular rotation of the servomotor was transmitted to a worm gear located in the gear reduction box. The worm gear drove an internally threaded gear which in turn drove the threaded propellant feedshaft. A bar mounted on the feedshaft perpendicular to the feedshaft axis prohibited the feedshaft from revolving when a torque was applied to the internally threaded gear. The gear reduction box and threaded propellant feedshaft were of the same design as employed by Osborn and Burick (24).

Burning rates of propellant samples were measured from the output of a tachometer which was incorporated in the servomotor. The tachometer was calibrated such that the speed of the propellant

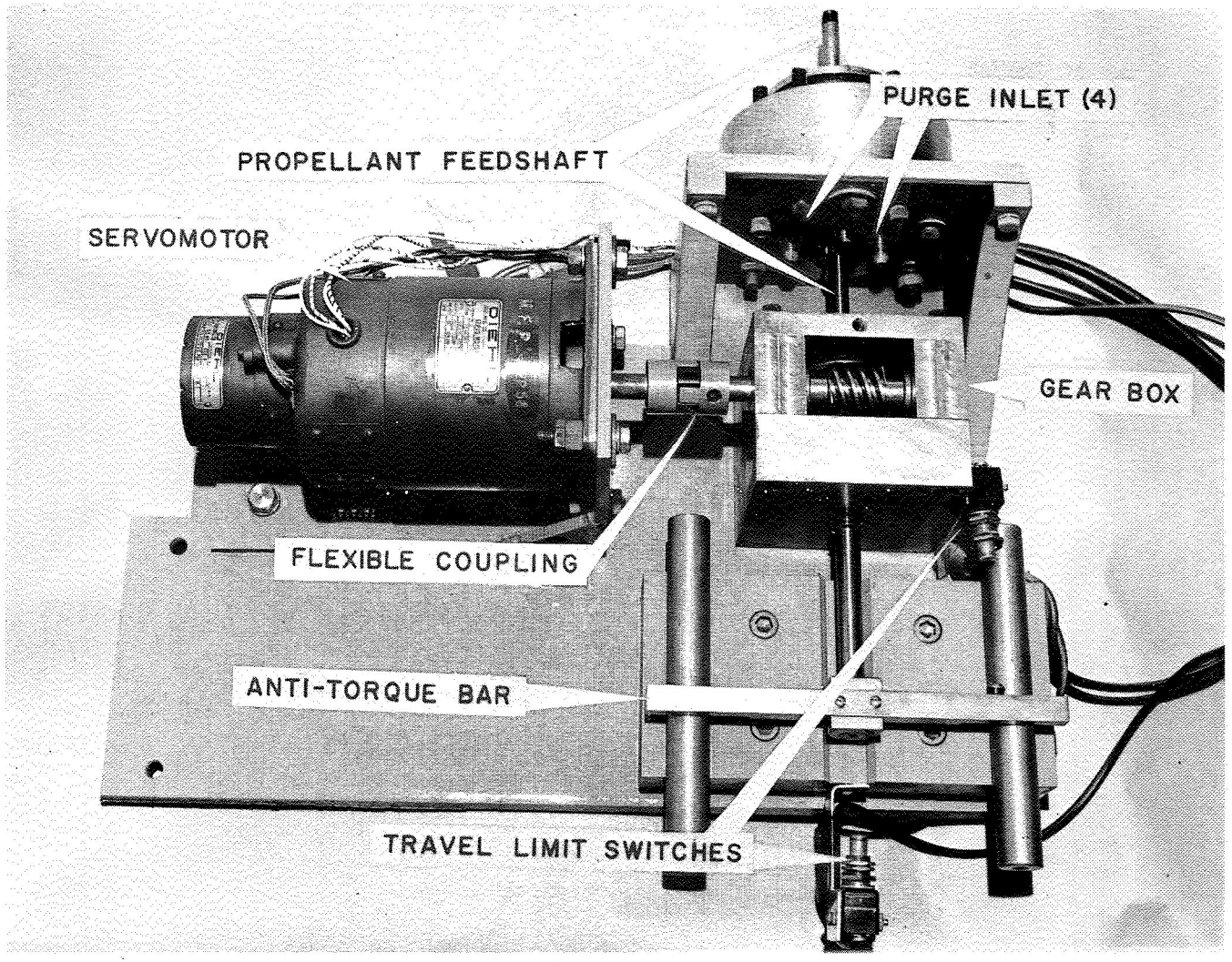

FIG. 12 SERVOMECHANISM MECHANICAL COMPONENTS

feedshaft was known as a function of the tachometer output. The calibration curve for the servomotor tachometer employed in the mechanical components is presented in Fig. 13. Since the propellant feedshaft was driven into a pressurized combustion bomb and the motor always revolved in the same direction when a propellant strand burned, backlash was not present in the gear train.

The Modified Line Reversal Pyrometer

The theory of the line reversal technique of measuring gas temperature is based on a straightforward application of Planck's law of radiation and Kirchhoff's law of radiation. The technique employs a calibrated radiation source, or a comparison source, whose spectral radiance is compared to the spectral radiance and absorptance of the gas whose temperature is to be measured. The wavelength range over which the comparison is made is restricted to a wavelength band corresponding to the resonance lines of an alkali metal which is seeded in the gas. The basis for the temperature measurement lies in the reversal condition which results when the spectral radiance of the comparison source is matched to the spectral radiance and absorptance of the gas such that the source cannot be differentiated from the flame when viewed through the flame over the above mentioned wavelength band. When this condition prevails, the temperature of the gas is equal to the brightness temperature of the source.

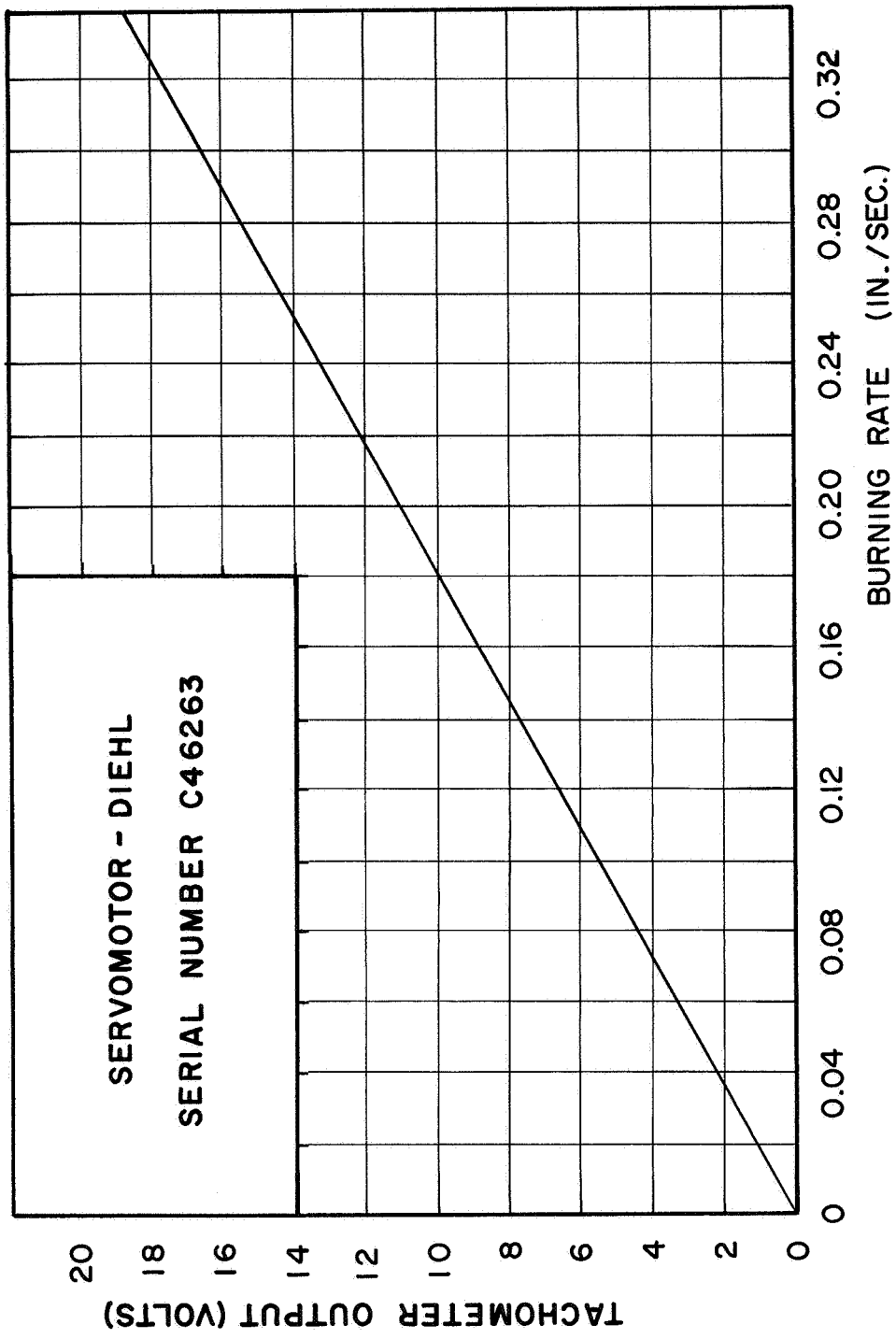

FIG. 13 TACHOMETER CALIBRATION CURVE

The line reversal technique of measuring temperature in gases was first developed around 1900. Kurlbaum (25) and Fery (26) are commonly referred to as being the originators of the technique; however, the basic principles for the technique date back many years before their work. In the many attempts at employing the technique since Kurlbaum and Fery's work, various modifications have been introduced. Probably the most significant improvement in the technique is the elimination of the eye as the radiation detector and the introduction of a modulated photoelectric device for rapid quantitative measurement of radiation levels. It was that method, termed the modified line reversal technique, which was employed in this research program.

A schematic of the optical system is presented in Fig. 14 which consists of the optics for examining the flame radiance, the monochromator for dispersing the radiation from the flame and the comparison source, and a sensitive photomultiplier tube (RCA-1P21) to detect the radiation levels. The comparison source optics are shown in Fig. 6. It should be noted that the lamp employed in the servomechanism VLBPDS is the same lamp utilized in the line reversal pyrometer. As described previously, the lenses L_1 and L_2 form an image of the tungsten strip lamp within the combustion bomb at the plane of the propellant strand.

Referring to Fig. 14, it can be seen that a beam splitter passed a fraction of the light leaving the bomb (approximately 30 percent) to the objective lens system of an American Optical Company

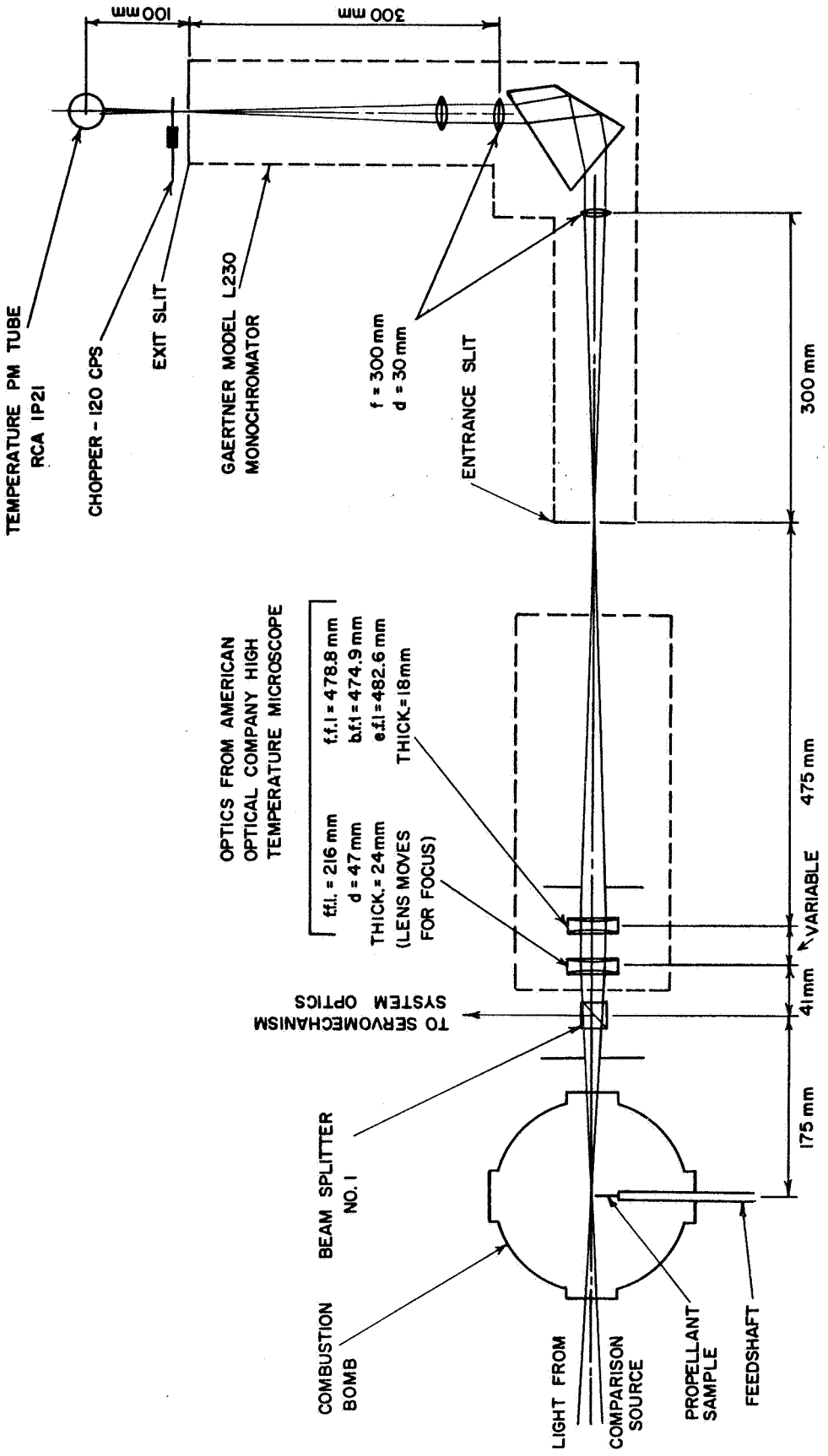

FIG. 14 OPTICAL SCHEMATIC OF LINE REVERSAL PYROMETER

High Temperature Microscope. It was the purpose of these optics to image the flame and tungsten strip lamp on the entrance slit of a Gaertner Model L230 monochromator. The size of the monochromator entrance slit dictated the size of the temperature measurement region and was constructed from the standard slit jaws (in the vertical dimension) and a pair of razor blades (in the horizontal dimension.) The monochromator served to disperse the light and allow only the band of wavelength chosen for the experiment to pass out of the exit slit. A 120 cps chopper was located between the exit slit and the temperature photomultiplier tube (hereafter referred to as TPM tube).

The output of the TPM tube was passed through a 5 megohm potentiometer as shown in the electrical schematic presented in Fig. 15. This potentiometer was adjusted for maximum voltage output for the low light levels detected by the photomultiplier tube. The anode current-to-voltage-divider current ratio of 0.10 was not exceeded as recommended by the photomultiplier tube manufacturer (27). The voltage output formed across the potentiometer was then amplified by an operational amplifier which was capable of amplifying feeble voltages up to 100 times. The resulting amplified output was then recorded on a third channel of the Ampex Tape recorder.

The equation defining the temperature of the gas in terms of the TPM tube output is derived in Appendix B and is

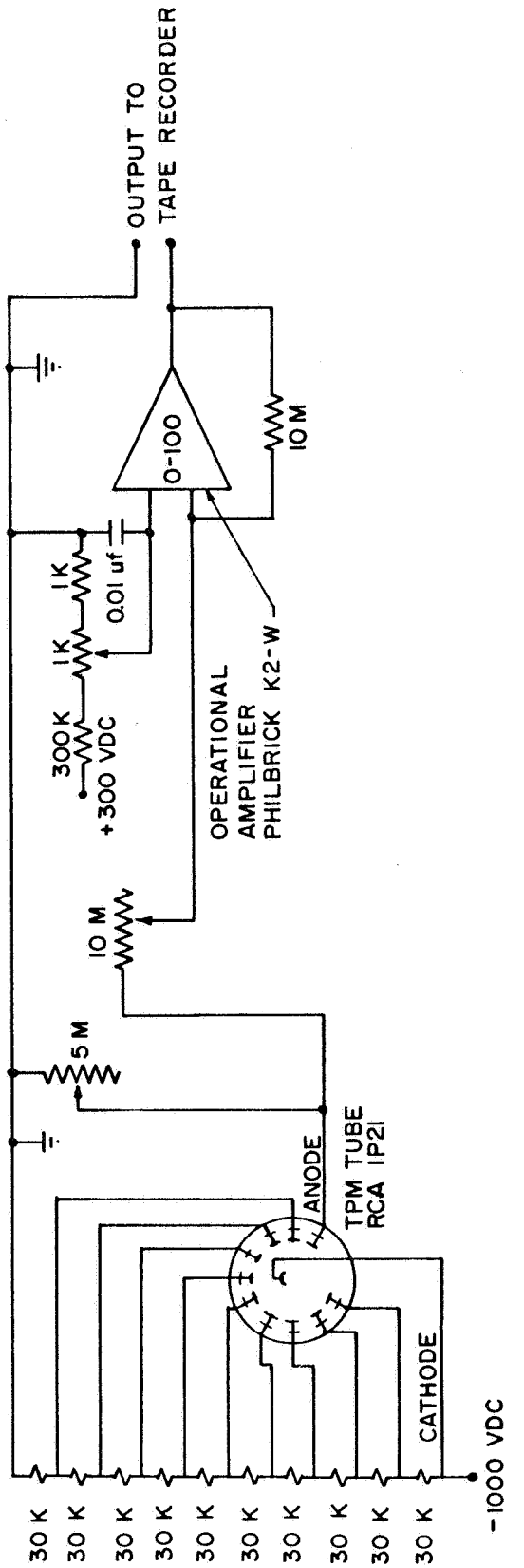

FIG. 15 TEMPERATURE PHOTOMULTIPLIER TUBE - ELECTRICAL SCHEMATIC

$$T_F = \frac{\lambda}{C_2} \ln\left\{\frac{I_L - I_{L-F}}{I_F}\left[\exp(C_2/\lambda T_L)-1\right]+1\right\}$$

where

I_F = the output of the TMP tube due to the spectral radiance of the flame alone at the wavelength λ.

I_{L-F} = the output of the TPM tube due to the spectral radiance of the comparison source passing through the flame at the wavelength λ.

I_L = the output of the TPM tube due to the spectral radiance of the comparison source alone at the wavelength λ.

λ = wavelength at which experiment is performed.

T_L = brightness temperature of comparison source at the position of the flame.

The TPM tube output I_L was obtained by recording the output of the TPM tube before the strand of propellant was ignited as shown in the idealized TPM tube output of Fig. 16. Following the placement of the propellant strand and the subsequent ignition of the strand, the choppers CH_1 and CH_2 served to modulate the light and allow the detection of the light levels I_F and I_{L-F}.

In the experiments, the sodium D line band was used for the temperature measurement. To determine the flame temperature rapidly once the ratio $\frac{I_L - I_{L-F}}{I_F}$ was known, a plot of that ratio versus the flame temperature was constructed for a range of comparison source brightness temperatures. This plot is shown in Fig. 17. The brightness temperature of the comparison source at the position of the flame measurement with a disappearing filament pyrometer (Leeds and Northrup Pyrometer Model 360). A detailed description of the calibration procedure is given in Appendix C.

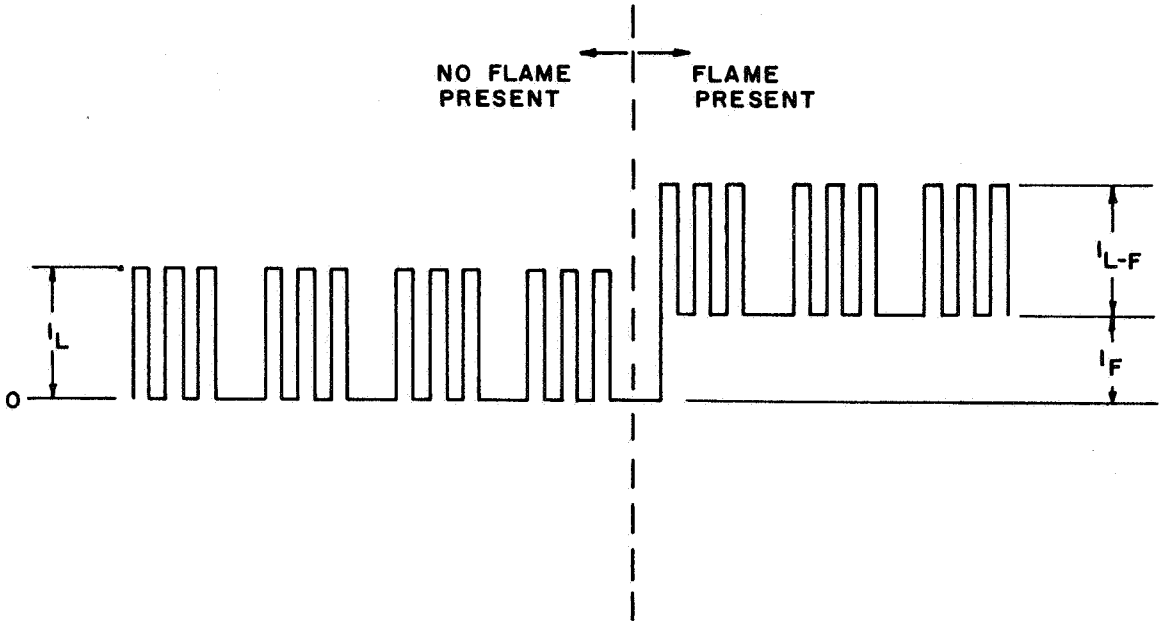

FIG. 16 IDEALIZED TEMPERATURE PHOTOMULTIPLIER TUBE OUTPUT

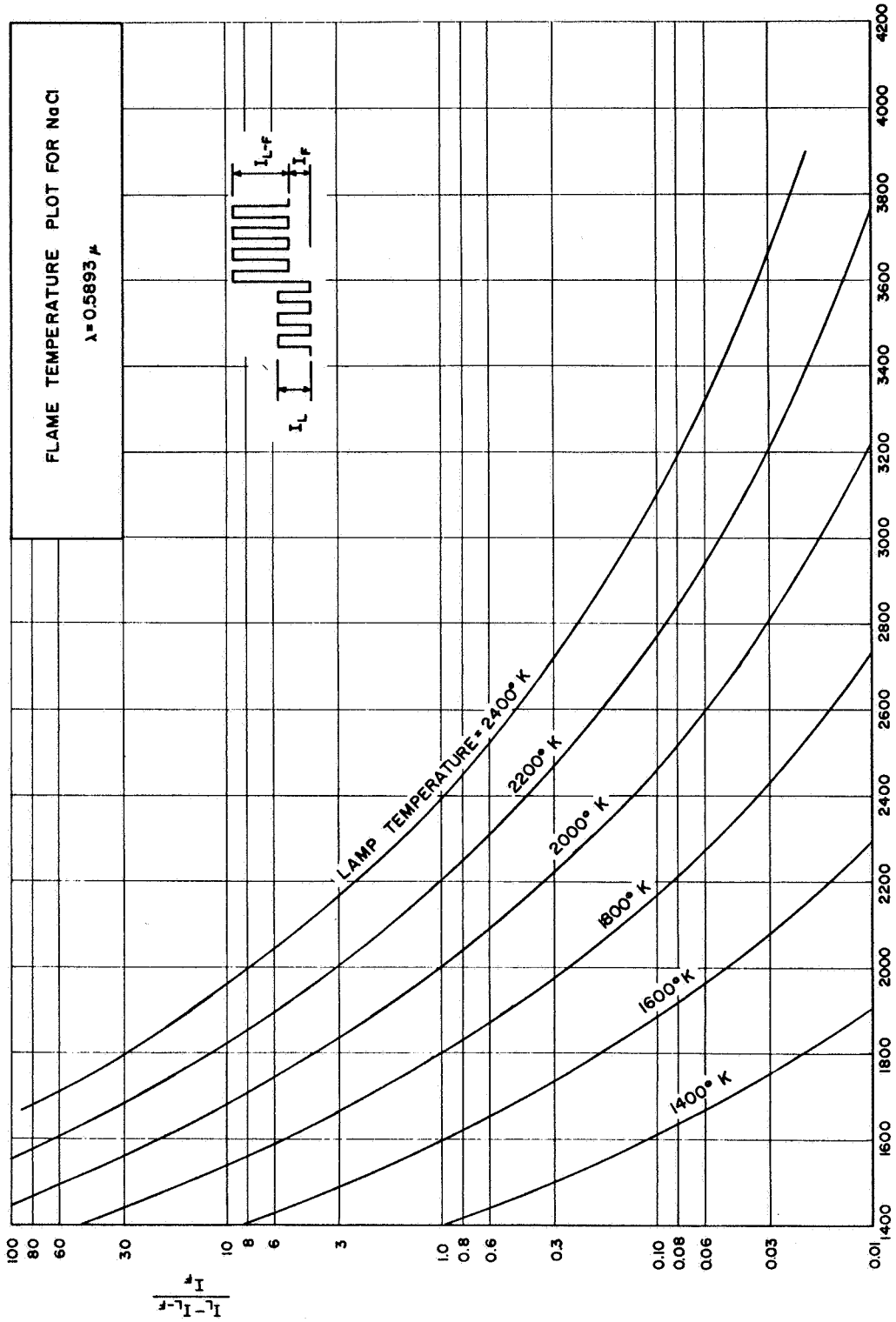

FIG. 17 FLAME TEMPERATURE FOR A FLAME SALTED WITH SODIUM CHLORIDE

The Combined System

The combined servomechanism and temperature measurement apparatus is shown in the photograph presented in Fig. 18. As mentioned previously, the comparison source was a tungsten strip lamp which served as the lamp in the servomechanism VLBPDS and the comparison source in the line reversal pyrometer. The following discussion deals with the various procedures employed in the operation of the system to measure temperature profiles.

Operation of the Temperature Measuring System. When burning a strand of propellant, four types of data were recorded on the Ampex tape recorder; viz.,

1. The output of the position photomultiplier tube (PPM tube),
2. The output of the position correction photomultiplier tube (PCPM tube),
3. The output of the temperature photomultiplier tube (TPM tube), and
4. The output of the servomotor tachometer.

A typical output of these data as a function of time for a strand of propellant burning at 100 psig is shown in Fig. 19 as a function of time.

At time t = 0, the strand of propellant blocked the beam of light originating from the comparison source; thus, the servomotor was not operating and the tachometer output was zero. In addition, since no light was allowed to pass to the photomultiplier

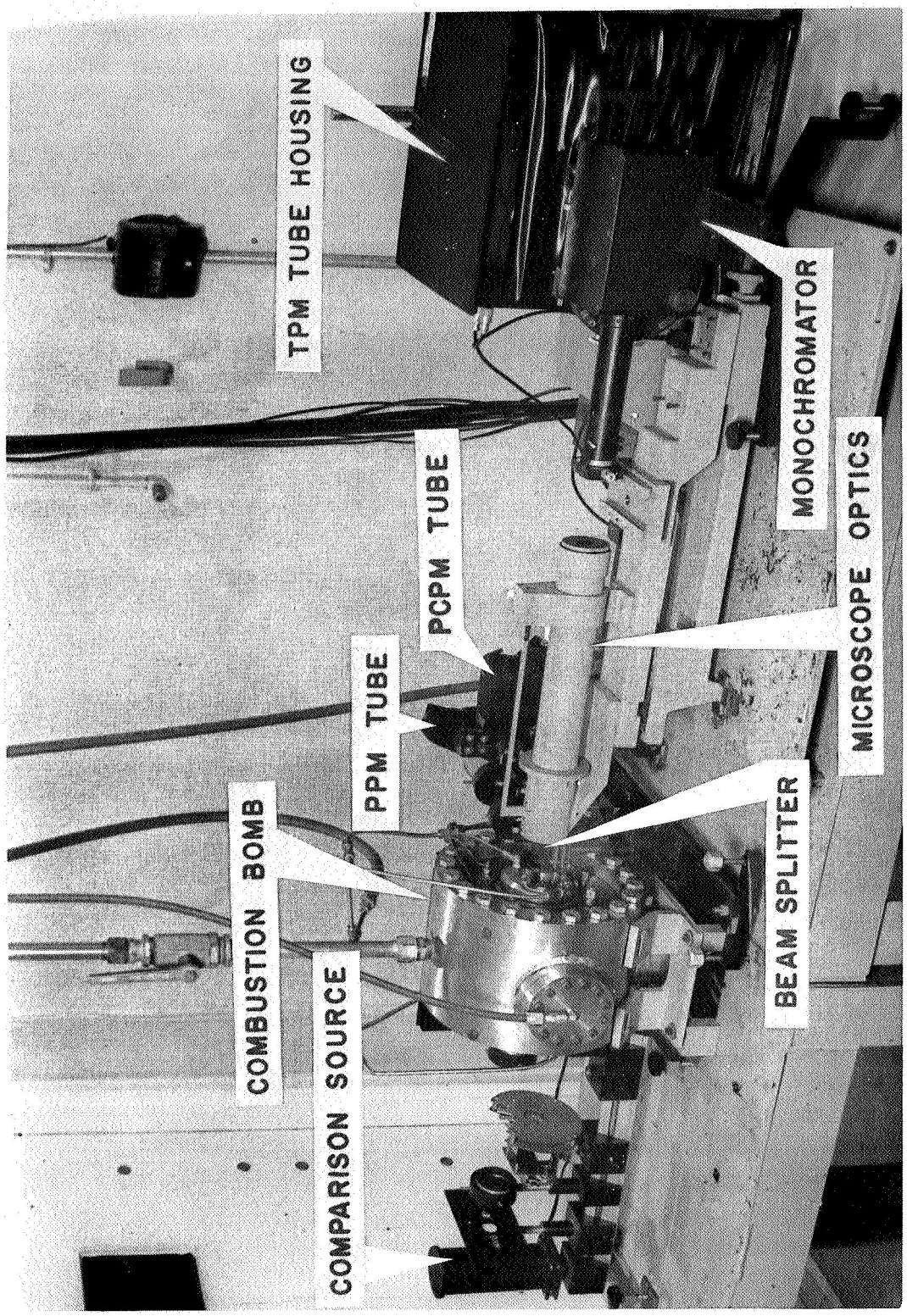

FIG. 18 TEMPERATURE MEASUREMENT SYSTEM

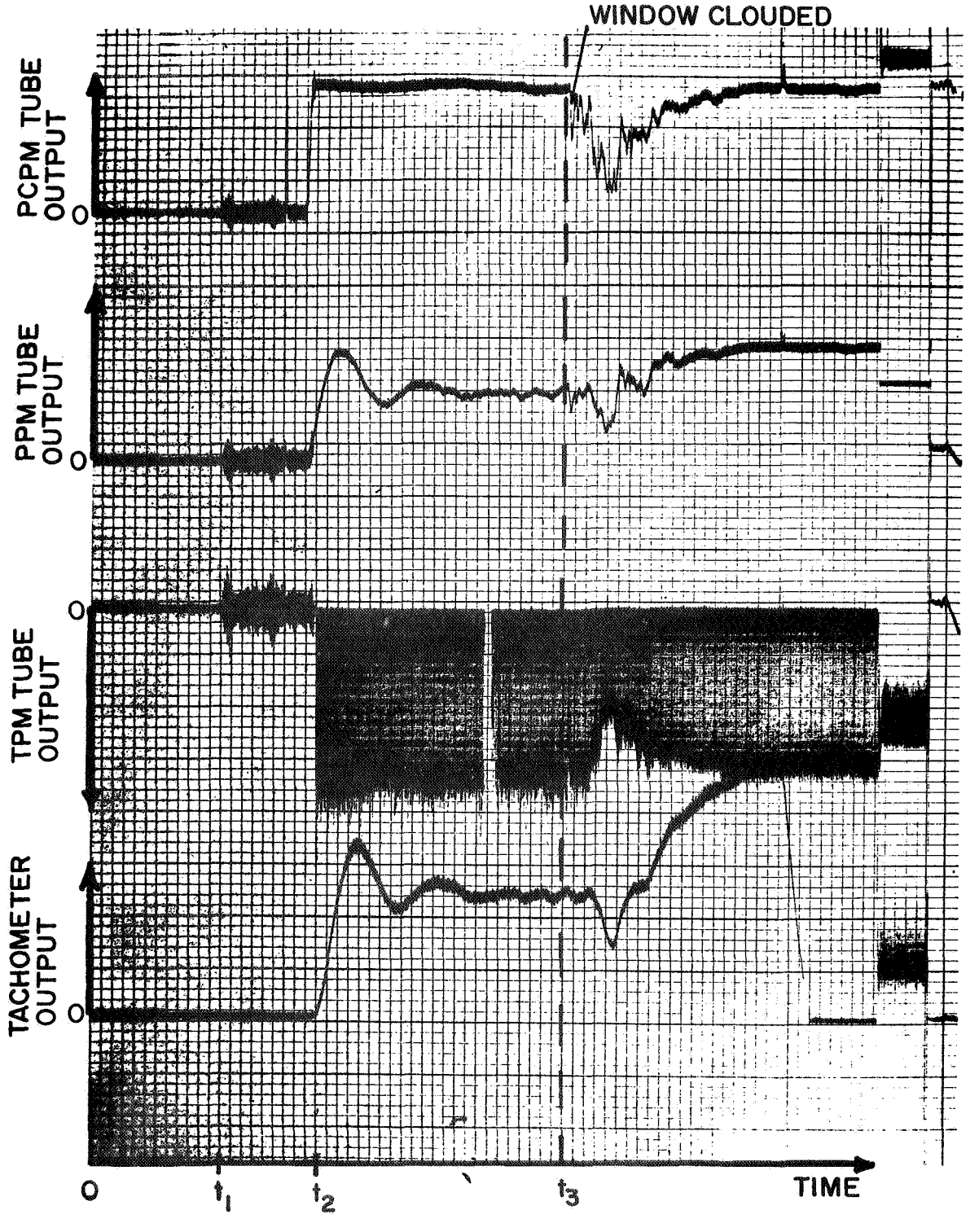

FIG. 19 TEMPERATURE MEASUREMENT SYSTEM DATA OUTPUT

tubes, the outputs of the PPM tube, the PCPM tube, and the TPM tube were zero.

At time $t = t_1$, the strand was ignited and the strand surface burned in a direction parallel to the axis of the propellant feedshaft. At time $t = t_2$, the burning surface reached the upper edge of the comparison source image located at the plane of the propellant sample. As the surface continued to burn, light was detected by the photomultiplier tubes and the servomotor started to drive the strand in a direction opposite to that of the burning and at a speed directly proportional to the PPM tube output. After a short period of time, the servomechanism system stabilized and the PPM tube showed that the propellant feedshaft was driving the propellant strand upward at the same rate at which it was burning downward.

The output of the PCPM tube is observed to attain a maximum value immediately after the surface passes the upper portion of the comparison source image. As explained previously, this indication shows that no attenuation of the light has occurred due to soot on the windows or excessive scattering of the comparison source beam by the flame. At time $t = t_3$, the output of the PCPM tube shows a sharp deviation from its maximum value. From this indication, the remainder of the run is deemed inaccurate as a result of the reasons mentioned previously.

Determination of the Temperature Region Size. The size of the temperature region was dictated by the projected image of the monochromator entrance slit in the flame. Since the direct measurement of the size of the slit was difficult and the calculation of the projected slit in the flame inaccurate, a calibration technique was devised which allowed the direct recording of the size of the temperature measurement region. The procedure was first to locate the unburned propellant surface below the comparison source beam such that the photomultiplier tubes detected the full beam of light from the comparison source. Second, the strand was driven upward and the outputs of the photomultiplier tubes were recorded. A typical output of this type is shown in Fig. 20. At time t = 0, the propellant surface is located below the comparison source image and at time t = t_1, the strand has been driven upward such that the light entering the TPM tube has been blocked. By measuring the output of the PPM tube from the point where the surface first begins to block the light detected by the TPM tube to the point where all light detected by the TPM tube is blocked, a voltage change for the PPM tube is known which can be converted to a distance change by referring to the VLBPDS calibration curve shown in Fig. 7. Thus, in the sample shown, the voltage change is 2.5 volts and the temperature measurement region is 50 microns in height above the surface.

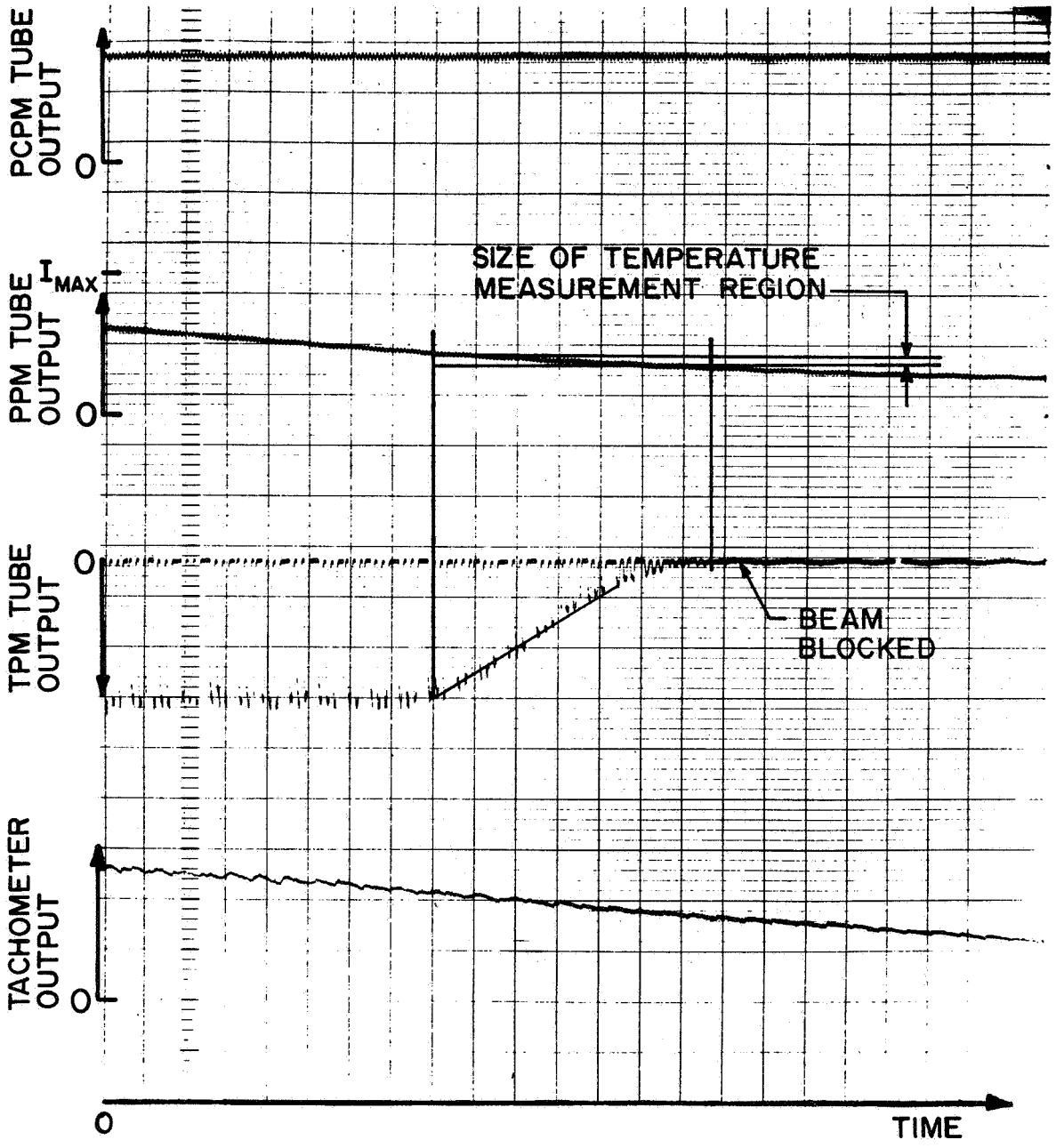

FIG. 20 SIZE OF THE TEMPERATURE MEASUREMENT REGION

Determination of the Distance from the Burning Surface to the Temperature Measurement Region. In order to obtain a temperature profile above the burning surface of a strand of propellant, it was necessary to measure the distance from the burning surface to the region of temperature measurement for each temperature measurement. This distance measurement was obtained from the output of the PPM tube as illustrated in Fig. 21. At time t = 0 the burning surface of the propellant sample was located above the temperature measurement region; as a result, the TPM tube output was zero. The movement of the surface at time t = 0 is indicated by the increasing output of the PPM tube. At time t = t_1, the surface was located at the upper edge of the temperature measurement region. As the propellant continued to burn, the TPM tube output increased until the region was no longer blocked. The time at which that occurred is determined from the change in the PPM tube output which corresponds to the size of the temperature measurement region (see Fig. 20). For the example, this time occurred at time t = t_2. At times greater than t_2, the output of the PPM tube is utilized to calculate the distance from the center of the temperature measurement region to the burning surface. This is accomplished in terms of the voltage change as indicated at time t = t_3 in Fig. 21. Once the voltage change is known, the slope of the PPM calibration curve, Fig. 7, gives the actual distance of interest. It should be mentioned that this procedure is only valid when the PCPM tube is a maximum because the PPM calibration curve is not valid when the comparison source beam is attenuated by anything other than the propellant surface.

The operation of the temperature measurement system is thus established. Detailed design criteria for the line reversal pyrometer is given in Appendix B.

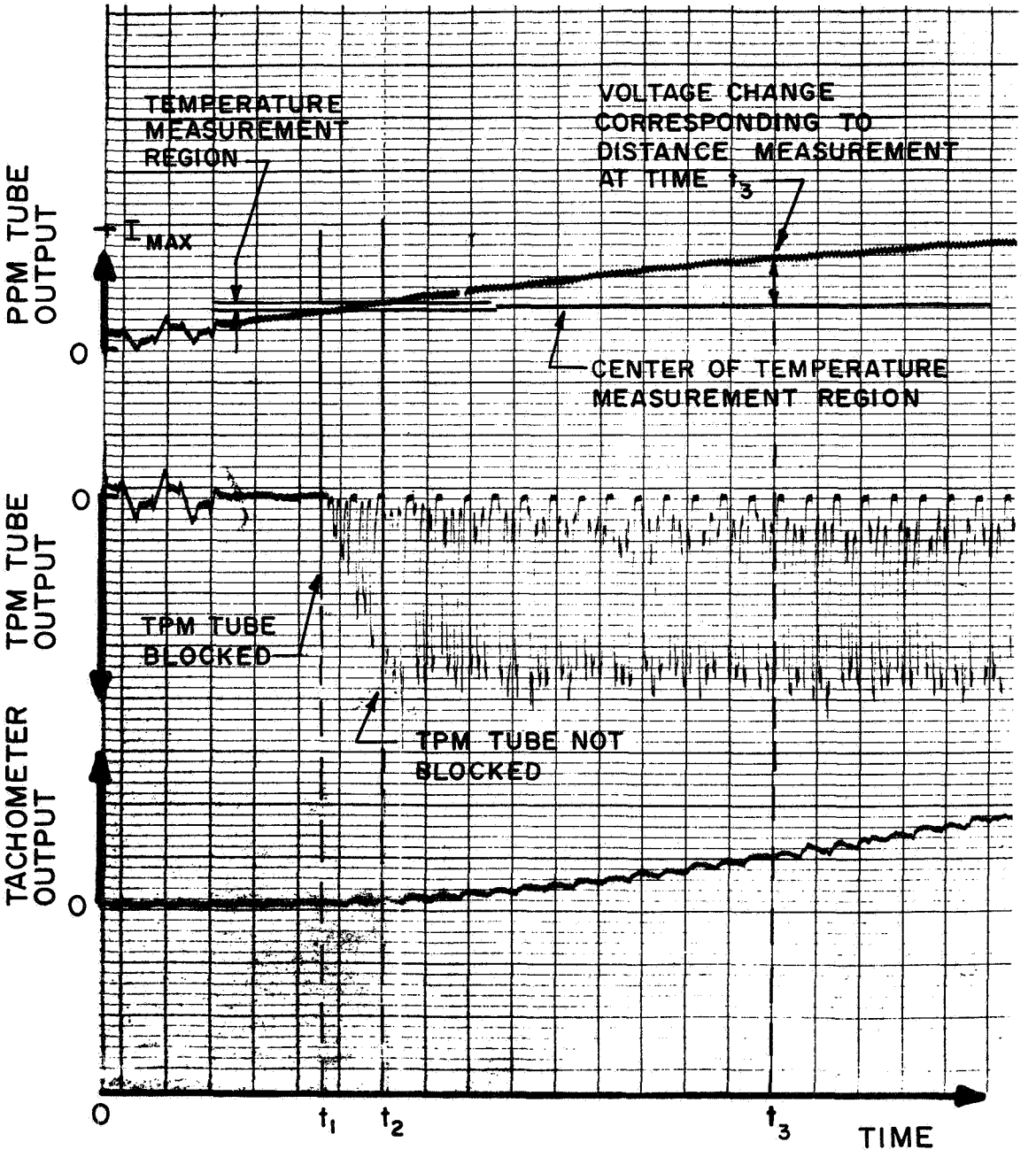

FIG. 21 MEASURING DISTANCE FROM THE PPM TUBE OUTPUT

EXPERIMENTAL RESULTS

The experiments conducted in this research program can be separated into two phases. First, a film study was conducted in which burning samples of a composite solid propellant were photographed as the servomechanism system positioned the burning surface of the propellant sample. Second, the temperature of the gases above the burning surface of a composite solid propellant was measured as a function of the distance from the burning surface to the temperature measurement region. The temperature measurement system was employed for these measurements.

Before the results are described, the type of propellant used in the experiment will be discussed. Following this, the experiments will be discussed in terms of their objectives and results.

The Solid Propellant Used in the Experiments

The solid propellant used in the experimental program was a polysulfide-ammonium perchlorate propellant. The formulation of the propellant was taken from Reference 28 and is given in Table 1. The reason for using this propellant type was that it has been a well characterized propellant in terms of flame temperature, burning rate, and physical properties due to its extensive use in solid

TABLE I.

Propellant Composition

(Concentrations given as percent weight)

LP-3 (Thiokol)	32.6
p-Quinone Dioxime	2.2
Sulfur (Flowers)	0.2
Ammonium Perchlorate	65.0

propellant rocket engines. In addition, the combustion characteristics of the propellant are such that the propellant burns well over a wide range of pressure with fine oxidizer grinds of unimodal distribution.

The propellants used in the experiments were supplied by the Thiokol Chemical Corporation, Huntsville, Alabama, and consisted of two different unimodal oxidizer grinds. The mean diameter of the coarse grind oxidizer was 50 microns (the diameter where 50 percent of the oxidizer is greater than that diameter) whereas the mean diameter of the fine grind oxidizer was 6 microns as measured on a micromerograph. The propellant samples were received in pint cartons and were cut into wafers of 500 and 1000 microns with a laboratory microtome (American Optical Company, Model 900) for the film study and temperature measurement.

As mentioned previously, the sodium D line band was employed for the line reversal temperature measurement; thus, it was necessary to introduce a small fraction of NaCl to the propellant formulation. In introducing the NaCl, it was recognized that the sodium must mix uniformly throughout the propellant before curing and must vaporize quickly at the burning surface of the propellant; thus, the NaCl was ground as finely as possible. A micronizer (Helme Products Inc., Laboratory Model) was employed to grind the NaCl. The resulting powder was examined under a microscope and found to be of diameters less than ten microns. The quantity of salt added was 0.5 percent by weight, this being the optimum amount of salt in terms of flame emissivity as determined by Sutherland (5).

The Film Study Experiments

Description of the Film Study Experiments

The film study was conducted to determine (A) the ability of the servomechanism system to position the burning surface of a strand of propellant for the temperature measurement of the gases above the surface, (B) the asperity of the burning surface as it was positioned for the temperature measurement by the servomechanism system, and (C) the physical characteristics of the gaseous combustion zone as the burning surface was positioned by the servomechanism system. The first two objectives were primarily intended to supply information pertaining to the operation of the temperature measurement system, while the third was intended as an experimental investigation of the gaseous reaction zone which was independent from that of the temperature measurements.

In order to gain information pertaining to the operation of the servomechanism system in the temperature measurement system, the movie camera was mounted at the rear of the High Temperature Microscope. By mounting the camera at this point, the strand of propellant could be viewed along the optical axis of the line reversal pyrometer and the microscope could be employed to give high magnifications of the burning surface. In this way, the field of view of the camera included the burning surface and the temperature measurement region. It should be noted that the microscope as employed here included the power changing lenses necessary for high magnification filming whereas only the forward optics were necessary in the previously described line reversal pyrometer optics. The camera was a Paillard-Bolex (Model H16 F25) 16 mm framing camera which was operated at a speed of 64 frames per second. The film type was Kodak Ektachrome ER film, Type B.

Results of the Film Study Experiments

Films were obtained of strands burning as their burning surfaces were positioned by the servomechanism system. The strands were burned over pressures varying from atmospheric to 275 psig for both the fine and coarse oxidizer grind propellants.

The ability of the servomechanism system to operate satisfactorily was established by comparing the films of the burning surface to the position photomultiplier tube (PPM tube) output. Comparison for each run showed excellent agreement between the PPM

tube output and the surface location as observed from the film. Thus, it was established that the visible light beam position detection system (VLBPDS) could detect the location of the burning surface and the output of the PPM tube could be relied upon to determine the location of the burning surface at any given time.

A further indication of the ability of the servomechanism to position the burning surface of the propellant was obtained from measurements of the propellant burning rate with the servomechanism system. This was accomplished by recording the output of the tachometer and PPM tube and measuring the output of the tachometer at the point where the PPM tube showed that the propellant surface was positioned. The tachometer output was then converted to burning rate from the tachometer calibration curve shown in Fig. 13. Burning rates measured in this manner are shown in Fig. 22 for the pressure range of atmospheric to 275 psig.

The asperity of the burning surface of the propellant strands was studied from films in which the High Temperature Microscope magnification was set at 35X. This magnification corresponded to a field of view of approximately 2000 microns over the 16 mm film with a spatial resolution of approximately 10 microns. The films showed that the surface roughness of strands inhibited by water leaching the oxidizer from the propellant surface and passing a column of nitrogen adjacent to the propellant surface would vary from large irregularities of 100 to 200 microns down to a smooth surface with irregularities of about 10 to 20 microns. In examining

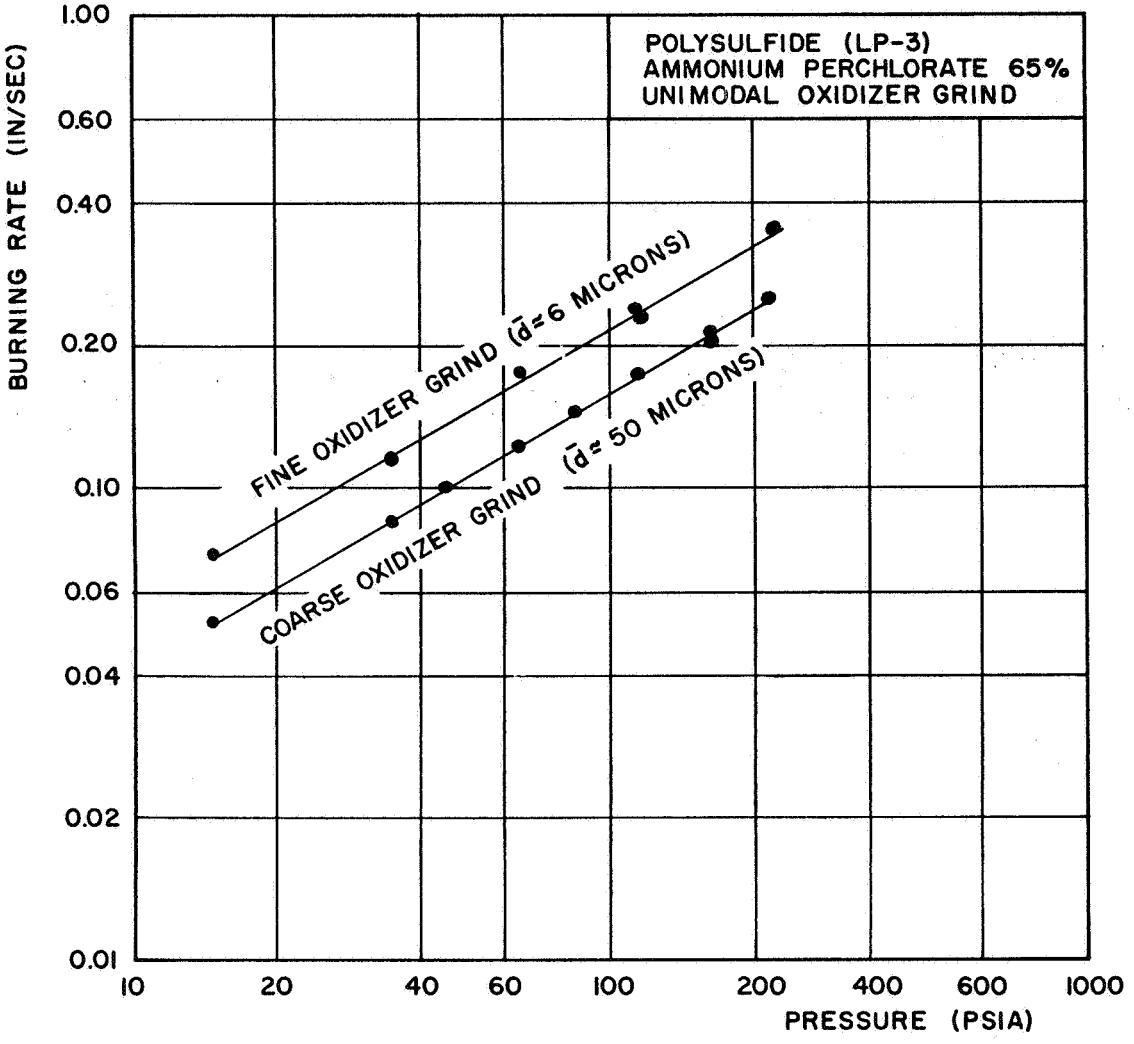

FIG. 22 BURNING RATE OF POLYSULFIDE-AP PROPELLANT

the films and the PPM tube output, it was discovered that the large irregularities were related to the tilting of the burning surface either toward or away from the comparison source as the propellant strand burned.

Quite obviously, the larger surface irregularities could not be tolerated in the temperature measurement. Since the camera record was not available when temperatures were measured, a means of identifying the surface characteristics of the strand was necessary from the PPM tube output alone. Fortunately, the means of accomplishing that objective were present in the system. It was noted that when the strand burned such that an irregular surface prevailed, the PPM tube output became erratic when compared to the output of that tube when the strand burned with a smooth surface.

To illustrate this, the outputs of the PPM tube and tachometer are shown in Fig. 23 for a fine oxidizer grind propellant burning at a pressure of 222 psia. At time $t = t_1$, the propellant was ignited and the burning surface burned past the lamp image. As the servomotor accelerated, the strand was driven upward until the burning surface again interrupted the lamp image at time $t = t_2$. At time $t = t_3$, the surface was positioned, and the tachometer showed the servomotor operating at a constant speed. The output of the PPM tube in this case is smooth and the film of the burning surface shown in Fig. 24 confirms this surface condition.

A similar example for the coarse oxidizer propellant burning at a pressure of 207 psig is shown in Figs. 25 and 26. Here again

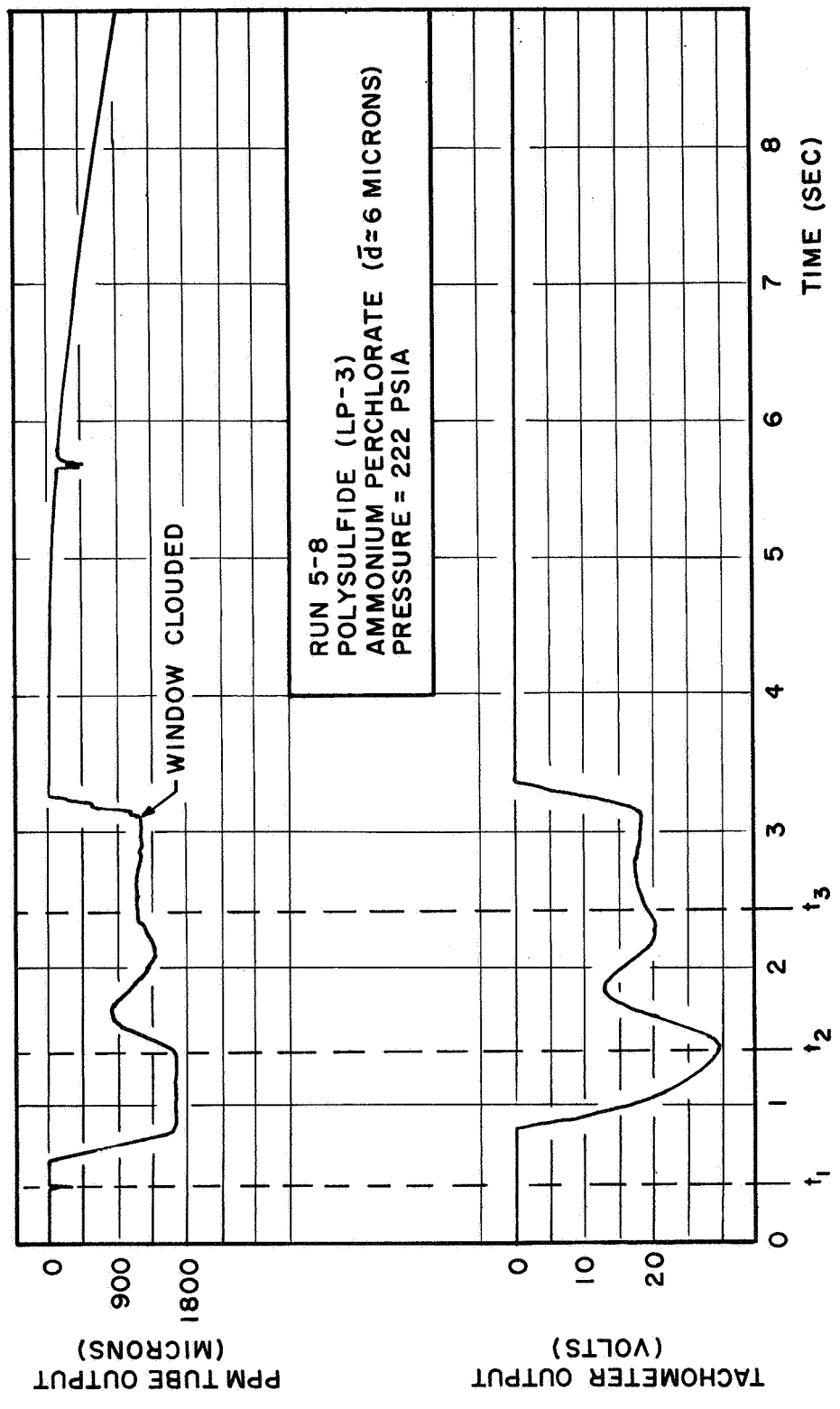

FIG. 23 FINE OXIDIZER GRIND PROPELLANT BURNING WITH A SMOOTH SURFACE

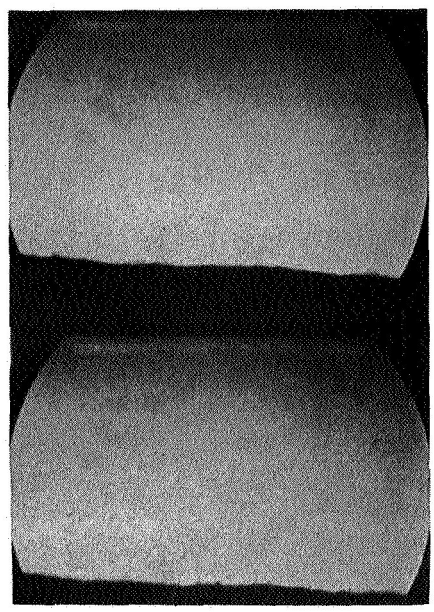

200 MICRONS

FIG. 24 FINE OXIDIZER GRIND PROPELLANT — SMOOTH BURNING SURFACE

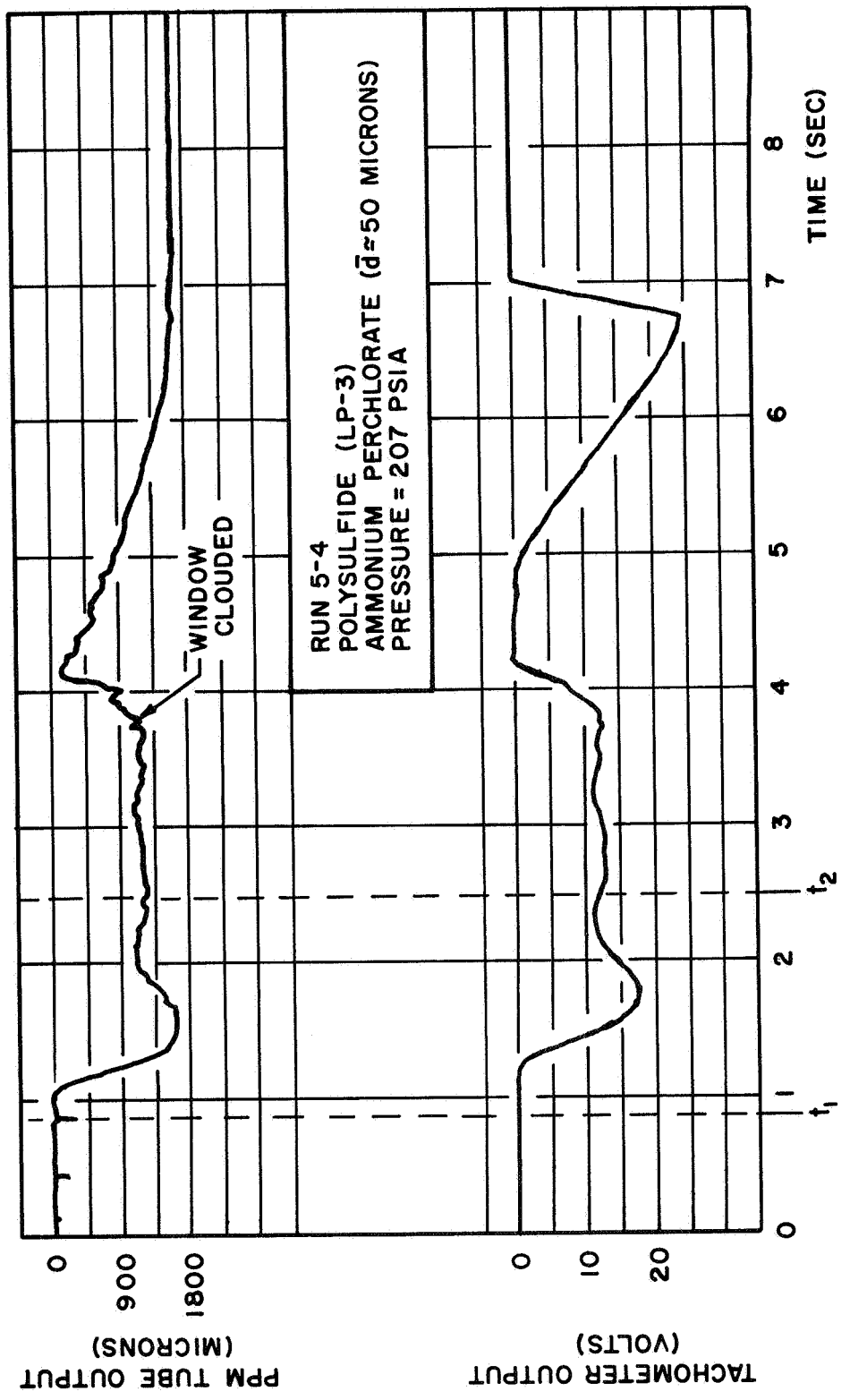

FIG. 25 COARSE OXIDIZER GRIND PROPELLANT BURNING WITH A SMOOTH SURFACE

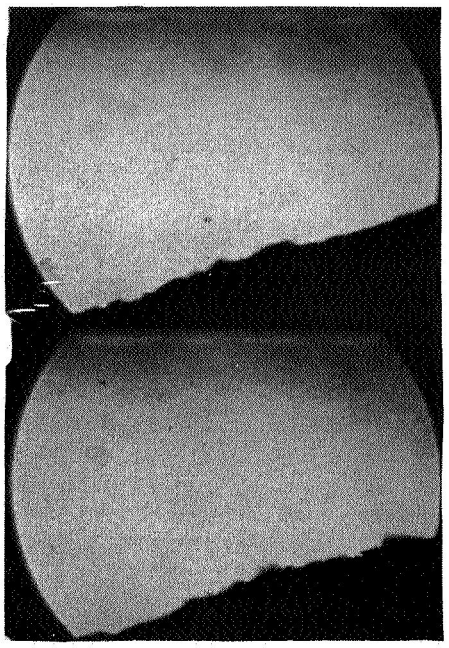

200 MICRONS

FIG. 26 COARSE OXIDIZER GRIND PROPELLANT—
SMOOTH BURNING SURFACE

the strand surface is smooth and the corresponding PPM tube output confirms this condition.

An example of a coarse oxidizer grind propellant strand burning with an irregular surface at 262 psia is shown in Figs. 27 and 28. Here, the surface of propellant is smooth up to time $t = t_4$ at which time some unknown defect in the strand (possibly a void) caused the surface to burn on a slant. From Fig. 26 undulations in the PPM tube output can now be seen, which correspond to the surface roughness shown in Fig. 28.

The results of studying the films for information pertaining to the combustion of the solid propellant strands were not very extensive due to the slow framing rate of the camera and the fact that all of the films were of burning surfaces backlighted with the comparison source. However, one result of the films was very interesting. In the burning of both the fine and coarse oxidizer grind propellants, it was noted that white streaks were present in the gaseous reaction zone at pressures above about 115 psia. The origin of the streaks was not clearly established due to the slow framing speed of the camera. In some cases, the light emanated directly from the propellant surface as shown in Fig. 29a. In others, the streak appeared abruptly above the surface as shown in Fig. 29b. In still other instances, the streak appeared faintly for a distance of about 300 microns and then appeared bright over the remainder of the field of view.

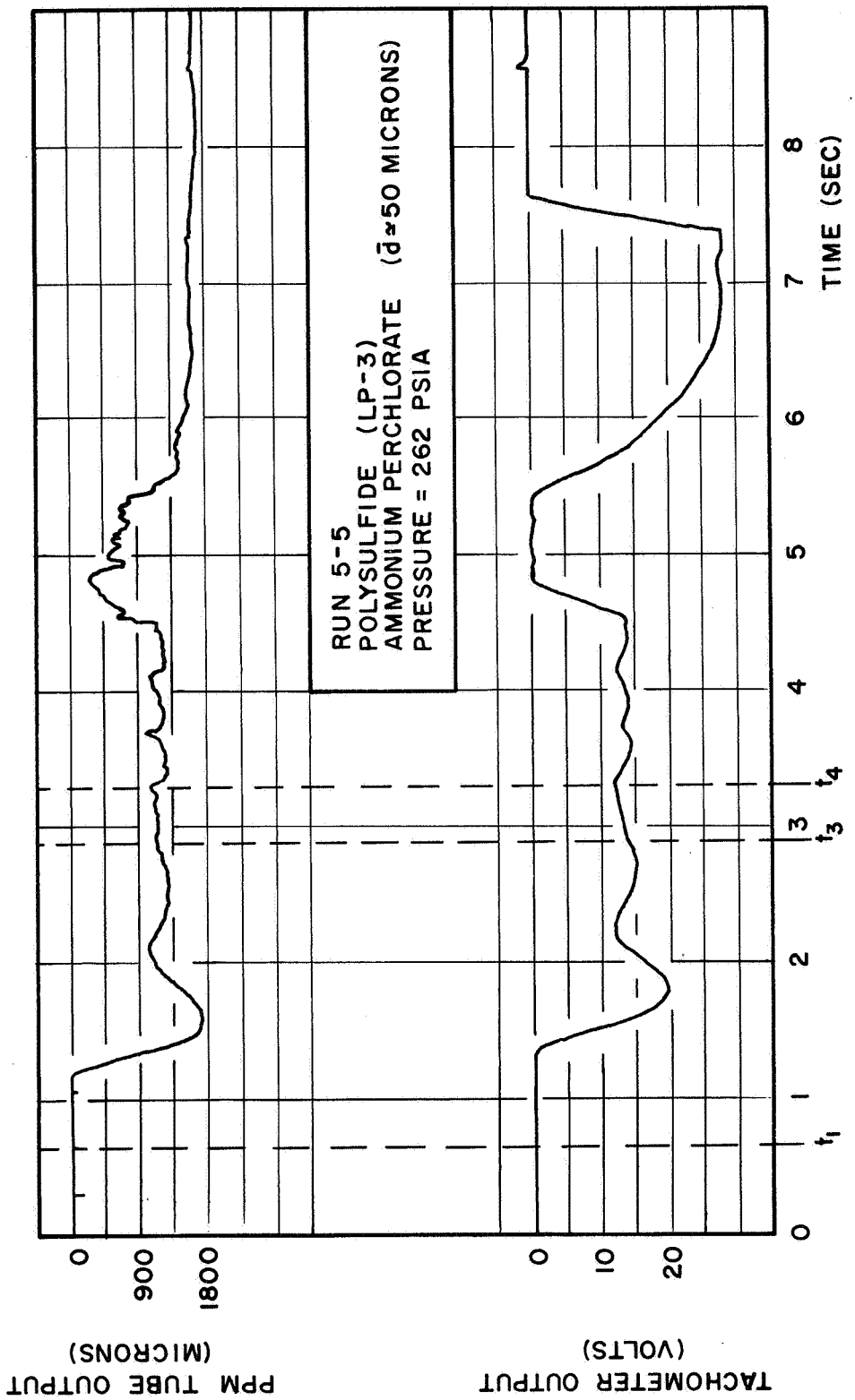

FIG. 27 COARSE OXIDIZER GRIND PROPELLANT BURNING WITH A ROUGH SURFACE

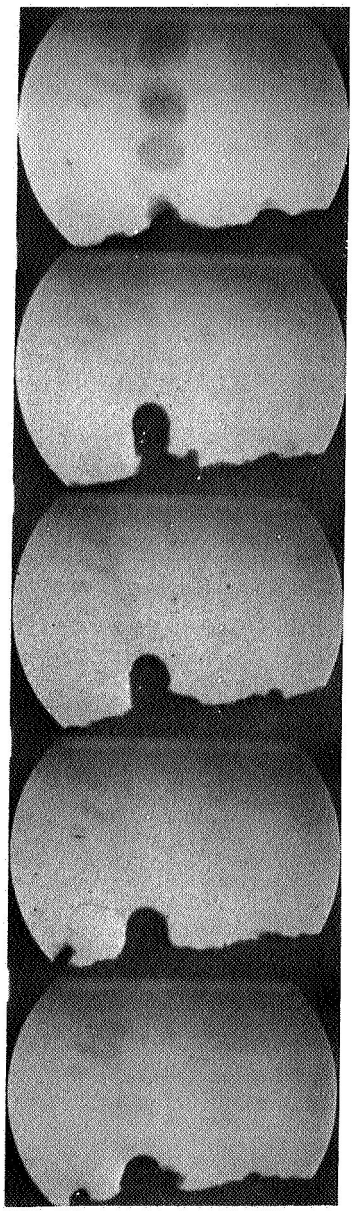

200 MICRONS

FIG. 28 COARSE OXIDIZER GRIND PROPELLANT— ROUGH BURNING SURFACE

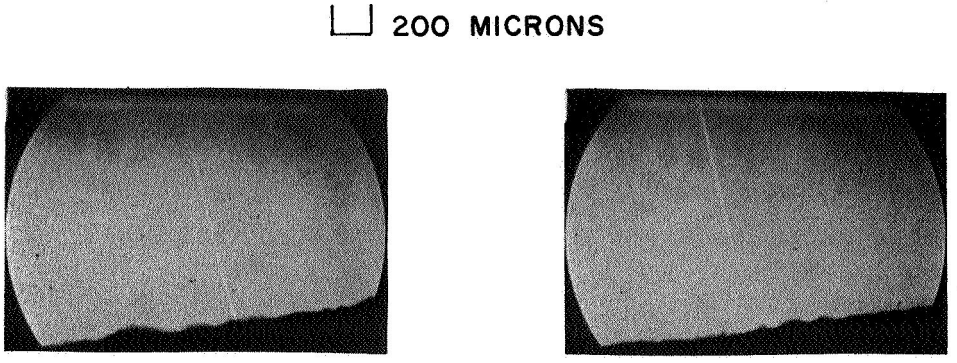

FIG. 29 STREAKS OCCURING IN GASEOUS REACTION ZONE

The frequency of occurrence of the light streaks was also difficult to establish due to the slow framing rate of the camera; however, it was observed that the frequency increased with pressure. For pressures less than about 115 psia, no streaks were observed.

The Temperature Measurement Experiments

Description of the Temperature Measurement Experiments

The previously described temperature measurement system was employed for the temperature measurements in these experiments. The experiments were conducted using both the fine and coarse oxidizer grind propellant and the propellants were burned over a pressure range of 115 to 215 psia. The flow settings for the strand and windows purges were the same as the settings found to yield satisfactory burning surface characteristics from the film study.

The Results of the Temperature Measurement Experiments

The results of the temperature measurements over the pressure range of 115 to 215 psia showed that the gaseous reaction zone is very inhomogeneous. In particular, the temperature measurements showed that no average, one-dimensional temperature profiles exist above the burning surface of the propellant at any of the pressures examined. The temperature measurements of both the fine and coarse oxidizer grind propellants over the scanning range of the instrument (up to 1000 microns above the surface) showed temperatures varying from the lower limit of accurate temperature measurement (1800 K)

to the adiabatic flame temperature of the polysulfide propellant (about 2200 K). The size of the temperature measurement zone in preliminary measurements was about 60 microns in height by 40 microns in width and the propellant thickness was 1000 microns. Since the results were so erratic, the height of the temperature measurement region was increased to 120 microns in order to average the temperature over a larger region. This situation again resulted in the erratic temperature results. A further attempt to measure a temperature profile was made by reducing the thickness of the strand to 500 microns; however, again the results were of a very erratic nature.

A plot of the temperature measured for a fine oxidizer grind propellant burning at a pressure of 215 psia is shown in Fig. 30. Here it can be seen from four separate runs that there is no specific distance from the surface at which a high temperature is favored. At distances of about 100 microns from the surface, the adiabatic flame temperature was recorded, however, this was not found consistently. In some cases the temperature was below the lower limit of the instrument (1800 K). The accuracy of the distance measurements was $\pm$ 15 microns and the temperature measurement was about $\pm$ 60 K, which does not account for the scatter shown here.

A similar plot of the temperature measured above the burning surface of a coarse oxidizer grind propellant burning at a pressure of 215 psig is shown in Fig. 31. For this plot, the results of two

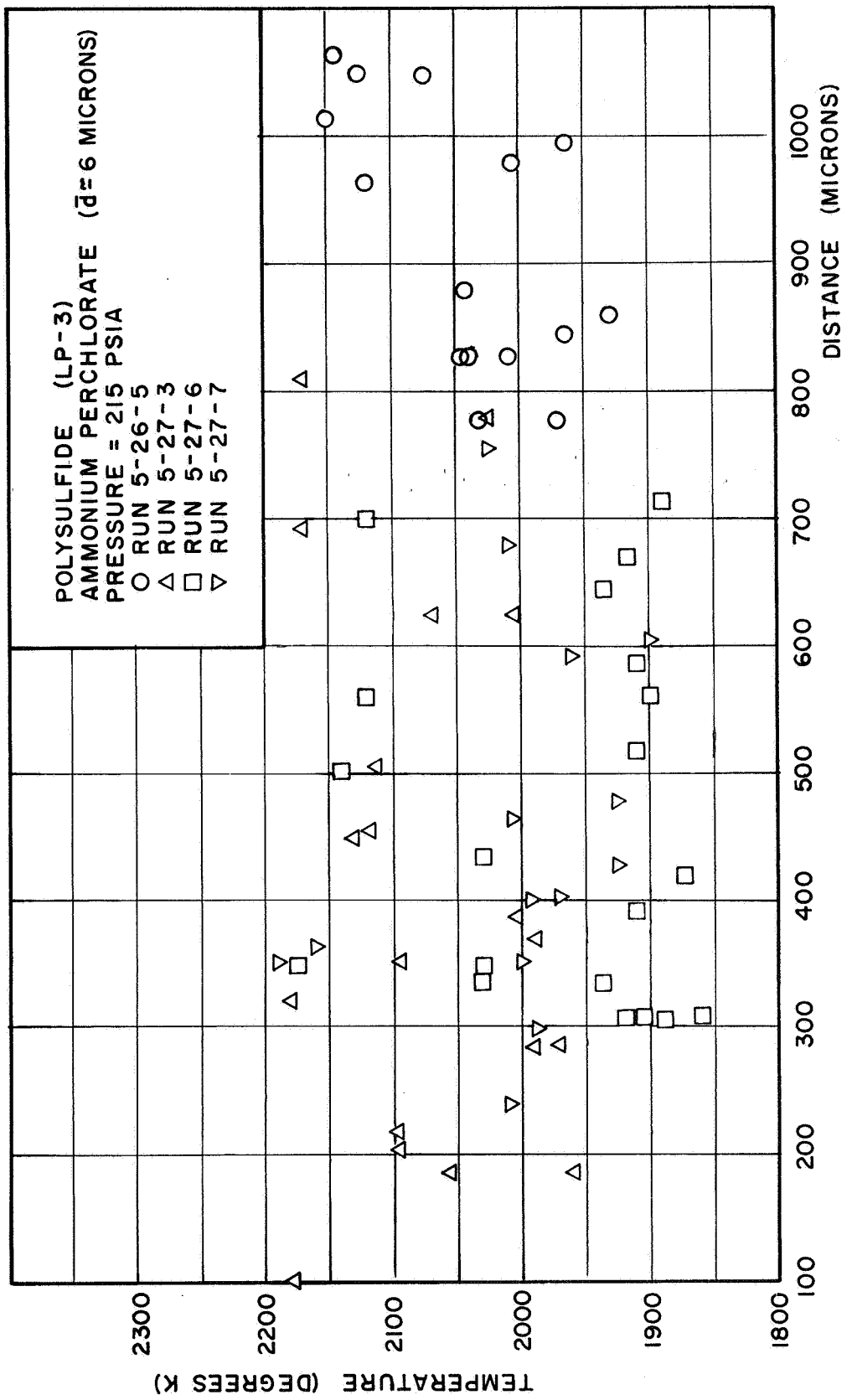

FIG. 30 FLAME TEMPERATURE OF FINE OXIDIZER GRIND PROPELLANT

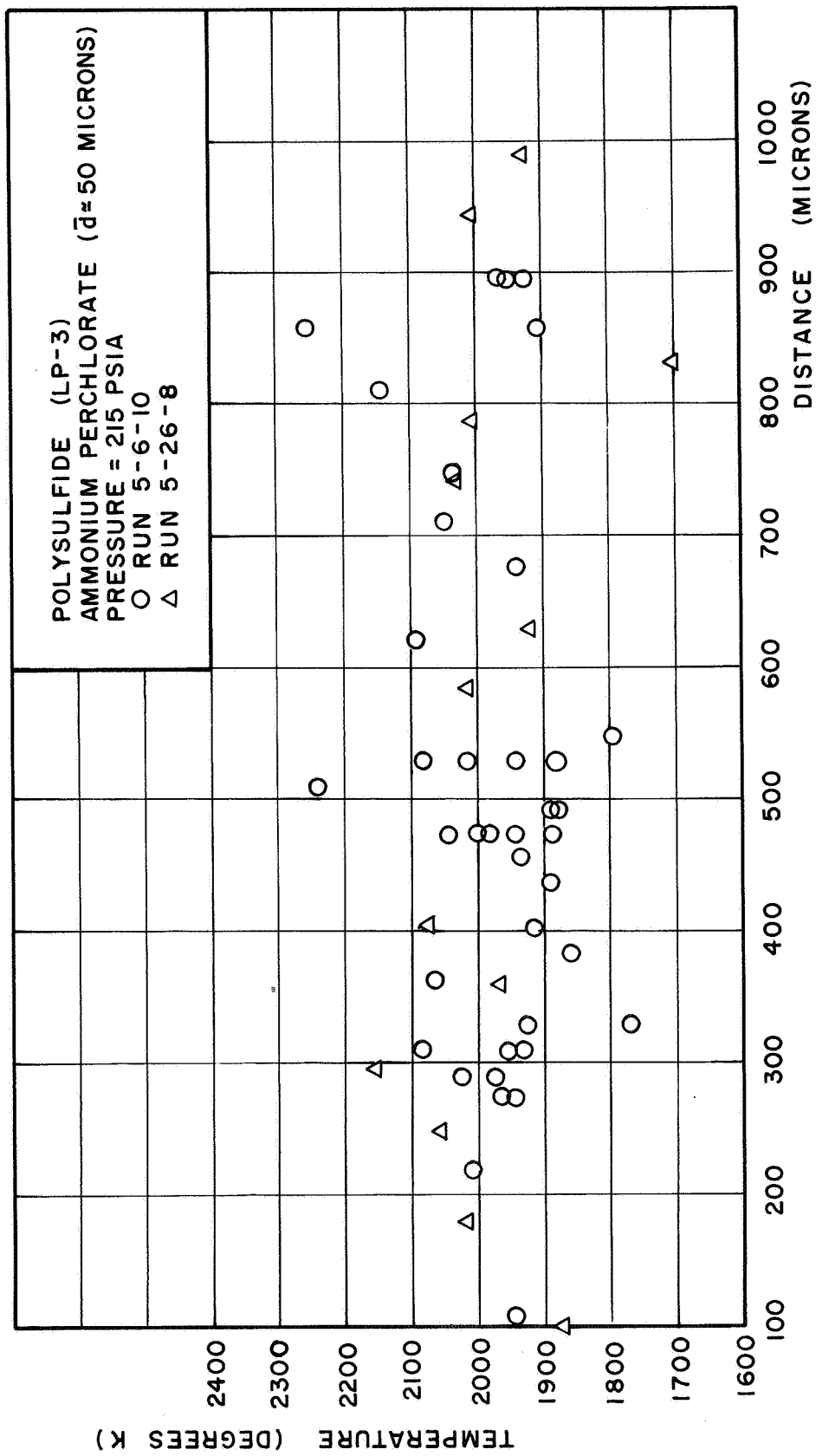

FIG. 31 FLAME TEMPERATURE OF COARSE OXIDIZER GRIND PROPELLANT

separate runs show that the temperature varies from the previously mentioned lower limit to that of the adiabatic flame temperature over the entire scanning range of the instrument.

In light of the discovery that the temperature measurement system did not yield a temperature profile as found in previous research programs (5,6) the attempt was made to measure profiles in the same manner that had been employed in those investigations. That is, the servomotor was turned off and the burning surface was allowed to burn by the temperature measurement region. Results of this type for the fine oxidizer grind propellant burning at 215 psia are shown in Fig. 32. Here the temperatures were measured as a function of time and by recording the output of the PPM tube concurrently with the TPM tube, the instantaneous burning rate could be calculated as the propellant burned by the temperature measurement region from the VLBPDS calibration curve shown in Fig. 7. The size of the temperature measurement region was 120 microns in height and 40 microns in width. The propellant thickness was 1000 microns. The results show that a profile could be inferred where the maximum temperature is attained at a distance of about 300 microns.

A similar plot for the coarse oxidizer grind propellant is shown in Fig. 33. Here again, the temperature distribution is such that a profile could be inferred where the maximum temperature lies in the vicinity of 300 microns from the surface. Again the temperature measurement region was 120 microns by 40 microns and the strand thickness was 1000 microns. These results will be discussed in more detail in the next section.

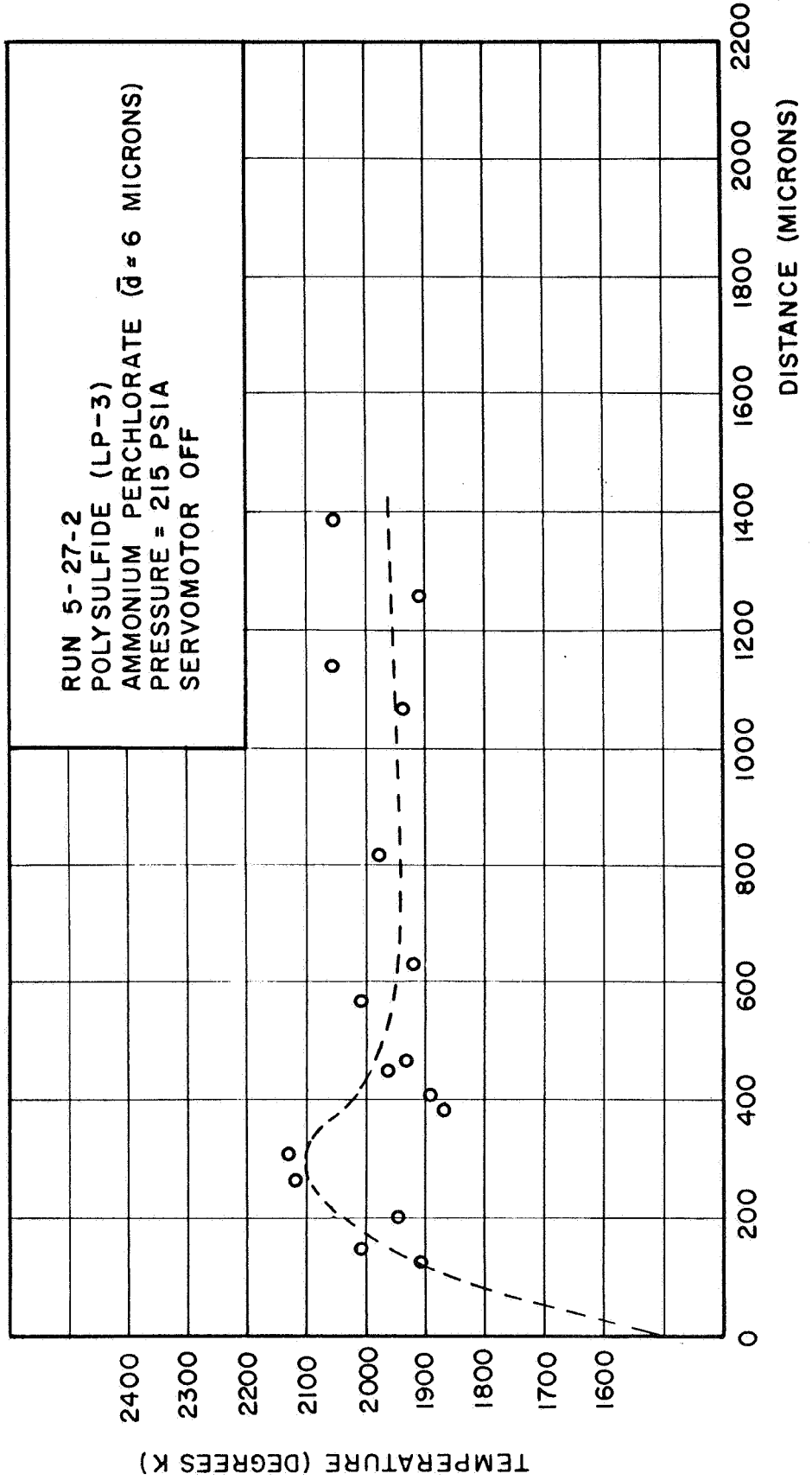

FIG. 32 TEMPERATURE PROFILE MEASUREMENTS WITH SERVOMOTOR OFF

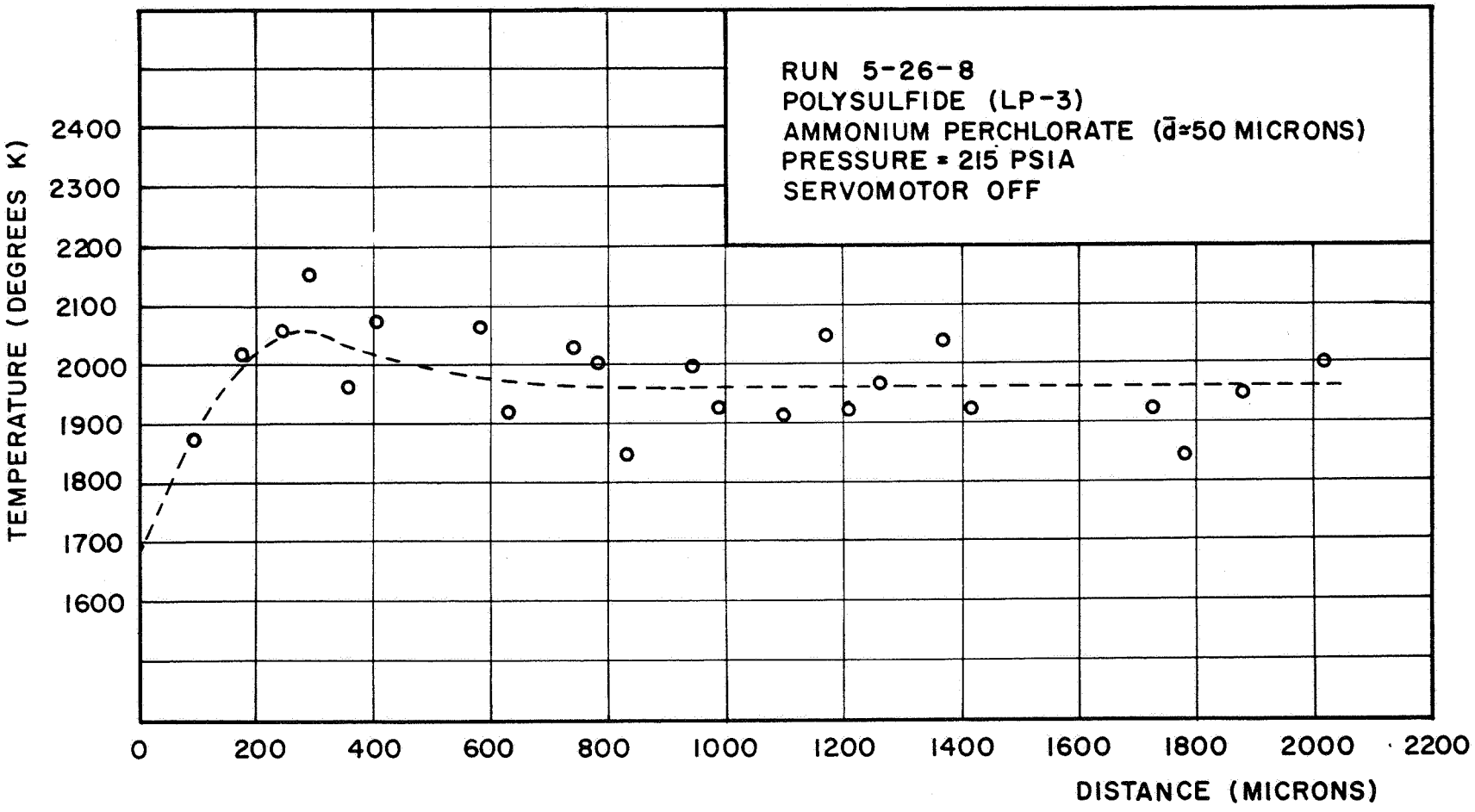

FIG. 33 TEMPERATURE PROFILE MEASUREMENT WITH SERVOMOTOR OFF

One observation which was evident over the pressure range examined was that the fluctuations of temperature in the coarse oxidizer grind propellant were much more pronounced than those of the fine oxidizer grind at a given distance from the propellant surface. An illustration of this can be seen by comparing the temperature plots shown in Figs. 34 and 35. In these plots, the temperature has been recorded, with uncertainties, as a function of time as the servomechanism system positioned the strand such that temperature measurement region was approximately 500 microns from the burning surface. The temperature measurement region was 120 microns by 40 microns and the strands were 1000 microns thick. In the case of the fine oxidizer grind propellant, the temperature can be seen to fluctuate from a temperature of about 1950 K to 2150 K over a time period of 140 milliseconds. However, in the case of the coarse oxidizer grind propellant, a fluctuation of about 1800 K to 2230 K exists over the same time period. The variation shown is typical of the temperature behavior over the pressure range of 115 to 215 psia.

Summary of Experimental Results

The results obtained from the experiments performed in this research program can be summarized as follows:

1. The servomechanism system is capable of positioning the burning surface of the solid propellant strands such that temperature measurements can be made over a flame zone for a controlled length of

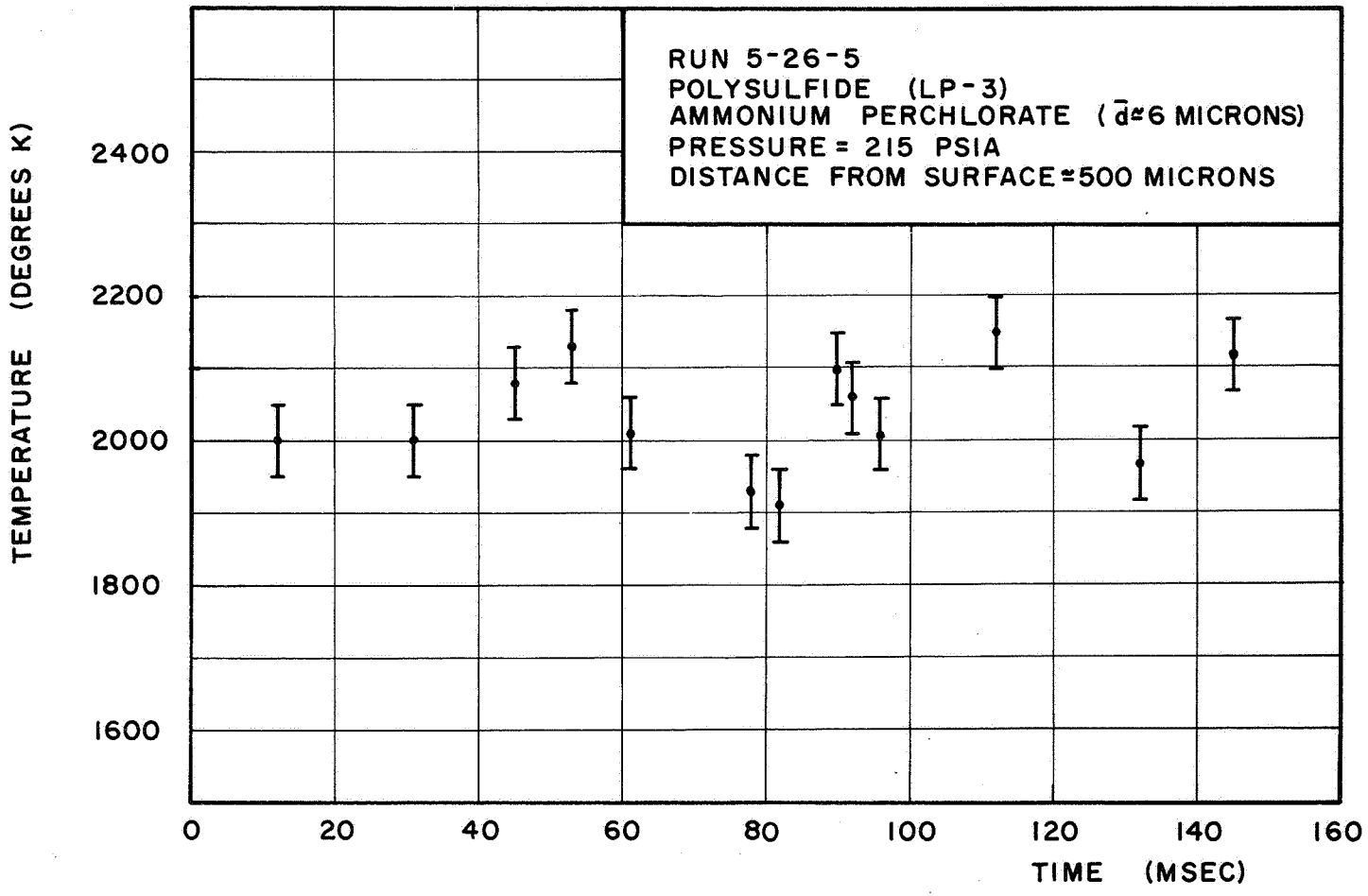

FIG. 34 TEMPERATURE FLUCTUATIONS IN FINE OXIDIZER GRIND PROPELLANT

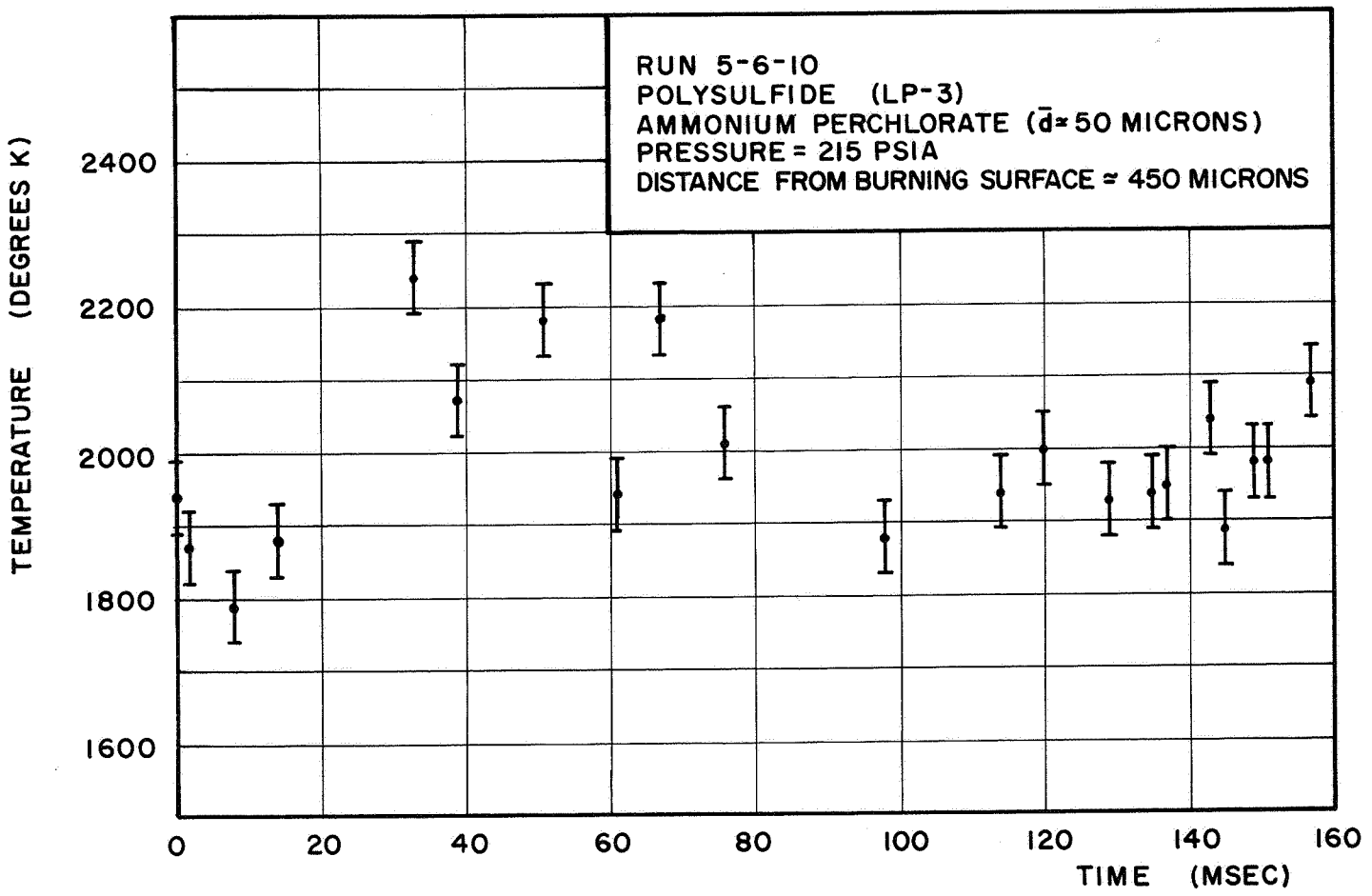

FIG. 35 TEMPERATURE FLUCTUATIONS IN COARSE GRIND OXIDIZER PROPELLANT

time. Furthermore, the VLBPDS is capable of locating the burning surface within the detection zone at any given time.

2. Light streaks have been observed for the coarse and fine oxidizer grind propellants at pressures of 115 psia and greater. These streaks appear to emanate from the burning surface, however, the precise location of the streak sources is not possible due to the low framing rate of the movie camera.

3. Temperatures close to the adiabatic flame temperature exist very close to the propellant surface (within 100 microns) over the pressure range of 115 to 215 psia for both the fine and coarse oxidizer grind propellants.

4. The temperature of the gases fluctuates over a range of 1800 K to 2200 K at distances of 100 to 800 microns above the surface of the propellant at pressures of 115 to 215 psia.

5. The temperature fluctuations occur more frequently for the coarse oxidizer grind propellant ($\bar{d} \simeq 50$ microns) than for the fine oxidizer grind propellant ($\bar{d} \simeq 6$ microns).

6. A temperature profile can be inferred provided the temperature measuring system is operated without the servomechanism.

DISCUSSION OF RESULTS

The following discussion is concerned with the interpretation of the results found in this experimental program and the comparison of those results with the results obtained in previous investigations. In particular, an attempt has been made to explain the differences between the experimental work of Sutherland (5), who found a steep temperature gradient in the gas phase adjacent to the surface, and the work of other researchers (6,7) who did not find a steep temperature gradient adjacent to the surface.

Interpretation of Experimental Results

The experimental findings from this research program have been summarized at the end of the preceding section. Included was the result that high temperatures, of the order of the adiabatic flame temperature of the propellant, have been measured at distances of 100 microns and less from the propellant surface. It has been shown previously that in order for the gaseous reaction between the fuel and oxidizer to supply the total energy necessary to sustain the surface reactions, a steep temperature gradient must exist adjacent to the propellant surface such that the flame temperature is attained at a distance of about 10 to 50 microns from the propellant

surface. Thus, the above-mentioned result of temperature measurements at distances 100 microns and less from the surface tends to substantiate the premise that the gaseous phase reactions are supplying a large fraction of the energy required to sustain the surface reactions. However, the experimental results show that the temperatures within the 100 micron zone are subject to violent changes wherein the temperatures recorded were observed to range from an upper limit of the adiabatic flame temperature (2200 K) down to the temperature at which the measuring instrument would no longer give reliable results (1800 K). Thus, it appears that the location of the high temperature zone is not restricted to a thin zone which is smaller than the temperature measurement region.

Turning attention to the results obtained above the region close to the surface, it is possible to see further evidence of temperature fluctuations. For the measurements at a distance of 100 to 1000 microns from the surface, the temperatures again have been observed to fluctuate over a broad temperature range.

As a result, it appears that the gaseous reactions between the fuel and oxidizer are occurring both very close to the surface and at distances well above that estimated thin reaction zone which precludes the need for subsurface reactions. Thus, a very inhomogeneous reaction zone where inhomogeneities are of the order of hundreds of microns has been found above the burning surface of the propellants examined in this experimental program.

Unfortunately, an accurate detailed description of the gaseous phase reaction zone is not possible in terms of structure or dimension from the experimental results due to the averaging effect which results from looking through a finite depth of such an inhomogeneous regime. In particular, the temperature and distance measurements in the zone which is 100 microns or less from the surface are subject to inaccuracies which deserve attention here. First, the problem of defining the surface is difficult for a medium which is a composite of oxidizer crystals and binder. It is not practical to believe that the surface burns in a perfectly rectilinear planar fashion. Rather, it would be more realistic to believe that undulations of the order of oxidizer crystal size exist across this surface. In the case of the fine oxidizer grind propellant, this would mean that the irregularities are of the order of 6 microns which is not excessive for measurements of distance in the zone less than 100 microns from the surface. However, for the coarse oxidizer grind propellant, the surface would be of the order of 50 microns. In this case the roughness of the surface cannot be ignored and spatial resolution in the sense of a one-dimensional profile within a distance of 100 microns from the surface is meaningless. A second factor which must be considered is the effect of the surface tilt which has been mentioned previously. For a strand of 1000 microns thickness, a large error in distance measurement could result due to excessive surface tilt. However, the

results of the film study showed that surface tilt could be identified from the output of the PPM tube; thus, runs with surface tilt were not considered in the final data analysis.

In the case of errors in temperature measurement close to the surface, the possibility of error in the ratio $\frac{I_L - I_{L-F}}{I_F}$ due to the gradual uncovering of the projected image of the monochromator entrance slit (or the temperature measurement region) by a tilted surface has been recognized in a previous experimental investigation of solid propellant flame temperatures (5). However, since all of the runs with surface tilt were disregarded, this error is not considered to be present in this experimental program. A related error is that of measuring temperatures as the temperature measurement region is uncovered by a non-tilted surface. Indeed, temperature measurements cannot be made as the monochromator slit is uncovered because the reference output of the TPM tube, I_L, is known only for the case where the monochromator slit is completely illuminated with light from the comparison source. Hence, the output of the TPM tube was not considered for temperature measurements in the experiments until the surface had burned past the temperature measurement region. Considering the height of the temperature measurement region, this means that the gas temperature was not measured until the surface was a distance equal to one-half the height of the temperature measurement region from the center of the temperature measurement region. Since that region

was approximately 120 microns and 40 microns for the experiments reported, the averaging over the region of 100 microns or less from the surface is evident.

From the above described error and averaging effects, it can be seen that the temperatures measured in the zone 100 microns or less in distance from the surface is at best an average over that entire zone. However, it is certain from the results presented that the gaseous reaction zone does originate very close to the surface (within 100 microns) and extends up to a distance of about 1 mm above the burning surface for combustion pressures of from 115 psia to 215 psia. Considering the estimated thin zone necessary for complete energy transfer from the gaseous phase reactions, this is further interpreted as evidence that the gaseous reaction between the fuel and oxidizer is not the sole provider of energy to the sustaining surface reactions.

Evidence of the importance of the gaseous reaction zone on the overall combustion process can be inferred from the finding of more frequenct temperature fluctuations in the gases at distances of about 500 microns above the surface of the coarse oxidizer grind propellant when compared to the fluctuations in the fine oxidizer grind propellant at about the same distance. The indication here is that the gaseous reactions between the fuel and oxidizer are occurring farther from the surface for the coarse oxidizer grind propellant. As a result, the energy transfer

from the gaseous phase reactions to the surface is less for the coarse oxidizer grind propellant. Since the burning rate for the coarse oxidizer grind propellant is slower than that of the fine oxidizer grind propellant as shown in Fig. 22, the indication is that the energy contribution from the gaseous reaction zone is still significant and must not be ignored completely.

The light streaks observed in the motion picture study have been considered as the source of the sudden temperature changes noted in the gaseous reaction zone of the coarse and fine oxidizer propellants. In the past, similar light streaks have been observed in film studies of the gaseous reaction zone of composite propellants by Marxman (29). In that study, the phenomenon was attributed to the explosive deflagration of single ammonium perchlorate crystals. If this is indeed the case, it would stand to reason that the path of the light streak would be of a higher temperature than that of the surrounding gases; thus, if the streak passed through the temperature measurement region, a temperature fluctuation would occur. Confirmation of this is unfortunately not possible from the motion picture study of this research program because of the slow framing rate of the camera. However, the results of Marxman show that the deflagration of single crystals appears in less than 1/2% of the ammonium perchlorate present. If this is also true for the polysulfide propellants used in this research program, the possibility of the streak passing through the temperature region is remote.

Thus, it appears more probable that the temperature fluctuations are not a result of the observed light streaks; rather, they are indeed a result of the more extensive gaseous phase reactions which are occurring above the burning surface.

Comparison of Results to Previous Experiments

The one important result that arises from the postulated gaseous reaction zone structure is the key to understanding the discrepancies of previous investigations. Because, if the reaction zone is of an inhomogeneous nature where the inhomogeneities could be of the order of hundreds of microns, the experimental approaches of previous attempts to measure temperature profiles could lead to erroneous results. In all of the past experimental approaches, the procedure followed has consisted of fixing the temperature measurement point (or region) at a point below the surface of the propellant sample. The propellant is ignited and the surface then burns past the measurement point such that a single temperature scan of the gaseous reaction zone is obtained. Since the gaseous reactions are occurring at various points throughout the zone traversed by the temperature measurement point and the locations of these reactions are changing constantly as the surface regresses away from the temperature measurement point, it is conceivable that almost any shape of temperature profile is possible above the burning surface. Indeed, the results of the

temperature measurements in this experimental program with the servomotor off show that temperature profiles can be inferred as shown in Figs. 32 and 33. Thus, single scan temperature measurements can lead to serious errors in the study of the combustion zone structure.

From Sutherland's temperature measurement (5), the following results are noted. First, the adiabatic flame temperature was reached at a distance of 100 microns from the surface. The second is that the flame zone was microscopically inhomogeneous with inhomogeneities of the order of at least ten microns, a situation which was inferred from the rippling of the signal when the radiation from the flame was recorded.

The technique for measuring temperatures as employed by Sutherland was basically the same as that employed in this investigation. The major difference was the employment of a single temperature scan technique in Sutherland's experiments instead of a surface controlling technique as employed in the present experimental approach. As a result, it was expected that there would be agreement between the experimental results. Upon comparison of the results, it appears that there is agreement in the existence of high temperatures close to the surface. At zones farther from the surface, temperature fluctuations are noted which is also in agreement with this experiment. Thus, the experimental results are in agreement.

However, the conclusions drawn from the experimental results are not in agreement. In Sutherland's work, the conclusion is drawn that the results lend support to a gaseous flame adjacent to the burning surface precluding the need of subsurface reactions to sustain the overall combustion process. It is evident from the results of this investigation that such a conclusion is unfounded if it is based upon results obtained from a single temperature scan experiment. If Sutherland had introduced a means of measuring the temperature over a fixed region with respect to the burning surface as done in this experimental approach, the presence of temperature fluctuations over that zone would have been established. Thus, he would not have been led to the conclusion of a steep temperature gradient at the surface.

The results of Penzias (6) are of the type which substantiate the results of this experiment. Two comments appear to be necessary before discussion of those results. First, an infrared technique was employed in the experiments of Penzias which involved measurements of absorptivity and radiance of the propellant flame at 23 different wavelengths. The results were based upon separate strand burning in which each measurement yielded information at only one wavelength. Second, an indirect means of measuring the distance from the measurement region to the burning surface was employed which required the independent measurement of the burning rate under

experimental conditions. As the propellant surface burned by the detection region, the measurements of emissivity and radiance were made as a function of time. The data were then converted by the burning rate value from a time to a spatial distribution. As a result of these comments and the fact that this was again a single scan technique, it is emphasized that the possibility of error is present in locating the distance where the maximum temperature occurs.

An interesting result included in Penzias' work is an observed temperature fluctuation measured at a wavelength of 3.30 microns, which is shown in Fig. 36. Here, Penzias has noted the extremely violent temperature fluctuations that were observed in the burning of strands of propellants in this research program. Thus, the results of Penzias at this wavelength are consistent with the results that the gaseous reaction zone is of a very inhomogeneous nature.

The results of Sabadell's thermocouple experiments (7) are again based on a single temperature scan of the gaseous reaction zone. The results of the study are again consistent with the postulated extensive gaseous reaction region. In fact, Sabadell suggested the existence of such a reaction zone (7) to explain the very slow rise in temperature experienced by the thermocouple after emerging from the burning surface. The absence of temperature fluctuations from the thermocouple is not surprising due to the thermal lag present in the thermocouple output.

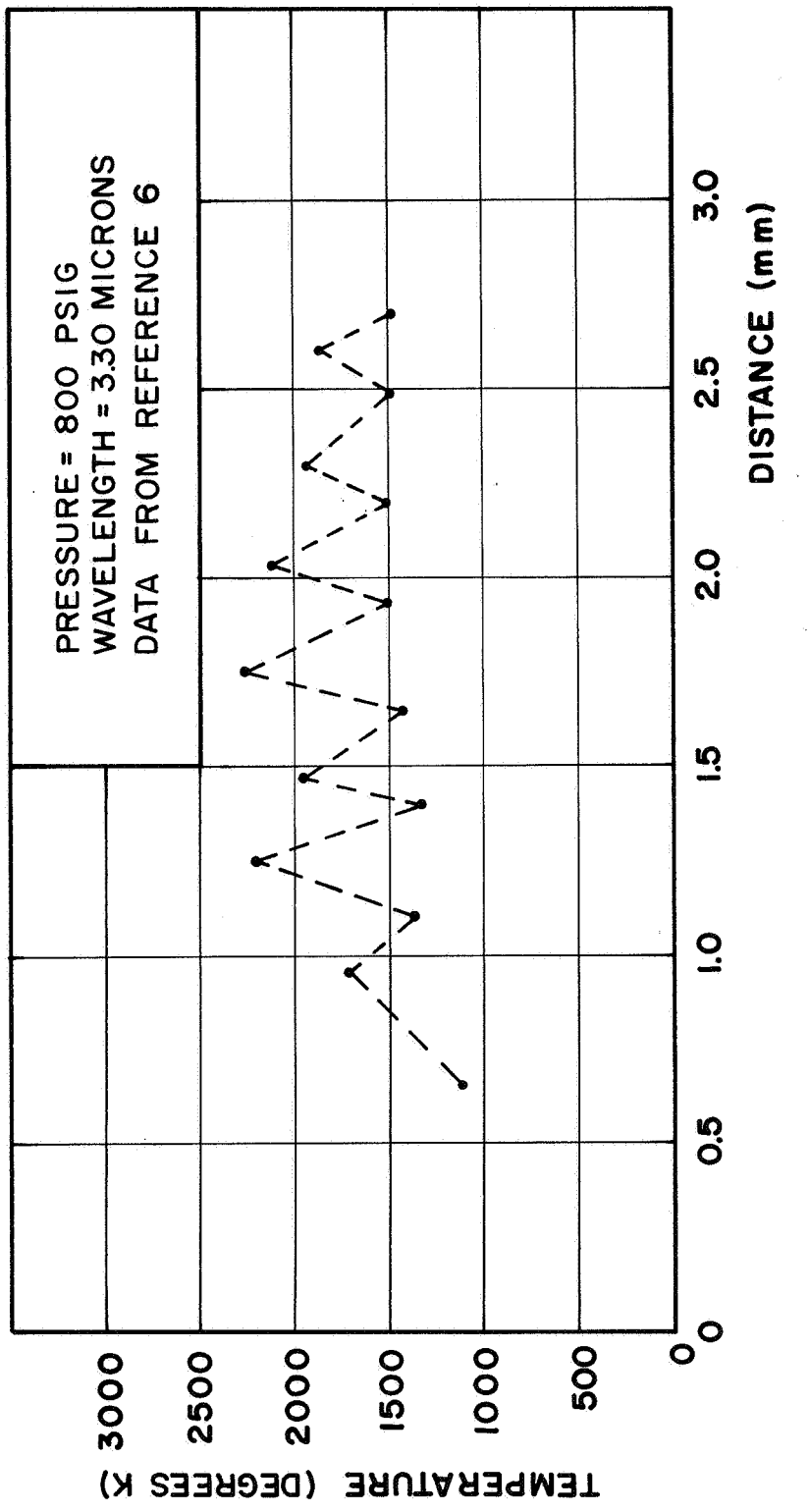

FIG. 36 TEMPERATURE FLUCTUATIONS OF POLYVINYL-AP FLAME

Finally, the results of Povinelli (20) and Waesche (21) from the spectroscopic studies of the flame in which sites of CN radiation were measured confirm the results established in this investigation. The results of both of these studies showed that the reaction zone extended to distances of about one to two mm above the surface. In regard to fluctuations in the reaction zone, the spectrographic technique is not suitable for drawing meaningful results. The radiation is recorded on a photographic plate which integrates the total radiation from the flame over the time the strand burns by the detecting slit. Thus, the output is not known for very short time intervals.

CONCLUSIONS

The main result of this investigation has been the conclusion that the gaseous reaction zone of a composite propellant is not confined to a very thin layer adjacent to the propellant surface such that the gaseous reaction between the fuel and oxidizer is the sole source of energy for sustaining the controlling surface reactions. Also, it has been found that previous attempts to measure the heat transfer characteristics of the gaseous phase by means of single temperature scans of that zone have led to erroneous conclusions in some cases. Furthermore, it has been determined that the gaseous reaction zone cannot be represented by a one-dimensional temperature profile.

In regard to the overall combustion process of composite propellants, the results of this investigation indicate that heat generation at or below the propellant surface is necessary in order to supplement the energy transfer from the gaseous reaction zone to the propellant surface. However, the finding of greater temperature fluctuations in the gases above the surface of the coarse oxidizer grind propellant when compared to the fine oxidizer grind propellant indicates that the gaseous reactions between fuel and oxidizer must not be ignored completely.

In light of the findings of this research program, it is concluded that one-dimensional theoretical and experimental approaches to the steady state combustion of a composite solid propellant will never supply the answers to the more complicated areas of non-steady combustion. In particular, it appears that studies in the gaseous phase must now be directed towards understanding reactions that occur in a zone which is at least 1000 microns thick and contains inhomogenieties of the order of several hundred microns; as a result, a three-dimensional approach appears necessary to represent the combustion process.

LIST OF REFERENCES

LIST OF REFERENCES

1. Summerfield, M., Sutherland, G. S., Webb, M. J., Taback, H. J., Hall, K. P., "Burning Mechanism of Ammonium Perchlorate Propellants," Vol. I of ARS Progress in Astronautics and Rocketry: Solid Propellant Rocket Research, Academic Press, 141-82, 1960.

2. Hermance, C. E., "A Physical Model of Composite Solid Propellant Combustion Which Includes the Oxidizer Particle Size and Surface Heat Generation," Third Aerospace Science Meeting, New York, January 1966.

3. Capener, E. L., Dickinson, L. A., and Marxman, G. A., "Response of a Burning Propellant Surface to Erosive Transients," First Quarterly Report, Stanford Research Institute, April 1966.

4. Waesche, R. H. W. and Wenograd, J., "Investigation of Solid Propellant Decomposition Characteristics and Their Relation to Observed Burning Rates," ICRPG/AIAA Second Solid Propulsion Conference, Anaheim, June 1967.

5. Sutherland, G. S., "Mechanism of Combustion of an Ammonium Perchlorate-Polyester Resin Composite Solid Propellant," Ph.D. Thesis, Aeronautical Engineering, Princeton, 1956.

6. Penzias, G. J., Liang, E. T., and Tourin, R. H., "Infrared Radiation and Temperature Measurements in Solid Propellant Flames. I. Preliminary Study of Arcite 368," TR-800-5, Warner and Swasey Co., October 1962.

7. Sabadell, A. J., Wenograd, J., and Summerfield, M., "The Measurement of Temperature Profiles through Solid Propellant Flames Using Fine Thermocouples," Solid Propellant Conference, AIAA, January 1964.

8. Geckler, R. D., "The Mechanism of Combustion of Solid Propellant," Selected Combustion Problems, 289-339, Butterworths, 1954.

9. Huggett, C., "Combustion of Solid Propellants," Solid Propellant Rockets, 3-63, Princeton University Press, 1956.

10. Geckler, R. D., "Unsolved Problems in Solid Propellant Combustion," Fifth Symposium (Int.) on Combustion, 29-40, Reinhold, New York, 1955.

11. Barrere, M., and Williams, F., "Analytical and Experimental Studies of the Steady State Combustion Mechanism of Solid Propellants," TR-240, ONERA, April 1965.

12. Schultz, R. D., Green, L., and Penner, S. S., "Studies of the Decomposition Mechanism, Erosive Burning, Sonance and Resonance for Solid Composite Propellants," Combustion and Propulsion, 367-420, Pergamon Press, New York, 1958.

13. Anderson, R., Brown, R., Shannon, L., "Critical Comparison of Solid-Propellant Ignition Theories," TM-34-63-U2, UTC, 1963.

14. Anderson, R., Brown, R., Shannon, L., "Heterogeneous Reactions in Ignition and Combustion of Solid Propellants," AIAA J., 2, 179-180, January 1964.

15. Gutman, V. R., "Solid Propellant Burning Rate Theory," Aircraft Engineering, 37, 255-260, September 1960.

16. Boys, S. F., and Corner, J., "The Structure of the Reaction Zone in a Flame" J. Proc. Roy. Soc. London, A197, 90, 1949.

17. Friedman, R., "Experimental Techniques for Solid Propellant Combustion Research," AIAA J., 5, 1217-1223, July 1967.

18. Hightower, J. D., and Price, E. W., "Two-Dimensional Experimental Studies of the Combustion Zone of Composite Propellants," ICRPG Second Combustion Conference, Los Angeles, May 1966.

19. McGurk, J. L., "Microscopic Determination of Propellant Combustion Surface Temperatures," ICRPG Combustion Instability Conference, Orlando AFB, November 1964.

20. Povinelli, L. A., "Study of Composite Solid Propellant Flame Structure Using A Spectral Radiation Shadowgraph Technique," AIAA J., 3, 1580-1584, September 1965.

21. Waesche, R. H. W., "A Spectroscopic Technique for the Study of Solid Propellant Combustion," Special Report No. S-75, Rohm and Haas Company, July 1965. [C]

22. Stammler, M., Comment on paper of H. Selzer, Eleventh Symposium (Int.) on Combustion, 446, The Combustion Institute, Pittsburgh, 1967.

23. Osborn, J. R., Burick, R., and Panella, R., "Continuous Measurement of Solid Propellant Burning Rates," Rev. Sci. Instr., 37, 86-92, January 1966.

24 Burick, R. J., and Osborn, J. R., "Erosive Combustion of Solid Rocket Propellants," Ph.D. Thesis, Mechanical Engineering, Purdue, 1967. [C]

25. Kurlbaum, F., Physik. Z, 3, 332, 1902.

26. Fery, M. Ch., Compt. rend. 137, 909, 1903.

27. RCA Product Bulletin for IP2I Multiplier Phototube.

28. Bastress, E. K., "Modification of the Burning Rates of Ammonium Perchlorate Solid Propellants By Particle Size Control," Ph. D. Thesis, Aeronautical Engineering, Princeton, 1961.

29. Marxman, G. A., Capener, E. L., and Wooldridge, C. E., "Response of a Burning Propellant Surface to Erosive Transients," Fifth Quarterly Report, Stanford Research Institute, May 1967.

30. Silverman, S., "The Determination of Flame Temperatures by Infrared Radiation," J. Opt. Soc. of Amer., 39, April 1949.

31. Millar, G. H., Winans, J. G., Uyehara, O. A., and Myers, P. S., "A Fast, Electro-Optical, Hot-Gas Pyrometer," J. Opt. Soc. of Amer., 43, 609-617, July 1953.

32. Heidmann, M. F., and Priem, R. J., "A Modified-Sodium-Line Reversal Technique for the Measurement of Combustion Temperatures in Rocket Engines," ARS J., 23, 248-253, July-August 1953.

33. Colucci, S. E., and Adams, J. M., "Flame Temperature Measurements in Metallized Propellants," Aerojet-General Corporation, Report SRO 20, November 1965.

34. Jones, G. W., Lewis, B., Friauf, J. B., and Perrott, G. St. J., "Flame Temperature of Hydrocarbon Gases," J. Amer. Chem. Soc., 53, 869-883, March 1931.

35. Gaydon, A. G., and Wolfhard, H. G., "Flames - Their Structure, Radiation and Temperature, Chapman and Hall Ltd. London, 1953.

36. Lewis, B., and von Elbe, G., "Flame Temperature," Temperature, Its Measurement and Control in Science and Industry," Reinhold Publishing Corp., New York, 1941.

APPENDIX A

NOMENCLATURE

APPENDIX A

NOMENCLATURE

Symbol

A_1	area of the monochromator slit illuminated by radiation from the source.
A_2	area of the monochromator slit illuminated by radiation from the radiating specie in the flame.
B (T)	total radiant energy emitted over the wavelength interval S .
C_1	first radiation constant.
C_2	second radiation constant.
I	output of photomultiplier tube.
J (λ,T)	emitted blackbody radiant energy.
K	calibration constant for photomultiplier tube output.
T	temperature.
T_1	brightness temperature.

Greek Symbols

α (λ,T)	spectral absorptivity.
ϵ (λ,T)	spectral emittance.
λ	wavelength.
τ_1	transmission coefficient of the optics between the comparison source and the flame.
τ_2	transmission coefficient of the optics between the flame and the photomultiplier tube.

ω_1 solid angle for the radiation from the source as it enters the collimating lens of the monochromator.

ω_2 solid angle for the radiation from the radiating species as it enters the collimating lens of the monochromator.

Subscripts

L lamp.

F flame.

L-F lamp transmitted through flame.

Abbreviations

AP ammonium perchlorate.

PBAA polybutadiene-acrylic acid.

PCPM position correction photomultiplier.

PPM position photomultiplier.

SCR silicon control rectifier.

TPM temperature photomultiplier.

VLBPDS visible light beam position detection system.

APPENDIX B

DESIGN CRITERIA FOR THE LINE REVERSAL PYROMETER

APPENDIX B

DESIGN CRITERIA FOR THE LINE REVERSAL PYROMETER

The temperature measurement technique chosen for the temperature measurement system was a line reversal technique. In the following discussion, the theoretical basis for the line reversal is presented. Included are the important assumptions in the theory which lead to design criteria necessary for the fabrication of a line reversal pyrometer. Following that discussion, the pyrometer employed in this research program is discussed in terms of the design criteria.

Development of the Line Reversal Theory

The line reversal technique of measuring flame temperature consists of introducing an atomic radiating specie in the flame and comparing the absorption and emission characteristics of that radiating specie to the radiant energy characteristics of a calibrated light source (or comparison source). The validity of the technique depends mainly upon the existence of thermal equilibrium between the flame and the radiating specie. The measurement is actually that of the effective electronic

excitation temperature for the particular specie used in the flame. Thus, if the specie is not in equilibrium with the translational degree of freedom of the gas molecules or atoms, the temperature measurement is meaningless.

Development of the Theory

The radiant energy emitted at a given wavelength and temperature from a blackbody is given by Planck's radiation law. Hence, the radiant energy emitted from the comparison source over the wavelength interval at which the specie added to the flame radiates and absorbs, $\delta\lambda$, is given by

$$B_L(T_L) = \int_{\lambda_1+\delta\lambda}^{\lambda_1} \varepsilon_L(\lambda,T_L)J_L(\lambda,T_L)d\lambda \qquad (1)$$

where

$\varepsilon_L(\lambda,T_L)$ = spectral emittance of the lamp filament

$J_L(\lambda,T_L)$ = blackbody radiant energy emitted from the lamp filament as expressed by Planck's law.

In the same manner, the radiant energy emitted from the radiating specie in the flame is

$$B_F(T_F) = \int_{\lambda_1+\delta\lambda}^{\lambda_1} \epsilon_F(\lambda,T_F)J_F(\lambda,T_F)d\lambda \qquad (2)$$

where

$\epsilon_F(\lambda,T_F)$ = spectral emittance of the flame

If the radiant energy from the comparison source is passed through the flame, a fraction of that energy will be absorbed by the radiating and absorbing specie over the wavelength interval $\delta\lambda$ resulting in a reduced radiant energy over that wavelength interval. Thus,

$$B_{L-F}(T_L,T_F) = \int_{\lambda_1+\delta\lambda}^{\lambda_1} [1-\alpha_F(\lambda,T_F)]\epsilon_L(\lambda,T_L)J_L(\lambda,T_L)d\lambda \qquad (3)$$

where

$\alpha_F(\lambda,T_F)$ = spectral absorptivity of the flame.

The condition for line reversal exists when the radiant energy over the wavelength interval $\delta\lambda$ from the comparison source is viewed through the flame such that the radiant energy of the flame equals the radiant energy of the lamp before entering the flame. Hence,

$$B_{L-F}(T_L,T_F)+B_F(T_F) = B_L(T_L) \qquad (4)$$

Introducing the Planck radiation equation

$$J(\lambda,T) = \frac{C_1}{\pi\lambda^5(e^{C_2/\lambda T}-1)}$$

where C_1 = first radiation constant

C_2 = second radiation constant

into equations 1, 2, and 3 and substituting that group of equations in equation 4, after cancellation of like terms, yields

$$\int_{\lambda_1+\delta\lambda}^{\lambda_1}\left[1-\alpha_F(\lambda,T_F)\right]\varepsilon_L(\lambda,T_L)\lambda^{-5}(e^{C_2/\lambda T_L}-1)^{-1}d\lambda + \int_{\lambda_1+\delta\lambda}^{\lambda_1}\varepsilon_F(\lambda,T_F)\lambda^{-5}$$

$$\cdot\,(e^{C_2/\lambda T_F}-1)^{-1}d\lambda = \int_{\lambda_1+\delta\lambda}^{\lambda_1}\varepsilon_L(\lambda,T_L)^{-5}(e^{C_2/\lambda T_L}-1)^{-1}d\lambda \quad (5)$$

In order to simplify this relationship, the assumption is made that the quantities $\varepsilon_L(\lambda,T_L)$, $\varepsilon_F(\lambda,T_F)$, and $\alpha_F(\lambda,T_F)$ are constant across the wavelength interval $\delta\lambda$. In addition, the assumption is made that Kirchhoff's radiation law is valid in the flame such that

$$\varepsilon_F(\lambda,T_F) = \alpha_F(\lambda,T_F) \quad (6)$$

Thus, equation 5 can be integrated by the trapezoidal rule to give

$$\varepsilon_L(\lambda,T_L)(e^{C_2/\lambda T_L}-1)^{-1} = (e^{C_2/\lambda T_F}-1)^{-1} \qquad (7)$$

Introducing the concept of brightness temperature (that is the temperature of a blackbody at a given wavelength with the same radiant energy as the lamp filament surface at the same wavelength) equation 7 becomes

$$(e^{C_2/\lambda T_L'}-1)^{-1} = (e^{C_2/\lambda T_F}-1)^{-1}$$

or

$$T_F = T_L' \qquad (8)$$

where

T_L' = brightness temperature of the lamp filament.

Thus, the measurement of the flame temperature with the line reversal technique involves matching two radiant energies as described in equation 4 by adjusting the comparison source intensity. Once the match is obtained the system is said to be reversed and the flame temperature is equal to the comparison source brightness temperature.

The method of measuring flame temperatures as described above is too slow for the measurements made in this research program. However, the modified line reversal technique increases the speed

of the temperature measurement to a rate which is compatible to the needs of the temperature profile study. The modified line reversal technique was first introduced by Silverman (30) and has had widespread application in measuring gas temperature (31, 32, 33). In this approach a photomultiplier tube is employed to measure the previously defined radiant energy levels.

The outputs of the photomultiplier tube for these energy levels are given by

$$I_L = \tau_1\tau_2\omega_1 A_1 K \int_{\lambda_1+\delta\lambda}^{\lambda_1} \varepsilon_L(\lambda,T_L)J_L(\lambda,T_L)d\lambda \qquad (9)$$

$$I_F = \tau_2\omega_2 A_2 K \int_{\lambda_1+\delta\lambda}^{\lambda_1} \varepsilon_F(\lambda,T_F)J_F(\lambda,T_F)d\lambda \qquad (10)$$

$$I_{L-F} = \tau_1\tau_2\omega_1 A_1 K \int_{\lambda_1+\delta\lambda}^{\lambda_1} \left[1-\alpha_F(\lambda,T_F)\right]\varepsilon_L(\lambda,T_L)J_L(\lambda,T_L)d\lambda \qquad (11)$$

where

τ_1 = transmission coefficient of the optics between the comparison source and flame

τ_2 = transmission coefficient of the optics between the flame and the photomultiplier tube.

ω_1 = solid angle for the radiation from the source as it enters the collimating lens of the monochromator.

ω_2 = solid angle for the radiation from the radiating specie in the flame as it enters the collimating lens of the monochromator.

A_1 = area of the monochromator slit illuminated by radiation from the source.

A_2 = area of the monochromator slit illuminated by radiation from the radiating specie in the flame.

In the modified line reversal technique, it is convenient to group the three photomultiplier tube outputs to give

$$\frac{I_L - I_{L-F}}{I_F} = \left(\frac{\omega_1 A_1}{\omega_2 A_2}\right) \frac{(e^{C_2/\lambda T_F} - 1)}{(e^{C_2/\lambda T_L'} - 1)} \tag{13}$$

Where T_L' = brightness temperature of the comparison source at the flame.

Solving equation 13 for the flame temperature yields

$$T_F = \frac{\lambda}{C_2} \ln \left\{ \left[\frac{\omega_1 A_1}{\omega_2 A_2}\right] \left[\frac{I_L - I_{L-F}}{I_F}\right] \left[\exp(C_2/\lambda T_L') - 1\right] + 1 \right\}$$

By the proper optical design, the ratio $\omega_1 A_1 / \omega_2 A_2$ is equal to unity. Hence,

$$T_F = \frac{\lambda}{C_2} \ln \left\{ \frac{I_L - I_{L-F}}{I_F} \left[\exp(C_2/\lambda T_L') - 1\right] + 1 \right\} \tag{14}$$

Thus, the temperature of the flame is measured in terms of the three photomultiplier tube outputs and reversal is not required in the

modified line reversal technique. Discrimination between the radiant energy levels is accomplished by introducing two choppers in the pyrometer optics. One chopper interrupts the light path between the comparison source and flame while the other interrupts the light path between the flame and photomultiplier tube. Thus, the number of temperature measurements over a given time is determined by the chopping frequency.

Pyrometer Design Criteria

Several important criteria for accurate temperature measurements with a modified line reversal pyrometer can be established from the above theory development. These can be summarized as follows:

1. Thermal equilibrium must exist between the radiating specie and the flame gases.

2. The quantities $\epsilon_L(\lambda,T_L)$, $\epsilon_F(\lambda,T_F)$, and $\alpha_F(\lambda,T_F)$ must be constant over the wavelength interval $\delta\lambda$

3. Radiant energy from the comparison source can be reduced only from absorption by the radiating species in the flame. Solid particles which could cause scattering of that radiant energy must not exist in the flame. Also, the windows must be maintained free of dirt or soot throughout the period of temperature measurement.

4. The design of the pyrometer optics must be such that $A_1\omega_1 = A_2\omega_2$.

5. The photomultiplier tube output must be linear with input radiant energy.

The Design of the Pyrometer

The importance of thermal equilibrium between the radiating specie and the flame has been emphasized previously. In this research program, the radiating specie added to the flame was sodium and the wavelength interval was centered about the sodium D lines. This wavelength band has been used in the past (31,32) and was selected because sodium is generally accepted as being in thermal equilibrium with the flame (34, 35, 36). Although there is no way to prove that thermal equilibrium was present between the sodium atoms and the flame, previous examinations have shown satisfactory agreement between theoretically predicted and experimental flame temperatures.

The comparison source employed in the pyrometer was a GE tungsten strip lamp. The spectral emissivity of the tungsten strip is constant within the accuracy of experimental data for the spectral properties of tungsten (37). Thus, the requirement that $\epsilon_L(\lambda,T_L)$ be maintained constant over the experiment wavelength was realized for the pyrometers.

The spectral emissivity and absorptivity of the radiating specie in the flame are a function of the concentration of radiating specie in the flame. However, the width and shape of the spectral lines are also important in establishing the emissivity and absorptivity. As a result, the exit slit of the monochromator was adjusted carefully to allow only the spectral lines emitted by

the sodium atoms such that $\epsilon_F(\lambda,T_F)$ and $\alpha_F(\lambda,T_F)$ were constant over the experiment wavelength.

The problem of scatter in the flame was not present for the simple nonmetalized propellant used in the research program. However, the problem of clouded windows was present in some instances. The frequency of occurrence of that problem was reduced by purging the windows with nitrogen. The detection of dirty windows was accomplished by monitoring the position correction photomultiplier tube (PCPM tube) as described previously. Thus, although this problem was not eliminated in the pyrometer, a means was available to detect when the problem was present.

The design of the optical system for the pyrometer is illustrated schematically in Fig. 6 and 14. In order to satisfy the fourth design criterion, the optics were designed such that the areas of the monochromator slit illuminated by the flame, A_1, and the comparisons source, A_2, were equal. This was accomplished by ensuring that both the radiant energy from the comparison source and flame completely covered the slit opening. In addition, the requirement on the solid angles ω_1 and ω_2 was met by introducing an iris diaphragm between the flame and the photomultiplier tube as shown in Fig. 14. Since the f number of the lens L_2 shown in Fig. 6 was smaller than that of the microscope objective lens, the iris diaphragm served to limit the solid angle of both the flame and comparison source radiant energy. As a result, the solid

angles ω_1 and ω_2 were equal. Thus, the fourth design criterion was met in the pyrometer.

The temperature measurement photomultiplier tube (TPM tube) was designed such that the ratio of the voltage divider current to anode current was always less than 0.1 for maximum linearity as specified by the photomultiplier tube manufacturer (27). A Kodak neutral density step tablet was employed to check the TPM tube linearity. The check confirmed that the TPM tube output was linear for the radiant energy levels entering the photocathode of the photomultiplier tube.

Thus, the previously defined design criteria necessary for fabricating a modified line reversal pyrometer have been realized in the pyrometer employed in this research program.

APPENDIX C

CALIBRATION OF THE COMPARISON SOURCE

APPENDIX C

CALIBRATION OF THE COMPARISON SOURCE

The comparison source was a tungsten strip lamp (GE Model 18A/T10/2P). The lamp served two purposes in the temperature measurement system. First, the lamp was employed as a continuous light source for the line reversal pyrometer. Second, the lamp was employed as the source of light necessary for the operation of the servomechanism detection system (VLBPDS). Current was supplied to the lamp from six 12 v storage batteries wired in parallel. Regulation of the current level was accomplished by a one ohm rheostat (Ohmite Model T 1Ω) wired in series between the lamp and the battery output. In order to achieve maximum lamp stability, the lamp was annealed at a current of 12 amp for a period of several hundred hours.

Temperature Calibration of the Comparison Source

As discussed previously, the brightness temperature of the comparison source must be known at the flame location in order to calculate the flame temperature from equation 14. Calibration to find the brightness temperature of the lamp was accomplished with a disappearing filament pyrometer (Leeds and Northrup Model 360).

The pyrometer was mounted and focused such that the image of the tungsten strip lamp was observed through the telescope of the pyrometer. Values of the lamp brightness temperature were obtained as a function of lamp current from 8 amps to 13.5 amps. The brightness temperature measurements were for a wavelength of 0.653 μ. Since the experiment wavelength was 0.5893 μ, it was necessary to calculate the brightness temperature corresponding to the experiment wavelength from the measured brightness temperature.

Representing the radiant energy of the tungsten lamp by Planck's radiation law, the true temperature of the lamp can be expressed in terms of the brightness temperature of the lamp. Hence,

$$\varepsilon_L(\lambda_{RED},T_L)(e^{C_2/\lambda_{RED}T_L}-1)^{-1} = (e^{C_2/\lambda_{RED}T'_{RED}}-1)^{-1} \qquad (15)$$

where

λ_{RED} = wavelength of pyrometer measurement (.653 μ)

T_L = true temperature of the lamp

T'_{RED} = brightness temperature of the lamp at λ_{RED}

$e_L(\lambda_{RED},T_L)$ = spectral emissivity of tungsten

Solving equation 15 for the true lamp temperature required a trial and error solution. As a result, a computer program was written in which the true lamp temperature was calculated for a given brightness temperature. The values for the tungsten emissivity

were obtained from (37). Once the true lamp temperature was known, the brightness temperature of the lamp was calculated at the experiment wavelength. This was done by replacing the value of the wavelength, λ_{RED}, and emissivity, $\varepsilon_L(\lambda_{RED},T_L)$, with the values corresponding to the experiment wavelength. Thus, the brightness temperature of the lamp at the experiment wavelength was expressed by

$$T_L' = \frac{C_2}{\lambda \ln\left\{1 + \varepsilon_L(\lambda,T_L)\left[e^{C_2/\lambda T_L}-1\right] - 1\right\}} \qquad (16)$$

A plot of the measured and calculated lamp temperatures for the above mentioned current range is presented in Fig. 37.

Calibration of the VLBPDS

The calibration of the visible light beam position detection system (VLBPDS) was important in obtaining the plot of position photomultiplier tube (PPM tube) output versus distance as shown in Fig. 7. The calibration technique involved advancing the surface of a propellant strand (not burning) into the image of the tungsten strip lamp at known intervals of distance while the output of the PPM tube was recorded after each advancement of the propellant strand. The height of the lamp image was approximately 2 mm and the interval of advancement distance was 114 $\pm$ 5 microns. This small interval was attained by revolving

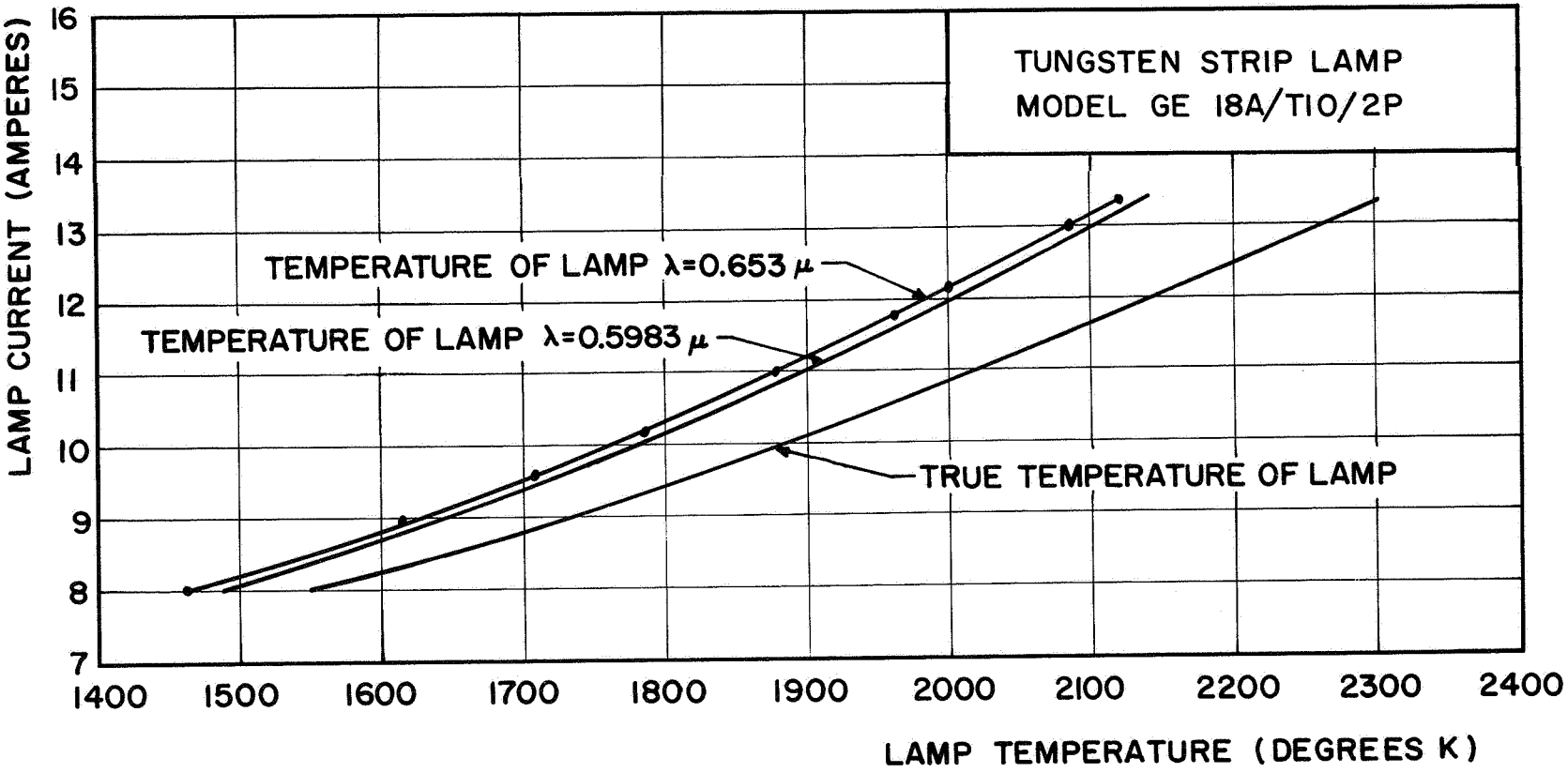

FIG. 37 COMPARISON SOURCE CALIBRATION CURVE

the servomotor driveshaft in one-quarter turn steps. The small error in position resulted by applying a downward pressure to the propellant feedshaft and revolving the servomotor driveshaft such that the feedshaft moved upward only.

Linearity of the VLBPDS calibration curve was important for the operation of the servomechanism and the accuracy of measuring the distance with the output of the PPM tube. In order to obtain linearity, it was found that the lamp current could not exceed 12 amp. At higher currents, the output of the PPM tube was saturated when the strand was not blocking the lamp image. When saturation prevailed, the slope of the VLBPDS curve, as shown in Fig. 7, was zero at small distances and was more negative at distances closer to 2000 microns. The optimum lamp current was about 11 amp. This then dictated the lamp current and brightness temperature for the temperature measurement (approximately 1850 K).

APPENDIX D

COMBUSTION BOMB SYSTEM

APPENDIX D

DESCRIPTION OF COMBUSTION BOMB SYSTEM

The experiments were performed in a combustion bomb which was incorporated in a purge flow system as illustrated schematically in Fig. 38. The combustion bomb and purge components, termed the combustion bomb system, were located in a test cell having reinforced concrete walls. Operation of the combustion bomb system was accomplished from a control room which was remote from the test cell for safety purposes.

The combustion bomb was fabricated from a stainless steel forging and was designed to operate safely up to a pressure of 2000 psia. The inside diameter of the combustion bomb was 9 1/2 in. and the length was 8 in. A 1 in. diameter plexiglas window was located at each end of the bomb in order to allow the photomultiplier tubes to detect the radiant energy from the flame and tungsten strip lamp image.

A nitrogen supply was used to pressurize the combustion bomb and purge the propellant strand and windows during a firing. The supply consisted of six nitrogen bottles coupled to a manifold. The flow of nitrogen to the combustion bomb was regulated by a 1/2 in. dome loaded flow regulator and a parallel combination of three

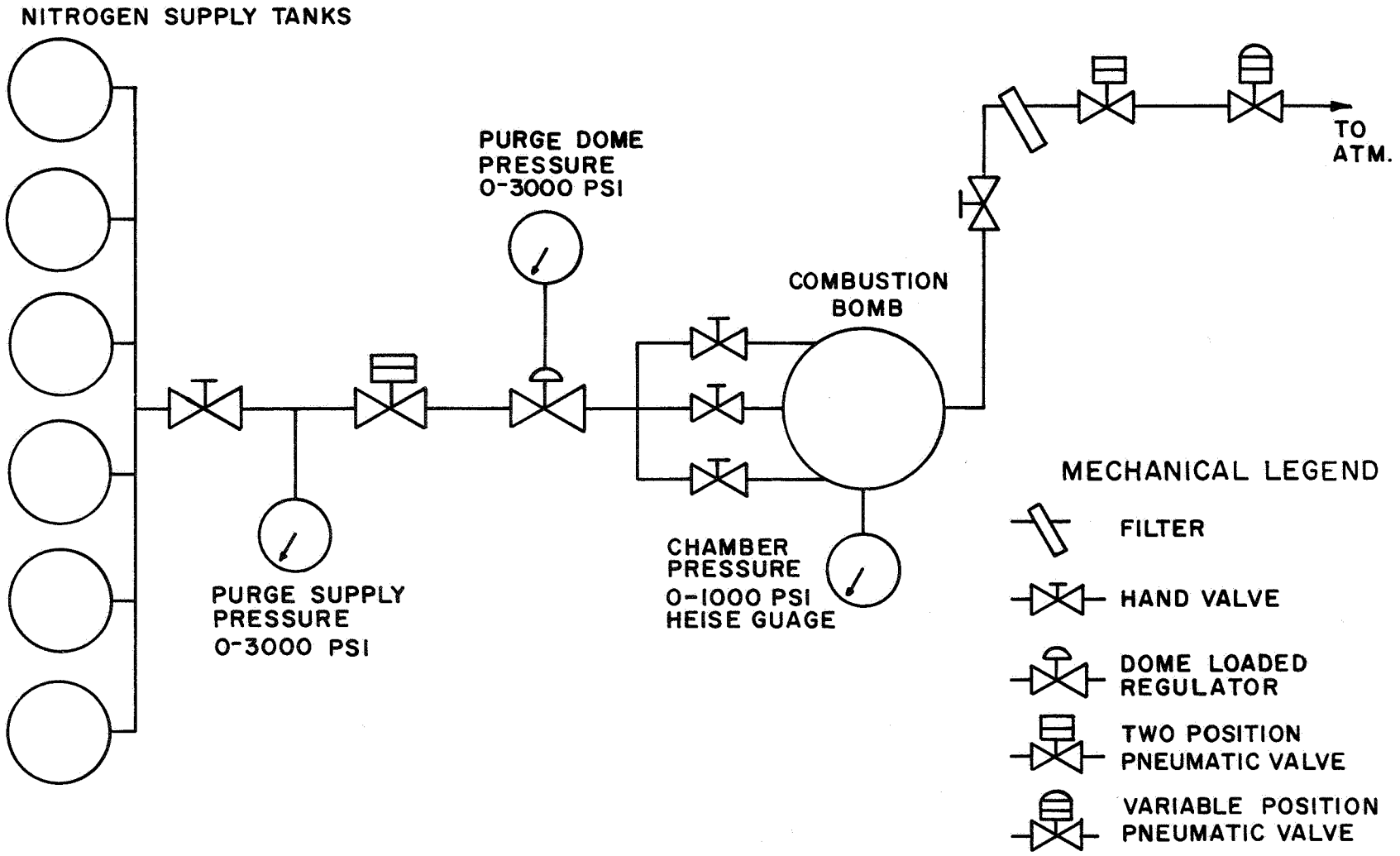

FIG. 38 PURGE FLOW SYSTEM

hand operated needle valves. The dome loaded regulator supplied a fixed upstream pressure to the needle valves; whereas the needle valves adjusted the flow rate of nitrogen to the strand and window purges.

The combustion bomb was vented with a 3/4 in. variable position pneumatic valve. That valve was adjusted such that the bomb pressure was constant and equal to the desired pressure during a firing. The pressure in the combustion bomb was measured with a 0 to 1000 psi Heise gauge.

UNCLASSIFIED

Security Classification

DOCUMENT CONTROL DATA - R&D

(Security classification of title, body of abstract and indexing annotation must be entered when the overall report is classified)

1. ORIGINATING ACTIVITY *(Corporate author)*
Jet Propulsion Center
School of Mechanical Engineering
Purdue University, Lafayette, Indiana

2a. REPORT SECURITY CLASSIFICATION
UNCLASSIFIED

2b. GROUP
N/A

3. REPORT TITLE

AN EXPERIMENTAL INVESTIGATION OF THE GASEOUS PHASE REACTION ZONE IN A COMPOSITE SOLID

4. DESCRIPTIVE NOTES *(Type of report and inclusive dates)*
Technical memorandum

5. AUTHOR(S) *(Last name, first name, initial)*
Derr, R. L.
Osborn, J. R.

6. REPORT DATE	7a. TOTAL NO. OF PAGES	7b. NO. OF REFS
September 1967	125	36

8a. CONTRACT OR GRANT NO.	9a. ORIGINATOR'S REPORT NUMBER(S)
NsG 382 and NsG 592	TM-67-6
b. PROJECT NO.	
c.	9b. OTHER REPORT NO(S) *(Any other numbers that may be assigned this report)*
d.	JPC-438

10. AVAILABILITY/LIMITATION NOTICES
No Restrictions

11. SUPPLEMENTARY NOTES	12. SPONSORING MILITARY ACTIVITY
N/A	National Aeronautics and Space Administration

13. ABSTRACT

This thesis discusses an experimental investigation of the gaseous reaction zone located above the burning surface of a composite solid propellant. In the investigation, the temperature profile within the gaseous reaction zone was measured with a modified line reversal pyrometer. In conjunction with this, a servo-controlled feedshaft was employed to drive the strand of propellant toward the temperature measurement region at the same rate at which the strand burned. This technique enabled a zone in the flame to be examined over a controlled length of time.

A polysulfide-ammonium perchlorate solid propellant was used in the study. The effect of oxidizer size on the temperature profile was investigated by using a propellant containing a fine oxidizer grind ($\bar{d}=6\mu$) and a propellant containing a coarse oxidizer grind ($\bar{d}=50\mu$). The propellants were burned at pressures ranging from atmospheric to 215 psia.

A motion picture study was conducted in which the gaseous reaction zone and burning surface of a propellant sample were photographed as the servomechanism operated. The results of this study demonstrated that the servomechanism was capable of positioning the burning surface satisfactorily.

The results of the temperature measurements showed that the gaseous reaction zone cannot be represented by a one-dimensional temperature profile. It was also found that the gaseous reaction zone is not confined to a thin region adjacent to the surface; rather, at the pressures examined, the reaction zone extends up to a distance of approximately 1 mm from the surface, a measurement which is greater than that found by some researchers.

DD FORM 1 JAN 64 1473

UNCLASSIFIED

Security Classification

14. KEY WORDS	LINK A		LINK B		LINK C	
	ROLE	WT	ROLE	WT	ROLE	WT
Combustion Solid Propellants Temperature Profile Servomechanism Flame Temperature						

INSTRUCTIONS

1. ORIGINATING ACTIVITY: Enter the name and address of the contractor, subcontractor, grantee, Department of Defense activity or other organization *(corporate author)* issuing the report.

2a. REPORT SECURITY CLASSIFICATION: Enter the overall security classification of the report. Indicate whether "Restricted Data" is included. Marking is to be in accordance with appropriate security regulations.

2b. GROUP: Automatic downgrading is specified in DoD Directive 5200.10 and Armed Forces Industrial Manual. Enter the group number. Also, when applicable, show that optional markings have been used for Group 3 and Group 4 as authorized.

3. REPORT TITLE: Enter the complete report title in all capital letters. Titles in all cases should be unclassified. If a meaningful title cannot be selected without classification, show title classification in all capitals in parenthesis immediately following the title.

4. DESCRIPTIVE NOTES: If appropriate, enter the type of report, e.g., interim, progress, summary, annual, or final. Give the inclusive dates when a specific reporting period is covered.

5. AUTHOR(S): Enter the name(s) of author(s) as shown on or in the report. Enter last name, first name, middle initial. If military, show rank and branch of service. The name of the principal author is an absolute minimum requirement.

6. REPORT DATE: Enter the date of the report as day, month, year; or month, year. If more than one date appears on the report, use date of publication.

7a. TOTAL NUMBER OF PAGES: The total page count should follow normal pagination procedures, i.e., enter the number of pages containing information.

7b. NUMBER OF REFERENCES: Enter the total number of references cited in the report.

8a. CONTRACT OR GRANT NUMBER: If appropriate, enter the applicable number of the contract or grant under which the report was written.

8b, 8c, & 8d. PROJECT NUMBER: Enter the appropriate military department identification, such as project number, subproject number, system numbers, task number, etc.

9a. ORIGINATOR'S REPORT NUMBER(S): Enter the official report number by which the document will be identified and controlled by the originating activity. This number must be unique to this report.

9b. OTHER REPORT NUMBER(S): If the report has been assigned any other report numbers *(either by the originator or by the sponsor)*, also enter this number(s).

10. AVAILABILITY/LIMITATION NOTICES: Enter any limitations on further dissemination of the report, other than those imposed by security classification, using standard statements such as:

(1) "Qualified requesters may obtain copies of this report from DDC."

(2) "Foreign announcement and dissemination of this report by DDC is not authorized."

(3) "U. S. Government agencies may obtain copies of this report directly from DDC. Other qualified DDC users shall request through _____."

(4) "U. S. military agencies may obtain copies of this report directly from DDC. Other qualified users shall request through _____."

(5) "All distribution of this report is controlled. Qualified DDC users shall request through _____."

If the report has been furnished to the Office of Technical Services, Department of Commerce, for sale to the public, indicate this fact and enter the price, if known.

11. SUPPLEMENTARY NOTES: Use for additional explanatory notes.

12. SPONSORING MILITARY ACTIVITY: Enter the name of the departmental project office or laboratory sponsoring *(paying for)* the research and development. Include address.

13. ABSTRACT: Enter an abstract giving a brief and factual summary of the document indicative of the report, even though it may also appear elsewhere in the body of the technical report. If additional space is required, a continuation sheet shall be attached.

It is highly desirable that the abstract of classified reports be unclassified. Each paragraph of the abstract shall end with an indication of the military security classification of the information in the paragraph, represented as *(TS), (S), (C), or (U)*.

There is no limitation on the length of the abstract. However, the suggested length is from 150 to 225 words.

14. KEY WORDS: Key words are technically meaningful terms or short phrases that characterize a report and may be used as index entries for cataloging the report. Key words must be selected so that no security classification is required. Identifiers, such as equipment model designation, trade name, military project code name, geographic location, may be used as key words but will be followed by an indication of technical context. The assignment of links, roles, and weights is optional.